

University of Cincinnati

Date: 3/10/2022

I, Richard T Niemeier, hereby submit this original work as part of the requirements for the degree of Doctor of Philosophy in Industrial Hygiene (Environmental Health).

It is entitled:

Examination of Factors Associated with the Dermal Penetration and Absorption of Inorganic Lead (Pb) Compounds for Occupational Risk Assessment

Student's name: Richard T Niemeier

This work and its defense approved by:

Committee chair: John Reichard, PharmD, Ph.D.

Committee member: Gerald Kasting, Ph.D.

Committee member: M. Maier, Ph.D.

Committee member: Glenn Talaska, Ph.D.

Committee member: Christine Whittaker, Ph.D.



41650

Examination of Factors Associated with the Dermal Penetration and Absorption of Inorganic Lead (Pb) Compounds for Occupational Risk Assessment

A dissertation submitted to the
Graduate School
of the University of Cincinnati
in partial fulfillment of the
requirements for the degree of
Doctor of Philosophy

in the Department of Environmental and Public Health Sciences
of the College of Medicine

by

Richard Todd Niemeier

B.A. (Psychology), University of Cincinnati, 1997

B.S. (Biology), University of Cincinnati, 2002

M.S. (Environmental and Industrial Hygiene), University of Cincinnati, 2004

Committee Chair: John Reichard, Pharm.D, Ph.D

Abstract

Inorganic Lead (iPb) exposure continues to be a public health issue in both occupational and non-occupational settings, with an estimated 1,465,000 U.S. workers having dermal exposures to iPb compounds. Four specific aims were completed to explore the potential for percutaneous absorption of iPb compounds. The first aim was to review published literature on iPb dermal studies to identify/calculate percutaneous absorption values (K_p and diffusion rate). Eleven articles containing relevant data were identified. Average diffusion rates for the pool of animal and human skin data ranged from 10^{-7} to 10^{-4} mg/cm²/h, and K_p values ranged from 10^{-7} to 10^{-5} cm/h. Most studies (92%) were not conducted using standard test guideline methods, and there is low confidence in the percutaneous absorption parameters estimates. A second aim was to determine the pH-dependent dissolution of iPb compounds (Pb Nitrate (PbN), Pb Acetate (PbA), Pb Oxide (PbO), Pb Red Oxide (PbRO)) in synthetic sweat (SSFL) and understand the dissolution kinetics of these compounds for up to 72 h. At 8 h, PbN and PbA exhibit dissolutions from 36.4%–61.1%, while PbO and PbRO range from 0.1%–2.5%, with pH having a significant effect ($p < 0.05$) on dissolution for all four compounds. PbA and PbN exhibit similar dissolution patterns, with rapid dissolution during the first 8 h, and slower dissolution between 8 and 24 h. PbO at both pH levels, and PbRO at pH 5.3, show similar patterns of dissolution but did not reach a slower dissolution until 24 h. PbRO at pH 6.5 slowly releases Pb ions into the SSFL through 72 h. A third aim was to conduct pilot studies of percutaneous absorption of PbN using human skin in a Franz cell assay over 24-72 h. Four studies conducted found Pb ion in washed skin layers ranging from 8.9%- 31.5% of the mass of Pb (applied). This is likely an underestimate of the Pb in washed skin, since Pb could not be fully accounted for in recovery studies of skin due to methodological issues to fully dissolve skin.. Pb was only sporadically found in receptor fluids, which may be due to selection of phosphate buffer saline

as a receptor fluid, which precipitates as Pb phosphate when mixed with PbN. Further studies are needed to determine appropriate receptor solutions and skin dissolution methodologies to determine Pb content. A final aim was to provide a screening model, based on K_p values and dissolution parameters for iPb compounds in SSFL, to estimate the impact of dermal exposures on blood lead levels (BLLs). The model suggests that dermal exposures may increase BLLs by as much as 0.7 $\mu\text{g}/\text{dL}$ for PbRO, 1.1 $\mu\text{g}/\text{dL}$ for PbO, and 1.5–8 $\mu\text{g}/\text{dL}$ for PbN and PbA. The screening estimates for PbO, PbA, and PbN exceed 1 $\mu\text{g}/\text{dL}$, which is the typical level of detection (LOD) for detecting Pb in blood. These results suggest that the impact of dermal exposures to some iPb compounds may increase BLLs beyond a *de minimus* additional exposure, suggesting the need for a more comprehensive evaluation of dermal absorption.

[Blank Page]

Acknowledgements

First, I would like to thank my Family for their love and support through these 6 long years of academic research, including through a global pandemic. Specifically, I would like to thank my beautiful wife, Maureen, for her kindness, reassurance, and taking the brunt to keep our house and home in order. Additionally, her editing skills never cease to amaze me, especially under pressured deadlines! I would like to thank my daughter Maggie, a current undergraduate student at the University of Cincinnati, College of Medicine, for many discussions on chemistry and math concepts that I learned long ago! She was also tremendously helpful in providing a quality control check on a publication related to this dissertation work. I would also like to thank my other daughter, Katie, whose humor and good-natured ribbing asking “when are you going to finish your dissertation, Dad?”, always motivated me to keep plodding ahead! And to the family dog Chloe, who has spent countless hours next to me and on my lap as I worked.

I would also like to thank my parents, Dr. Richard Niemeier and Carole Niemeier, who have never wavered in their confidence in me. I am so grateful for their love, support and guidance. They are truly both examples of hard work and perseverance, even through times of unspeakable tragedy. Knowing their hardships gave me the inspiration to keep pushing to finish this dissertation project. My father is an alum from the University of Cincinnati, Department of Environmental Health, a former NIOSH colleague, and a close friend. He is a great scientist who fueled my passion for science and worker safety and health. My mom, also a wonderful friend, was always able to give me the perspective of what it is like to be a “spouse of someone trying to finish their Ph.D”, which I was very appreciative to hear.

Next, I would like to thank my friends and work colleagues. Without their love and support, I would never have finished this project. I would specifically like to thank Dr. James Couch, a good friend and confidant, from whom I could always get great advice and find the motivation to keep pushing. I would also like to specifically thank Dr. Lauralynn McKernan, who strongly advocated for me for acceptance

into the NIOSH Long-Term Training program and never wavered in her support along the way. I also appreciate the support of NIOSH leadership including CAPT Lisa Delaney, CDR Chad Dowell, Dr. T.J. Lentz, Dr. Paul Schulte, and Dr. Margaret Kitt, among others, to give me time and space to finish up this dissertation work.

Lastly, I would like to thank my committee members, Dr. John Reichard, Dr. Andy Maier, Dr. Chris Whittaker, Dr. Jerry Kasting, and Dr. Glenn Talaska for their guidance, expertise, and patience. Without their support and encouragement, I would have not finished this work.

Table of Contents

Abstract.....	i
Acknowledgements.....	iv
List of Tables and Figures.....	ix
Tables.....	ix
Chapter 1.....	ix
Chapter 2.....	ix
Chapter 3.....	ix
Chapter 4.....	ix
Chapter 5.....	ix
Chapter 6.....	ix
Appendices.....	x
Figures.....	x
Chapter 1.....	x
Chapter 2.....	x
Chapter 3.....	x
Chapter 4.....	x
Chapter 5.....	x
Chapter 6.....	x
Appendices.....	xi
List of Appendices.....	xi
List of Abbreviations.....	xii
Chapter 1. Review of Dermal Penetration and Absorption of Inorganic Lead (Pb) Compounds for Occupational Risk Assessment.....	1
Introduction.....	1
Methods.....	6
Results.....	8
Pb Acetate.....	23
Pb Oxide and Pb Metal.....	25
Pb Nitrate.....	27
Other Pb Compounds (Pb subacetate, Pb orthoarsenate, and Pb sulfate).....	28
Discussion.....	29

Chapter 2. Dissolution of Inorganic Lead (Pb) Compounds in Synthetic Sweat Related to Dermal Route Risk Assessment	36
Introduction	36
Methods.....	44
Dissolution Assay	44
Statistical Analyses.....	45
Results.....	46
Dissolution Assay	46
Discussion.....	53
Chapter 3. Lead (Pb) Nitrate Percutaneous Absorption Pilot Studies Using a Franz Cell Assay	60
Introduction	60
Methods.....	62
Franz Cell Setup.....	62
Skin Samples	63
Electrical Resistance Testing (Skin Pre-screening).....	63
NIOSH SSFL.....	64
Preparation of Dosing Solutions	64
Skin Dissolution.....	65
Inductively Coupled Plasma-Atomic Emission Spectroscopy (ICP-AES) and Inductively Coupled Plasma-Mass Spectrometry (ICP-MS)	66
K _p and Diffusion Rate Calculations.....	66
Statistical Analysis.....	66
Specific Study Detail Objectives and Descriptions.....	67
Results.....	70
Study 1: Infinite dosing study using SSFL as donor solvent	70
Study 2: Finite dosing study- 24 h.....	71
Study 3: Finite dosing study- 72 h.....	73
Study 4: Finite dosing study- 24 h (epidermis only).....	75
Lead (Pb) Recovery Studies.....	76
Sample Size Power Calculations.....	77
K _p and Diffusion Rate Calculations.....	78
Discussion.....	79
Chapter 4. Analysis of Interaction between Lead (Pb) Nitrate and Buffers Used as Franz Cell Receptor Fluids	88

Introduction	88
Methods:.....	89
Study 1: Pb nitrate/PBS and McIlvaine buffer interaction.....	89
Study 2: Pb nitrate and Pb oxide/citrate buffer interaction	90
Study 3: Pb nitrate/synthetic sweat interaction.....	92
Results.....	92
Study 1: Lead (Pb) nitrate/PBS and McIlvaine buffer interaction.....	92
Study 2: Pb nitrate and Pb oxide/citrate buffer interaction	93
Study 3: Pb nitrate/synthetic sweat interaction.....	95
Discussion.....	96
Chapter 5. Screening Dermal Absorption Modeling Using Key Percutaneous Absorption and Dissolution Parameters.....	102
Introduction	102
Method	103
Results.....	105
Discussion.....	107
Chapter 6. Conclusions and Future Directions	110
Conclusions	110
Future Directions	112
Percutaneous Absorption Studies.....	113
Dissolution of Pb Compounds in SSFL.....	114
Dermal Absorption Modeling Refinement.....	115
Bibliography	117
Appendices.....	127
Appendix 1. Lead (Pb) Compounds and Search Strategy.....	127
Appendix 2. K_p and Diffusion Rate Calculation in Chapter 1.....	131
Appendix 3. K_p and Diffusion Rate Calculation Based on Skin Penetration Studies in Chapter 3.....	140

List of Tables and Figures

Tables

Chapter 1

Table 1-1. Water Solubility and Uses of Lead (Pb) Compounds with Available Dermal Penetration and Absorption Data

Table 1-2. Summary of K_p and Flux/Diffusion Rates for Inorganic Lead (Pb) Compounds

Table 1-3. Dermal Penetration and Absorption Studies Identified for Lead (Pb) Acetate

Table 1-4. Dermal Penetration and Absorption Studies Identified for Lead (Pb) Oxide and Pb Metal

Table 1-5. Dermal Penetration and Absorption Studies Identified for Lead (Pb) Nitrate

Table 1-6. Dermal Penetration and Absorption Studies Identified for Other Lead (Pb) Compounds (Pb Subacetate, Pb Ortho Arsenate, Pb Sulfate)

Chapter 2

Table 2-1. Dermal Loading of Lead (Pb) Compounds on Hands in Occupational Settings

Table 2-2. Estimate of Workers Potentially Dermal Exposed to Lead (Pb), 2019 (USCB, 2018; BLS, 2021)

Table 2-3. Dissolution Function Parameters for Four Lead (Pb) Compounds

Chapter 3

Table 3-1. Study 1 Results - Infinite Dosing of Lead (Pb) Nitrate in a Franz Cell Assay for 24 hours in Split Thickness Human Skin

Table 3-2. Study 2 Results - Finite Dosing of Lead (Pb) Nitrate in a Franz Cell Assay for 24 hours in Split Thickness Human Skin

Table 3-3. Study 3 Results - Finite Dosing of Lead (Pb) Nitrate in a Franz Cell Assay for 72 hours in Split Thickness Human Skin

Table 3-4. Study 4 Results - Finite Dosing of Lead (Pb) Nitrate in a Franz Cell Assay for 24 hours in Epidermis Layer of Human Skin

Table 3-5. Recovery of Lead (Pb) in Skin Samples Collected in Study 2 and Study 4

Table 3-6. K_p and Diffusion Rate Calculations Based on Lead (Pb) Skin Concentrations Determined in Studies 1–4

Chapter 4

Table 4-1. Dissolution of Lead Nitrate (PbN) and Lead Oxide (PbO) in 0.1M Citrate Buffer @36.3°C Over a 24-hour Period in a Dissolution Assay

Chapter 5

Table 5-1. Estimates of the Concentration of Lead (Pb) Ion Available on Skin to Estimate the Amount of Pb Absorbed Through the Hands and Impact on Blood Lead Levels

Chapter 6

No tables

Appendices

Table A1. Inorganic Lead (Pb) Names and Chemical Abstract System Identification Numbers (CAS#s)

Table A2. Dermal Search Terms

Figures

Chapter 1

No figures

Chapter 2

Figure 2-1. Mass fraction of Pb remaining (\pm SEM) versus time (t) and the model fit for PbA in synthetic sweat at pH 5.3 (a) and pH 6.5 (b)

Figure 2-2. Mass fraction of Pb remaining (\pm SEM) versus time (t) and the model fit for PbN in synthetic sweat at pH 5.3 (a) and pH 6.5 (b)

Figure 2-3. Mass fraction of Pb remaining (\pm SEM) versus time (t) and the model fit for PbO in synthetic sweat at pH 5.3 (a) and pH 6.5 (b)

Figure 2-4. Mass fraction of Pb remaining (\pm SEM) versus time (t) and the model fit for PbRO in synthetic sweat at pH 5.3 (a) and pH 6.5 (b)

Chapter 3

Figure 3-1. Diagram of Franz diffusion cell (adapted from Permagear, 2022)

Figure 3-2. Schematic of Electrical Screening Test to Verify Integrity of Skin Samples Mounted on a Franz Cell.

Figure 3-3a. Pb Content (μ g) (\pm SD) in Wash Water Collected on Skin Dosed with Pb Nitrate and Hourly Aliquots of Synthetic Sweat (SSFL) or Deionized Water (DI water) in Study 2

Figure 3-3b. Fraction of Total Pb in Wash Water Collected During Each Wash in Study 2

Chapter 4

Figure 4-1. Mass (mg) of precipitate formed with three buffers mixed with three concentrations of Pb nitrate in water

Figure 4-2. Dissolution (1 minus the cumulative fraction of dissolved mass) (\pm SEM) plotted versus time (t) for Pb nitrate (PbN) and Pb oxide (PbO) dissolved in 0.1 M citrate buffer solution over 24 hours

Figure 4-3. (a) Scanning electron micrograph and (b) energy dispersive x-ray (EDX) spectra analysis of Pb phosphate particles formed by mixing NIOSH synthetic sweat with Pb nitrate

Chapter 5

No figures

Chapter 6

No figures

Appendices

No figures

List of Appendices

Appendix 1. Lead (Pb) Compounds and Search Strategy

Appendix 2. K_p and Diffusion Rate Calculations in Chapter 1

Appendix 3. K_p and Diffusion Rate Calculations Based on Skin Penetration Studies in Chapter 3

List of Abbreviations

α	y intercept
ABLES	Adult Blood Lead Epidemiology and Surveillance
ACGIH	American Conference of Governmental Industrial Hygienists
ANOVA	Analysis of Variance
aq	aqueous
β_1	slope #1
β_{1skin}	adjusted slope #1 to account for the ratio between $M_{o(exp)}/V_{exp}$ and $M_{o(skin)}/V_{skin}$
β_2	slope #2 (multi-component model)
BEI[®]	Biological Exposure Indice
BLL	blood lead level
BLS	Bureau of Labor Statistics
BW	body weight
CAS RN	Chemical Abstract Service Registry Number
$C_{dis,skin}$ ($\mu\text{g/ml}$)	the dissolved concentration of Pb ions available on the skin at time (t)
C_{high} ($\mu\text{g/ml}$)	the maximum dissolved concentration of Pb ion in sweat in the experiment
DI	deionized
Diffusion rate ($\text{mg/cm}^2/\text{h}$)	$K_p \times$ concentration (at non-steady state)
EDX	energy dispersive x-ray analysis
exp	exponential function
FDA	Food and Drug Administration
Flux (J_{ss}) ($\text{mg/cm}^2/\text{h}$)	$K_p \times$ concentration (at steady state)
ICP-AES	inductively coupled plasma-atomic emission spectroscopy
ICP-MS	inductively coupled plasma-mass spectrometry
iPb	Inorganic lead
IRL	Interim Reference Level
K_a (h^{-1})	dermal absorption rate constant
K_p (cm/h)	the rate at which a chemical penetrates through the skin
LOD	limit of detection
LOQ	limit of quantification
M_{abs}/A ($\mu\text{g/cm}^2$)	the amount of Pb ion absorbed per area of skin
M_{MO} (%)	percent of undissolved metal mass to initial metal mass
MIMAD	mass median aerodynamic diameters
$M_{o(exp)}/V_{exp}$ ($\mu\text{g}/\mu\text{l}$)	the mass of Pb loaded onto filters in the volume of SSFL in the experiment
$M_{o(skin)}/V_{skin}$ ($\mu\text{g}/\mu\text{l}$)	maximum observed Pb loaded onto skin in occupational environments in an estimated volume of sweat on the skin surface ($\mu\text{g}/\mu\text{l}$)
n/a	not applicable
NAICS	North American Industry Classification System
NIOSH	National Institute for Occupational Safety and Health
OECD	Organisation for Economic Cooperation and Development
Pb	lead
PbA	lead acetate

<i>PbN</i>	lead nitrate
<i>PbO</i>	lead oxide
<i>PBPK</i>	physiologically based pharmacokinetic
<i>PbRO</i>	lead red oxide
<i>PBS</i>	phosphate buffer saline
<i>PTFE</i>	polytetrafluoroethylene
<i>Q</i>	quantile
<i>SAS</i>	Statistical Analysis Software
<i>SC</i>	subcutaneous
<i>SD</i>	standard deviation
<i>SEM</i>	standard error of the mean
<i>SQRT</i>	square root
<i>SSE</i>	sum of squared errors
<i>SSFL</i>	skin surface film liquids
<i>SUSB</i>	U.S. Census Statistics of U.S. Businesses

Chapter 1. Review of Dermal Penetration and Absorption of Inorganic Lead (Pb) Compounds for Occupational Risk Assessment

Introduction

Adverse health outcomes associated with lead (Pb) exposure are well established and include a variety of effects at low levels of exposure including cardiovascular, kidney, neurological effects, and reproductive and developmental effects in pregnant women with blood Pb levels below 5 µg/dl (NTP, 2012; Lanphear et al., 2018). Annually, as many as 1.5 million workers are exposed to Pb in the workplace in the U.S. (ATSDR, 2020a). Additionally, the National Institute for Occupational Safety and Health (NIOSH) Adult Lead Epidemiology and Surveillance (ABLES) program estimates a national prevalence rate of 15.8 adults per 100,000 employed having BLLs >10 µg/dL in 2016 based on 26 U.S. States reporting these data (NIOSH, 2022). Over 90% of the total BLL that were >10 µg/dL in adults identified in the NIOSH ABLES program had occupational exposures, including in four industry sectors (manufacturing, construction, services, and mining) (NIOSH, 2022).

Skin contact is a significant exposure route in the workplace and understanding this exposure pathway's overall contribution to body burden for Pb is necessary for a full aggregate occupational risk assessment. The need to better understand Pb dermal exposure and uptake information is likely to increase since regulatory focus on inhalation and oral exposure to Pb has increased exposure mitigation for these routes. Over time, the dermal pathway may represent a greater proportional contribution of aggregate or combined route occupational dose (OSHA, 1978; Julander et al., 2020). Additionally, industrial uses of Pb compounds include workplaces such as battery manufacturing, refineries, and construction settings in which other contributing factors, such as heat load and skin abrasions, may increase the potential for dermal absorption of Pb (Filon et al., 2006; NIOSH, 2016). Identification and evaluation of the available data on dermal Pb exposures and Pb uptake from the dermal route are a key step to understanding the role of dermal exposures on body burden for improving occupational risk assessments.

Pb compounds exist in both organic and inorganic forms, with most current occupational exposures coming from inorganic Pb (iPb) compounds (ATSDR, 2020b). Inorganic Pb compounds exist in three oxidation states of +0, +2, and +4, and exist in metallic, oxides, salts, and soap forms. Pb compounds are the most common in environmental exposures (ATSDR, 2020b). However, iPb⁴⁺ compounds are also relevant for risk assessment, particularly for Pb in drinking water attributed to the release of Pb directly from pipe materials and Pb-containing solder (Wang et al., 2010). Additionally, most organic Pb compounds, including tetraethyl Pb, have the +4-oxidation state (ATSDR, 2020b). Occupational uses and water solubilities of Pb compounds identified in this review are provided in Table 1-1.

The toxicokinetic behavior associated with oral and inhalation iPb exposures is well described (Kehoe, 1987; Leggett, 1993; O'Flaherty, 1993; NTP, 2012; ATSDR, 2020b; Vork and Carlisle, 2020; Sweeney, 2021). However, very few studies have evaluated dermal penetration (passive diffusion of a compound through the skin barrier) and dermal absorption (diffusion into skin layers that may become available for systemic distribution) of iPb compounds. The kinetics associated with dermally absorbed iPb compounds are largely unknown. Although physiologically based pharmacokinetic (PBPK) models have been published for the estimation of blood Pb levels through inhalation and oral exposure routes, the contribution of dermal exposure to body burden has not been included in these models (Leggett, 1993; O'Flaherty, 1993; Vork and Carlisle, 2020; Sweeney, 2021). The focus of the scientific community on inhalation and oral exposures to Pb is understandable, as these routes are likely the largest contributors of historical aggregate exposures (ATSDR, 2020b).

Table 1-1. Water Solubility and Uses of Pb Compounds with Available Dermal Penetration and Absorption Data

Compound (CAS#)	Water solubility	U.S. Manufacturing (where available) and Uses	Studies with dermal penetration/absorption data
Pb nitrate (10099-74-8)	59.7 g/100 ml @25°C	19,278 kg/year manufactured in U.S. (estimated) Uses: <ul style="list-style-type: none"> • dyeing, photography, and printing industries as a mordant • oxidizer and sensitizer in photographic, tanning, lithography, tanning, and process engravings industries • ore processing for titanium, electrolytic refining of Pb • recovery of precious metals from soils • manufacturing of plastics (rayon delustering, heat stabilization of nylon, and polyester catalyst) • production of matches, pyrotechnics, and explosives • electroluminescent and for electrodepositing Pb dioxide on nickel anodes (ATSDR, 2020a; PubChem, 2022a)	Sun et al., 2002; Pan et al., 2010
Pb acetate (301-04-2) Pb acetate trihydrate (commercial form) (6080-56-4)	44.3 g/100 ml @20°C	Uses: <ul style="list-style-type: none"> • hair dye (no longer used in U.S. as of 2017) • coatings for other metals • antifouling and paint additives • insecticide • gold cyanidation processing • analytical reagent • Dyeing of textiles (ATSDR, 2020a; PubChem, 2022b, c; FDA 2021)	Pounds, 1979; Moore et al., 1980; Bress and Bidanset, 1991; Pan et al., 2010
Pb subacetate (1335-32-6)	6.25 g/100 ml @15°C	Uses: <ul style="list-style-type: none"> • clarifying and decoloring agent (PubChem, 2022d) 	King et al., 1978

Pb sulfate (7446-14-2)	32 mg/L @15°C	2.03x10 ⁸ kg/year manufactured in U.S. (estimated) Uses: <ul style="list-style-type: none"> • battery manufacturing • pigments in paint, photography • manufacturing of electrical and vinyl compounds requiring high heat stability (PubChem, 2022e) 	Sun et al., 2002
Pb oxide (1317-36-8)	Insoluble	9.57x10 ⁷ kg/year manufactured in U.S. (estimated) Uses: <ul style="list-style-type: none"> • manufacturing of lead-acid batteries • vulcanizing agent and accelerator in the rubber industry • paints, enamels, varnishes and pottery glazing • assay of precious metal ores • manufacture of red lead and other lead compounds • cement additive (with glycerol) • acid resisting and match compositions (ATSDR, 2020a; PubChem, 2022f) 	Bress and Bidanset, 1991; Sun et al., 2002; Filon et al., 2006
Pb ortho arsenate (7645-25-2)	Insoluble	Uses: <ul style="list-style-type: none"> • historical use as pesticide; current usage unknown (Pubchem, 2022g) 	Kunze and Laug, 1948
Pb metal (7439-92-1)	Insoluble	1.58x10 ⁹ kg/year manufactured in U.S. (estimated) Uses: <ul style="list-style-type: none"> • production of batteries, alloys, solder, sheeting, pipes, ammunition and other products (ATSDR, 2020a; Pubchem, 2022h) 	Sun et al., 2002; Julander et al., 2020

To our knowledge, there are only a few studies that have attempted to evaluate the kinetics of iPb absorption through the skin, including the fundamental percutaneous zero-order rate constants, K_p , flux (J_{ss}), diffusion rate, and the first-order rate constant. K_p is the permeability coefficient through the skin (cm/h) (EPA, 1992). Flux refers to the amount of chemical absorbed across a defined surface area of the skin per unit time ($\text{mg}/\text{cm}^2/\text{h}$), at steady-state conditions (EPA, 1992) and is the permeability coefficient multiplied by the test compound concentration in the vehicle applied to the skin:

$$\text{Flux (mg/cm}^2/\text{h)} = K_p \text{ (cm/h)} \times \text{concentration (mg/cm}^3\text{) (at steady state).}$$

Diffusion rate is calculated using the same formula above; however, the calculated value does not assume steady-state absorption:

$$\text{Diffusion rate (mg/cm}^2/\text{h)} = K_p \text{ (cm/h)} \times \text{concentration (mg/cm}^3\text{) (at non-steady state).}$$

These rate constants are essential for determining human risks associated with dermal Pb exposures, since they enable estimation of systemic Pb doses (i.e., internal) resulting from skin deposition. In the absence of this knowledge, estimates of systemic Pb doses attributable to dermal exposure are highly uncertain. As a result, the risk from dermal Pb exposures is evaluated based on assumptions, rather than on scientific data.

The primary objective of this paper was to identify and evaluate published articles on dermal absorption kinetics of iPb, and to evaluate their utility for pharmacokinetic modeling, such as whether the studies were conducted according to standardized test guideline-compliant methods (EPA, 1992, 1998, 2007; OECD, 2004a,b, 2011; EFSA, 2012), and if tissue compartment-specific data were collected over multiple timepoints. Where possible, the fundamental percutaneous rate constant (K_p), flux (J_{ss} ; steady state), diffusion rate (non-steady state), and the dermal absorption rate were catalogued or calculated using

the available study data. A secondary objective of this effort was to summarize Pb concentrations in organ tissues after dermal dosing of Pb compounds to evaluate the evidence of Pb absorption through the skin.

Methods

A rapid review methodology was used to identify and evaluate literature related to the dermal exposure of iPb. First, a search was conducted in ChemIDPlus (2021) to identify iPb species and Chemical Abstract Service Registry Numbers (CAS RN) (Appendix 1). The chemical structures of the Pb species were evaluated to remove all organic Pb compounds from this review. Next, a search strategy was developed to identify scientific literature related to dermal exposures (Appendix 2). Using the National Library of Medicine PubMed®, three literature searches were conducted, including: (i) CAS RN (Appendix 1) with dermal exposure-related terms (Appendix 2); (ii) iPb species (Appendix 1) names with the dermal exposure terms (Appendix 2); (iii) Lead [MeSH] OR Lead poisoning [MeSH] OR 'lead poisoning' OR 'blood lead level' OR 'lead intoxication' OR 'lead toxicity' OR 'Plumbism' OR 'Saturnism' OR 'lead exposure' OR 'lead hazard' with the dermal exposure terms (Appendix 2). The search strategy was conducted in the National Library of Medicine PubMed in May 2017, with no date restrictions on the literature search. A follow-up literature search was conducted in May 2021 to identify additional articles published since the first literature search.

Two analyses were conducted to filter the results obtained from the PubMed searches. In the first analysis, references and abstracts were downloaded into Abstrackr (Wallace et al., 2012) and repeats were deleted. All abstracts were manually screened by the same researcher, applying the inclusion and exclusion criteria listed below. In a second level of literature analysis, references that met the inclusion criteria were downloaded for a full review of manuscript text. Articles were then categorized into human and animal experimental studies. Several methodological and result parameters were collected

from identified articles to obtain relevant data to determine whether rates of dermal penetration of iPb species across human skin could be determined. Study methodologies were evaluated to compare to standard test guideline-compliant methods (EPA, 1992, 1998, 2007; OECD, 2004a,b, 2011; EFSA, 2012). Where available, relevant data for PBPK modeling efforts to better elucidate the impact of dermal Pb exposure on systemic Pb distribution were collected or calculated, including documentation of K_p and flux values, or tissue compartment-specific data collected over multiple timepoints. If the study did not determine a permeation rate at steady-state conditions, a diffusion rate was calculated instead of flux. The assessments of the full text and data extraction were completed by the same researcher. All three researchers collaborated to evaluate data against the guidelines and synthesize the findings.

Calculations for K_p , flux, and diffusion rates, based on data identified in the articles, can be found in Supplementary Materials (available at *Annals of Work Exposures and Health* online). Where available, K_p , flux, and diffusion rates found in the literature are also provided and referenced accordingly.

Inclusion and exclusion criteria

Inclusion and exclusion criteria were applied for an initial screening review using the abstract of each study, including:

- Inclusion criteria: experimentally based dermal penetration studies of any iPb species in humans or animals (*in vivo* or *in vitro*).
- Exclusion criteria: (i) studies in languages other than English; (ii) organic Pb penetration/absorption data; (iii) studies that did not identify the species of Pb; (iv) cell culture studies (*in vitro*); (v) case studies and studies with no variability determinants (i.e., where only one participant was evaluated in one trial); (vi) studies where exposure dose was unknown; and (vii) studies where the route of exposure was not controlled.

Results

The literature identification and evaluation process included 1419 abstracts screened, with 98 publications reviewed. Eleven articles were selected for inclusion in this review, containing data for seven iPb compounds. Since most of the articles provided results for different experimental conditions (e.g., multiple animal species tested) or multiple Pb compounds tested within the same publication, the results below are reported as study summaries (n = 24).

Pb compounds identified in this paper include: Pb acetate, Pb nitrate, Pb oxide, Pb metal, Pb subacetate, Pb ortho-arsenate, and Pb sulfate. Over 1.88×10^9 kg of these Pb materials are manufactured in the U.S. per year (ATSDR, 2020b) and are used in a variety of industries, such as manufacturing of plastics, batteries, dyes, coatings, and pigments, among other uses (Table 1-1).

A summary of percutaneous absorption parameters that were calculated or identified in the literature is provided in Table 1-2. No articles identified dermal absorption rate constant (K_a ; h^{-1}).

Table 1-2. Summary of K_p and Flux/Diffusion Rates for Inorganic Lead (Pb) Compounds

	Human		Rat	Mouse	Guinea Pig	Pig
	<i>In vivo</i>	<i>In vitro</i>	<i>In vivo</i>	<i>In vitro</i>	<i>In vitro</i>	<i>In vitro</i>
Pb acetate						
K_p (cm/h)	$5 \times 10^{-7} - 4 \times 10^{-6}$ (a-c)		$2 \times 10^{-6} - 3 \times 10^{-5}$ (d)	$5.9 \times 10^{-7} - 1.0 \times 10^{-6}$ (e)		
Diffusion rate (mg/cm ² /h)	$1 \times 10^{-6} - 8 \times 10^{-6}$ (a)	1.6×10^{-4} (f)	$3 \times 10^{-5} - 3 \times 10^{-4}$ (c, d, i)		$9.6 \times 10^{-5} - 1.6 \times 10^{-4}$ (f, i, j, k)	
Pb oxide						
K_p (cm/h)						
Diffusion rate (mg/cm ² /h)	1.21×10^{-7} (g, h)				$< 3.0 \times 10^{-5}$ (f, i, k)	
Pb metal						
K_p (cm/h)						
Diffusion rate (mg/cm ² /h)	$1.1 \times 10^{-7} - 7.8 \times 10^{-7}$ (h)					
Pb nitrate						
K_p (cm/h)	$5.0 \times 10^{-7} - 1.1 \times 10^{-6}$ (e)					
Diffusion rate (mg/cm ² /h)	$1.9 \times 10^{-5} - 4.3 \times 10^{-5}$ (e)					

a. Moore et al., (1980)

b. EPA, (1992)

c. Hostýnek, (2003)

d. Pounds, (1979)

e. Pan et al., (2010)

f. Bress and Bidanset, (1991)

g. Filon et al., (2006)

h. Julander et al., (2020)

i. Hostýnek et al., (1993)

j. Franken et al., (2015)

k. Hostýnek et al., (1993) and Franken et al., (2015) identified the values reported in Bress and Bidanset, (1991) as flux.

The predominant Pb compounds evaluated were Pb acetate (n = 11, 46%) (Table 1-3), Pb oxide and Pb metal (n = 7, 29%) (Table 1-4), and Pb nitrate (n = 3, 13%) (Table 1-5). Additional studies for other Pb compounds (n = 3, 13%) are provided in Table 1-6. Most studies were conducted in animals (or animal skin) (n = 20, 83%) versus humans (or human skin) (n = 4, 17%). Additionally, most studies were conducted *in vivo* (n = 16, 67%).

Table 1-3. Dermal Penetration and Absorption Studies Identified for Lead (Pb) Acetate

Design	Results ^a
<p>Reference: (Pounds, 1979)</p> <p>Model (<i>in vitro/in vivo</i>): <i>in vivo</i></p> <p>Study design: experimental</p> <p>Species: Male Sprague-Dawley rats (300-400 g weight)</p> <p>N (technical and biological replicates each dose group): 4/group</p> <p>Concentration of Pb applied: 5 mg in 500 µl solution (Grecian formula or distilled water or 70% ethanol)</p> <p>Surface area of skin treated: 10 cm²</p> <p>Applied dose: (load): 0.5 mg/cm²</p> <p>Contact time (duration of application): 1 week or 2 weeks</p> <p>Recovery phase (time from dose removal to end of experiment): 0 days</p> <p>Total mass balance (applied-collected): unknown</p> <p>Mass balance reported?: No</p> <p>Standard test guideline-compliant methods: No</p> <p>Sample Media: Urine, feces, total body burden</p> <p>Frequency of collection: Cumulative; end of study</p> <p>Lower limit of detection or quantitation for each sample tested: Not reported</p>	<p>K_p: 7 days: 3x10⁻⁶—9x10⁻⁶ cm/h (Hostýnek et al., 1993) 14 days: 4x10⁻⁶cm/h—8x10⁻⁶ cm/h</p> <p>Diffusion rate: 7 days: 3x10⁻⁵—9x10⁻⁵ mg/ cm²/h (Hostýnek et al., 1993) 14 days: 4x10⁻⁵—8 x10⁻⁵ mg/ cm²/h</p> <p>F (% bioavailable): 2</p>
<p>Reference: (Pounds, 1979)</p> <p>Model (<i>in vitro/in vivo</i>): <i>in vivo</i></p> <p>Study design: experimental</p> <p>Species: Male Sprague-Dawley rats (400-500 g weight)</p> <p>N (technical and biological replicates each dose group): 4/group</p> <p>Concentration of Pb applied: 5 mg in 500 µl solution (Grecian formula or distilled water or 70% ethanol), applied 3 times per week for 4 weeks.</p> <p>Surface area of skin treated: 10 cm²</p> <p>Applied dose: (load): 0.5 mg/cm²</p> <p>Contact time (duration of application): 4 weeks, 8 weeks</p>	<p>K_p: 4 weeks: 2x10⁻⁵—3x10⁻⁵ cm/h 8 weeks: 2x10⁻⁶ cm/h</p> <p>Diffusion rate: 4 weeks: 2x10⁻⁴—3x10⁻⁴ mg/cm²/h (Hostýnek et al., 1993) 8 weeks: 2x10⁻⁴ mg/cm²/h</p> <p>F (% bioavailable): 2</p>

<p>Recovery phase (time from dose removal to end of experiment): 4-week study: 0 days 8-week study: 28 days Total mass balance (applied-collected): unknown Mass balance reported?: No Standard test guideline-compliant methods: No Sample Media: Urine, feces, total body burden Frequency of collection: Cumulative; end of study Lower limit of detection or quantitation for each sample tested: Not reported</p>	
<p>Reference: (Bress and Bidanset, 1991)</p> <p>Model (<i>in vitro/in vivo</i>): <i>in vitro</i> Study design: experimental, J diffusion tube Species: human (skin) N (technical and biological replicates each dose group): 20 Concentration of Pb applied: unknown^b Surface area of skin treated: 1.3 cm² Dose of Pb applied: 10 mg Applied dose: (load): 7.7 mg/cm² Contact time (duration of application): 24 hours Infinite or finite dose: infinite Flow type (static or continuous): static Recovery phase (time from dose removal to end of experiment): 0 hours Total mass balance (applied-collected): unknown Mass balance reported?: no Standard test guideline-compliant methods: no Sample Media: saline receptor solution Frequency of collection: Cumulative; end of study Lower limit of detection or quantitation for each sample tested: Not reported</p>	<p>K_p: n/a Diffusion rate: 1.6x10⁻⁴mg/cm²/h (Franken et al., 2015, Hostýnek et al., 1993)^c F (% bioavailable): n/a</p>

<p>Reference: (Moore et al., 1980)</p> <p>Model (<i>in vitro/in vivo</i>): <i>in vivo</i></p> <p>Study design: Experimental</p> <p>Species: human (males)</p> <p>N (technical and biological replicates each dose group): 8</p> <p>Concentration of Pb applied: 6 mM/liter of colloidal lotion, radiolabeled with Pb²⁰³ acetate (0.74 mBq) (1.95 mg/cm³) 0.1 ml applied</p> <p>Surface area of skin treated: 8 cm²</p> <p>Applied dose: (load): 2.44x10⁻² mg/cm²</p> <p>Contact time (duration of application): 12 h</p> <p>Recovery phase (time from dose removal to end of experiment): 12 h</p> <p>Total mass balance (applied-collected): unknown</p> <p>Mass balance reported?: No</p> <p>Standard test guideline-compliant methods: No</p> <p>Sample Media: urine, blood, calf whole body measurement via gamma counter</p> <p>Frequency of collection: urine- 24 h collection; blood- 1, 2, 4, 8, 12, 24 h; whole body measurement- 12, 24 h</p> <p>Lower limit of detection or quantitation for each sample tested: Sensitivity for whole body measurement and urine- 37 Bq (based on dose of 0.74 mBq); blood Pb measurements- 0.1 µmol/l</p>	<p>K_p: 4x10⁻⁶ cm/h— 5x10⁻⁷ cm/h (EPA, 1992; Hostýnek, 2003)</p> <p>Diffusion rate: 1x10⁻⁶mg/cm²/h— 8x10⁻⁶ mg/cm²/h</p> <p>F (% bioavailable): n/a</p>
<p>Reference: (Bress and Bidanset, 1991)</p> <p>Model (<i>in vitro/in vivo</i>): <i>in vitro</i></p> <p>Study design: experimental, J diffusion tube</p> <p>Species: guinea pig (skin)</p> <p>N (technical and biological replicates each dose group): 20 (10/group at 37°C, 10/group at 23°C)</p> <p>Concentration of Pb applied: unknown^b</p> <p>Surface area of skin treated: 1.3 cm²</p> <p>Dose of Pb applied: 10 mg</p>	<p>K_p: n/a</p> <p>Diffusion rate: @37°C: 9.6x10⁻⁵ mg/cm²/h @23°C: 1.6x10⁻⁴ mg/cm²/h</p> <p>F (% bioavailable): n/a</p>

<p>Applied dose: (load): 7.7 mg/cm² Contact time (duration of application): 24 hours Infinite or finite dose: infinite Flow type (static or continuous): static Recovery phase (time from dose removal to end of experiment): 0 hours Total mass balance (applied-collected): unknown Mass balance reported?: no Standard test guideline-compliant methods: no Sample Media: saline receptor solution Frequency of collection: Cumulative; end of study Lower limit of detection or quantitation for each sample tested: 1 µg</p>	
<p>Reference: (Pan et al., 2010)</p> <p>Model (<i>in vitro/in vivo</i>): <i>in vitro</i> Study design: experimental, static Franz cell Species: Nude mice (ICR-Foxn1nu strain) (dorsal skin) N (technical and biological replicates each dose group): 12 (4 per group) (Groups- intact skin in double distilled water (n=4), stratum corneum-stripped skin in double distilled water (n=4), or intact skin in synthetic sweat (n=4)) Concentration of Pb applied: 120 mM Pb in 0.5 ml in double distilled water or synthetic sweat (39.03 mg/ml) Surface area of skin treated: 0.785 cm² diameter Applied dose: (load): 24.86 mg/cm² Contact time (duration of application): 10 hours Infinite or finite dose: infinite Flow type (static or continuous): static Recovery phase (time from dose removal to end of experiment): 0 hours Total mass balance (applied-collected): unknown Mass balance reported?: No Standard test guideline-compliant methods: No</p>	<p>K_p: Intact skin (water): 5.9x10⁻⁷ cm/h SC stripped skin (water): 1.0x10⁻⁶ cm/h Intact skin (syn sweat): 3.3x10⁻⁷ cm/h</p> <p>Diffusion rate: Intact skin (water): 2.3x10⁻⁵ mg/cm²/h SC stripped skin (water): 4.0x10⁻⁵ mg/cm²/h Intact skin (syn sweat): 1.3x10⁻⁵ mg/cm²/h</p> <p>F (% bioavailable): n/a</p>

Sample Media: pH 7.4 buffer solution (unspecified) Frequency of collection: every 2 hours Lower limit of detection or quantitation for each sample tested: Not reported	
---	--

- Citations added where percutaneous absorption values were identified in the literature.
- The dosing was reported as 10 mg of total Pb. No information was provided on how the Pb was dosed on the skin.
- Franken et al., (2015) and Hostýnek et al., (1993) reported this value as flux.

Table 1-4. Dermal Penetration and Absorption Studies Identified for Lead (Pb) Oxide and Pb Metal

Design	Results ^a
Reference: (Bress and Bidanset, 1991) Compound: Pb oxide Model (<i>in vitro/in vivo</i>): <i>in vitro</i> Study design: experimental, J diffusion tube Species: guinea pig (skin) N (technical and biological replicates each dose group): 20 (10/group at 37°C, 10/group at 23°C) Concentration of Pb applied: unknown ^b Surface area of skin treated: 1.3 m ² Applied dose: (load): 7.7 mg/cm ² Contact time (duration of application): 24 hours Infinite or finite dose: infinite Flow type (static or continuous): static Recovery phase (time from dose removal to end of experiment): 0 hours Total mass balance (applied-collected): unknown Mass balance reported?: no Standard test guideline-compliant methods: no Sample Media: saline receptor solution Frequency of collection: Cumulative; end of study Lower limit of detection or quantitation for each sample tested: 1 µg	K_p: n/a Diffusion rate: <3x10 ⁻⁵ mg/cm ² /h (Hostýnek et al., 1993; Franken et al., 2015) ^c F (% bioavailable): n/a

<p>Reference: (Bress and Bidanset, 1991) Compound: Pb oxide Model (<i>in vitro/in vivo</i>): <i>in vivo</i> Study design: experimental Species: Guinea Pig N: 8 Concentration of Pb applied: Not reported Surface area of skin treated: 2 cm² Applied dose: reported as 300 mg/kg BW (calculated as 343 mg)^d Contact time (duration of application): daily for 7 days Recovery phase (time from dose removal to end of experiment): 0 days Mass balance reported?: No Total mass balance (applied-collected): unknown Standard test guideline-compliant methods: No Sample Media: Blood, brain, liver, kidney Frequency of collection: Cumulative; end of study Lower limit of detection or quantitation for each sample tested: Not reported</p>	<p>K_p: n/a Flux or Diffusion Rate: n/a F (% bioavailable): n/a</p>
<p>Reference: (Sun et al., 2002) Compound: Pb oxide Model (<i>in vitro/in vivo</i>): <i>in vivo</i> Study design: experimental Species: Albino Wistar rats N (technical and biological replicates each dose group): 4 Concentration of Pb applied: unk^b Surface area of skin treated: 12 cm² Applied dose: (load): 8.3 mg/cm² Contact time (duration of application): 12 days Recovery phase (time from dose removal to end of experiment): 0 days Total mass balance (applied-collected): unknown Mass balance reported?: no Standard test guideline-compliant methods: no Sample Media: urine Frequency of collection: every 2 days</p>	<p>K_p: n/a Flux or Diffusion Rate: n/a F (% bioavailable): n/a</p>

<p>Lower limit of detection or quantitation for each sample tested: not reported</p>	
<p>Reference: (Sun et al., 2002) Compound: Pb metal Model (<i>in vitro/in vivo</i>): <i>in vivo</i> Study design: experimental Species: Albino Wistar rats N (technical and biological replicates each dose group): 4 Concentration of Pb applied: unk^b Surface area of skin treated: 12 cm² Applied dose: (load): 8.3 mg/cm² Contact time (duration of application): 12 days Recovery phase (time from dose removal to end of experiment): 0 days Total mass balance (applied-collected): unknown Mass balance reported?: no Standard test guideline-compliant methods: no Sample Media: urine Frequency of collection: every 2 days Lower limit of detection or quantitation for each sample tested: not reported</p>	<p>K_p: n/a Flux or Diffusion Rate: n/a F (% bioavailable): n/a</p>
<p>Reference: (Filon et al., 2006) Compound: Pb oxide Model (<i>in vitro/in vivo</i>): <i>in vitro</i> Study design: experimental, static Franz cell Species: human skin (Full-thickness abdominal skin) N (technical and biological replicates each dose group): 8 Concentration of Pb applied: unknown* Applied dose: (load): 5mg/cm² Surface area of skin treated: 3.14 cm² Contact time (duration of application): 24 hours Infinite or finite dose: infinite Flow type (static or continuous): static Recovery phase (time from dose removal to end of experiment): 24 hours Total mass balance (applied-collected): unknown</p>	<p>K_p: n/a Diffusion Rate: 1.2x10⁻⁷ mg/cm²/h (Julander et al., 2020) F (% bioavailable): n/a</p>

<p>Mass balance reported?: no Standard test guideline-compliant methods: no Sample Media: receptor solution (disodium phosphate-based solution) Frequency of collection: cumulative, end of study Lower limit of detection or quantitation for each sample tested: 0.2 µg/L</p>	
<p>Reference: (Julander et al., 2020)</p> <p>Compound: Pb metal Model (<i>in vitro/in vivo</i>): <i>in vitro</i> Study design: experimental, static Franz cell Species: pig (skin- stillborn piglets) N (technical and biological replicates each dose group): 4 Concentration of Pb applied: 29-132 mg/kg (in metal cutting fluids) Surface area of skin treated: 0.64 cm² Applied dose: (load): 48.4-290 µg/cm² Contact time (duration of application): 2, 4, or 24 hours Infinite or finite dose: infinite Flow type (static or continuous): static Recovery phase (time from dose removal to end of experiment): 0 hours Total mass balance (applied-collected): unknown Mass balance reported?: partial Standard test guideline-compliant methods: OECD 428 (2004b) Sample Media: Phosphate Buffer Saline Frequency of collection: Cumulative; end of study Lower limit of detection or quantitation for each sample tested: <0.06 ppb</p>	<p>K_p: n/a Diffusion Rate: 1.1x10⁻⁷ (24 h)– 7.8x10⁻⁷ (2 h) mg/cm²/h (Julander et al., 2020) F (% bioavailable): n/a</p>

- a. Citations added where percutaneous absorption values were identified in the literature.
- b. The dosing was reported as 10 mg of total Pb. No information was provided on how the Pb was dosed on the skin.
- c. Franken et al., (2015) and Hostýnek et al., (1993) reported this value as flux.
- d. Guinea pig body weight was not reported. Dosage estimates were calculated off the average of standard body weights of male and female guinea pigs (average-875 g) (Clemons and Seeman, 2011).

Table 1-5. Dermal Penetration and Absorption Studies Identified for Lead (Pb) Nitrate

Design	Results
<p>Reference: (Sun et al., 2002)</p> <p>Model (<i>in vitro/in vivo</i>): <i>in vivo</i></p> <p>Study design: experimental</p> <p>Species: Albino Wistar rats</p> <p>N (technical and biological replicates each dose group): 4</p> <p>Dose of Pb applied: 100 mg</p> <p>Surface area of skin treated: 12 cm²</p> <p>Applied dose: (load): 8.3 mg/cm²</p> <p>Contact time (duration of application): 12 days</p> <p>Recovery phase (time from dose removal to end of experiment): 0 days</p> <p>Total mass balance (applied-collected): unknown</p> <p>Mass balance reported?: no</p> <p>Standard test guideline-compliant methods: no</p> <p>Sample Media: urine</p> <p>Frequency of collection: every 2 days</p> <p>Lower limit of detection or quantitation for each sample tested: not reported</p>	<p>K_p: n/a</p> <p>Flux/Diffusion Rate: n/a</p> <p>F (% bioavailable): n/a</p>
<p>Reference: (Pan et al., 2010)</p> <p>Model (<i>in vitro/in vivo</i>): <i>in vivo</i></p> <p>Study design: Experimental</p> <p>Species: Female nude mice (ICR-Foxn1nu strain) (8 wk old)</p> <p>N: 6</p> <p>Concentration of Pb applied: 120 mM solution in 0.6 ml vehicle</p> <p>Surface area of skin treated: 2.25 cm²</p> <p>Applied dose: (load): 53 mg/cm² (over 5 days)</p> <p>Contact time (duration of application): 5 days</p> <p>Recovery phase (time from dose removal to end of experiment): 0 days</p> <p>Mass balance reported?: No</p> <p>Total mass balance (applied-collected): unknown</p> <p>Standard test guideline-compliant methods: No</p>	<p>K_p: n/a</p> <p>Flux/Diffusion Rate: n/a</p> <p>F (% bioavailable): n/a</p> <p>Lag phase: n/a</p>

<p>Sample Media: Skin, liver, kidneys Frequency of collection: Cumulative; end of study Lower limit of detection or quantitation for each sample tested: Not reported</p>	
<p>Reference: (Pan et al., 2010)</p> <p>Model (<i>in vitro/in vivo</i>): <i>in vitro</i></p> <p>Study design: experimental, static Franz cell</p> <p>Species: Nude mice (ICR-Foxn1nu strain) (dorsal skin)</p> <p>N (technical and biological replicates each dose group): 12 (4 per group) (Groups- intact skin in double distilled water (n=4), stratum corneum-stripped skin in double distilled water (n=4), or intact skin in synthetic sweat (n=4))</p> <p>Concentration of Pb applied: 120 mM Pb in 0.5 ml in double distilled water or synthetic sweat (39.74 mg/ml)</p> <p>Surface area of skin treated: 0.785 cm²</p> <p>Applied dose: (load): 24.86 mg/cm²</p> <p>Contact time (duration of application): 10 hours</p> <p>Infinite or finite dose: infinite</p> <p>Flow type (static or continuous): static</p> <p>Recovery phase (time from dose removal to end of experiment): 0 hours</p> <p>Total mass balance (applied-collected): unknown</p> <p>Mass balance reported?: No</p> <p>Standard test guideline-compliant methods: No</p> <p>Sample Media: pH 7.4 buffer solution (unspecified)</p> <p>Frequency of collection: every 2 hours</p> <p>Lower limit of detection or quantitation for each sample tested: Not reported</p>	<p>K_p: Intact skin (water): 5.0x10⁻⁷ cm/h SC stripped skin (water): 1.1x10⁻⁶ cm/h Intact skin (syn sweat): 4.8x10⁻⁷ cm/h</p> <p>Diffusion Rate: Intact skin (water): 2.0x10⁻⁵ mg/cm²/h SC stripped skin (water): 4.3x10⁻⁵ mg/cm²/h Intact skin (syn sweat); 1.9x10⁻⁵ mg/cm²/h</p> <p>F (% bioavailable): n/a</p>

Table 1-6. Dermal Penetration and Absorption Studies Identified for Other Lead (Pb) Compounds (Pb Subacetate, Pb Ortho Arsenate, Pb Sulfate)

Design	Results
<p>Reference: (Kunze and Laug, 1948) Compound: Pb ortho-arsenate Model (<i>in vitro/in vivo</i>): <i>in vivo</i> Study design: experimental Species: rat N (technical and biological replicates each dose group): 6 Concentration of Pb applied: 102 mg of aqueous Pb acetate solution Surface area of skin treated: 29 cm² Applied dose: (load): 3.5 mg/cm² Contact time (duration of application): 24 h Recovery phase (time from dose removal to end of experiment): 0 h Total mass balance (applied-collected): unknown Mass balance reported?: no Standard test guideline-compliant methods: no Sample Media: kidney Frequency of collection: cumulative, end of study Lower limit of detection or quantitation for each sample tested: not reported</p>	<p>K_p: n/a Flux/Diffusion Rate: n/a F (% bioavailable): n/a</p>
<p>Reference: (King et al., 1978) Compound: Pb subacetate Model (<i>in vitro/in vivo</i>): <i>in vivo</i> Study design: experimental Species: human N (technical and biological replicates each dose group): 5 Concentration of Pb applied: 19-21.5% (W/W Pb acetate solution) Surface area of skin treated: 6 cm² Applied dose: (load): unknown Contact time (duration of application): 90 minutes Recovery phase (time from dose removal to end of experiment): 0 minutes Total mass balance (applied-collected): unknown</p>	<p>K_p: n/a Flux/Diffusion Rate: n/a F (% bioavailable) : n/a</p>

<p>Mass balance reported?: no Standard test guideline-compliant methods: no Sample Media: skin Frequency of collection: 2 time periods (20 min, 90 min) Lower limit of detection or quantitation for each sample tested: not reported</p>	
<p>Reference: (Sun et al., 2002) Compound: Pb sulfate Model (<i>in vitro/in vivo</i>): <i>in vivo</i> Study design: experimental Species: Albino Wistar rats N (technical and biological replicates each dose group): 4 Concentration of Pb applied: unk.^a Applied dose: (load): 8.3 mg/cm² Surface area of skin treated: 12 cm² Contact time (duration of application): 12 days Recovery phase (time from dose removal to end of experiment): 0 days Total mass balance (applied-collected): unknown Mass balance reported?: no Standard test guideline-compliant methods: no Sample Media: urine Frequency of collection: every 2 days Lower limit of detection or quantitation for each sample tested: not reported</p>	<p>K_p: n/a Flux/Diffusion Rate: n/a F (% bioavailable): n/a</p>

a. The dosing was reported as 100 mg of total Pb. No information was provided on how the Pb was dosed on the skin.

The vast majority of study summaries (n = 22, 92%) reported detectable levels of dermal absorption of iPb. Only two study summaries (8%) failed to show Pb absorption above the LOD. Both of these studies evaluated dermal absorption of Pb oxide and were conducted in *in vitro* systems using human and guinea pig skin (Bress and Bidanset, 1991). An in-depth review of all 24 study summaries showed most suffer from one or more elements of inadequate experimental design (described in the summaries below) and failed to adequately quantify Pb absorption. Among these 24 study summaries, dermal absorption was reported for all seven iPb species, including both water-soluble and water-insoluble forms.

Only one study was conducted using a standard test guideline-compliant method (Julander et al., 2020). This study dosed four different types of metal cutting fluids on *in vitro* stillborn pig skin using static Franz diffusion cells (Julander et al., 2020). The metal cutting fluids obtained from computer numeric-controlled machines in a brass foundry operation contained up to 20% Pb metal. Pb was detected in washed skin and Franz cell receptor fluid. Based on data collected in this study using both worker exposure and the *in vitro* animal testing data, the authors estimated that skin absorption could contribute 3.3–6.3 µg/dl blood in this exposure scenario (Julander et al., 2020). In another study, percutaneous uptake of radiolabeled Pb acetate was demonstrated in rats in both a single-dose study (~2% uptake of applied dose) and multidose study (~4% uptake of applied dose) (Pounds, 1979).

A summary of dermal penetration and absorption data for several Pb compounds is provided below:

Pb Acetate

Eleven study summaries were identified for the potential of dermal penetration and absorption of Pb acetate, including both *in vitro* skin penetration and *in vivo* assays in multiple animal species and humans (Table 1-3). Percutaneous penetration parameters were calculated or identified in the literature for humans and three animal species (rats, mice, guinea pigs) (Table 1-2). K_p values ranged from 5×10^{-7}

to 3×10^{-5} cm/h among humans and animal species data (Pounds, 1979; Moore et al., 1980; EPA, 1992; Hostýnek, 2003); diffusion rates ranged from 1×10^{-6} to 3×10^{-4} mg/cm²/h (Pounds, 1979; Moore et al., 1980; Bress and Bidanset, 1991; EPA, 1992; Hostýnek et al., 1993; Hostýnek, 2003; Pan et al., 2010; Franken et al., 2015). This included one human *in vivo* study that demonstrated increased urine and estimated whole body Pb levels after dermal dosing using a radioisotopic tracer technique (Moore et al., 1980). An *in vivo* study in rats, using radiolabeled Pb, estimated a percutaneous absorption rate of 2% and 4% in a single- and multidose study, respectively (Pounds, 1979). Two additional *in vitro* penetration studies in human abdominal skin (undefined), and in full-thickness mouse skin and guinea pig skin (undefined) detected Pb acetate in receptor fluid after either 10 or 24 h of exposure (Bress and Bidanset, 1991; Pan et al., 2010).

Other results include *in vivo* studies conducted in two animal species, where authors reported significant ($P \leq 0.05$) increases in delta-aminolevulinic acid dehydratase and tissue doses (kidney, liver, and muscle) of Pb after dermal dosing of Pb acetate (Rastogi and Clausen, 1976; Pan et al., 2010; Fang et al., 2014). Three additional studies also suggested accumulation of Pb in tissues after dermal dosing, though these results were not statistically compared with controls (Kunze and Laug, 1948; Bress and Bidanset, 1991; Pan et al., 2010).

These studies suggest that Pb acetate has the potential to penetrate through the skin and result in measurable absorbed systemic doses. This conclusion is based on data for multiple animal species and dose accumulation data in serum and tissues. However, none of the studies identified were conducted using guideline-compliant methods, which reduces confidence in quantitative percutaneous absorption-related kinetic parameter estimates. The *in vivo* studies were not adequate for PBPK modeling efforts, because they did not provide a fractional analysis of the dose applied, appropriate statistical analyses, or multiple timepoint collections of tissue dose.

Pb Oxide and Pb Metal

Pb Oxide

Four studies of Pb oxide dermal penetration and absorption were identified, including two *in vitro* penetration assays using human skin, and two *in vivo* studies conducted in guinea pigs or rats (Table 1-4). Two percutaneous absorption parameters were identified. Diffusion rate was calculated by Julander et al., (2020) to be 1.21×10^{-7} mg/cm²/h in human skin based on Filon et al., (2006). Flux was also calculated by Hostýnek et al., (1993) to be 1.21×10^{-7} mg/cm²/h in human skin based on Filon et al., (2006). Flux was also calculated by Hostýnek et al., (1993) to be $<3 \times 10^{-5}$ mg/cm²/h in guinea pig skin based on Bress and Bidanset, (1991). Two human *in vitro* skin penetration studies were identified for Pb oxide. The first study used a static Franz cell under infinite dosing conditions using full-thickness skin (Filon et al., 2006). A second study using a J-diffusion tube method did not detect Pb oxide in the receptor solution after a 24-h exposure period. One *in vitro* study dosed Pb oxide on guinea pig skin using a J-diffusion tube design, and also did not detect Pb above the LOD (Bress and Bidanset, 1991).

One study found Pb concentration in urine was statistically significantly increased compared with controls following dermal dosing with Pb oxide in rats over a 12-day study (Sun et al., 2002). Another study, conducted in guinea pigs, evaluated Pb levels in several tissue compartments after a 7-day exposure (Bress and Bidanset, 1991). Though Pb was identified in blood, brain, liver, and kidney, the authors indicated that the Pb levels were similar to those found in control animals, but they did not provide a statistical comparison of Pb-exposed versus control animals (Bress and Bidanset, 1991).

These studies suggest that Pb oxide has the potential to penetrate through the skin and result in measurable absorbed systemic doses. However, none of the studies identified were conducted using guideline-compliant methods, leading to low confidence in quantitative percutaneous absorption-related kinetic parameter estimates. The two *in vivo* studies were not adequate for PBPK

modeling efforts, because they did not provide a fractional analysis of the dose applied, appropriate statistical analyses, or multiple timepoint collections of tissue dose (Bress and Bidanset, 1991; Sun et al., 2002).

Pb Metal

Two studies evaluated dermal exposures of Pb metal (Table 1-4). Percutaneous absorption parameters were available, including a range of diffusion rates from 1.1×10^{-7} to 7.8×10^{-7} mg/cm²/h for stillborn pig skin (Julander et al., 2020) (Table 1-2). This range of values represents studies conducted using four metal cutting fluids in a static Franz diffusion cell under infinite dosing conditions, according to Organisation for Economic Cooperation and Development (OECD) guideline 428 (OECD, 2004a). Exposures were conducted for 2, 4, or 24 h. At the end of the experiments, concentration of Pb in the skin was 2.11–10.9% of the amount dosed, and 0.0001–0.004% in receptor fluid. Another study evaluated dermal absorption in rats (Sun et al., 2002). Dermal dosed Pb metal in rats resulted in statistically significantly increased concentrations of Pb in urine compared with controls by f over a 12-day study (Sun et al., 2002). The study did not provide data that may be useful for PBPK modeling because it did not provide a fractional analysis of the dose of Pb applied or tissue dose in other compartments other than urine (Sun et al., 2002). Percutaneous absorption parameters could not be calculated based on this study (Sun et al., 2002).

These studies suggest that Pb metal has the potential to penetrate through the skin of multiple animal species and accumulate in organ tissues; however, only one of the studies identified was conducted using guideline-compliant methods (Julander et al., 2020). Neither of the studies accounted for the total mass balance of the Pb in the experimental systems. Mass balance is crucial for assessing the overall recovery of the administered dose. The *in vivo* study was not adequate for PBPK modeling efforts,

because it did not provide a fractional analysis of the dose applied, appropriate statistical analyses, or multiple timepoint collections of tissue dose (Sun et al., 2002).

Pb Nitrate

Three studies were identified for the potential of dermal penetration and absorption of Pb nitrate, including both *in vitro* skin penetration and *in vivo* assays in multiple animal species (Table 1-5).

Percutaneous absorption parameters were calculated based on the data in Pan et al., (2010) (Table 1-2).

K_p values ranged from 5×10^{-7} to 1.1×10^{-6} cm/h, and diffusion rates ranged from 1.9×10^{-5} to 4.3×10^{-5} mg/cm²/h. In this study, Pb penetration was evaluated through full-thickness and stratum corneum-stripped mouse skin using a static Franz cell methodology under infinite dosing conditions. Pb was detected in receptor fluid solutions in both full-thickness and stratum corneum-stripped skin (Pan et al., 2010).

Other results include two animal studies evaluating dermal absorption of Pb nitrate in mice and rats over multiple-day exposures. Both studies detected an increase of Pb in different organ systems including skin, liver, and kidney in the mouse study (Pan et al., 2010), and in urine for the rat study (Sun et al., 2002); however, mass balance of the Pb in the experimental system was not documented.

These studies suggest that Pb nitrate has the potential to penetrate through the skin and result in measurable absorbed systemic doses. However, none of the studies identified were conducted using guideline-compliant methods, leading to low confidence in quantitative percutaneous absorption-related kinetic parameter estimates. Two *in vivo* studies were not adequate for PBPK modeling efforts, because they did not provide a fractional analysis of the dose applied, appropriate statistical analyses, or multiple timepoint collections of tissue dose.

Other Pb Compounds (Pb subacetate, Pb orthoarsenate, and Pb sulfate)

Three additional studies were identified for other lead compounds and are summarized below:

Pb Subacetate

One human experimental study was identified in which Pb subacetate was painted onto the forearm of one female volunteer (age 25) and sampled by tape stripping after 20 and 90 min (Table 1-6) (King et al., 1978). At both timepoints, Pb penetrated through four layers of stripped stratum corneum, with an increased concentration of Pb noted in the tape samples collected in the 90-min sample. However, statistical inference testing was not performed to compare concentrations in different skin layers between the two timepoints (20 and 90 min).

Data are inadequate to provide a conclusion regarding percutaneous absorption. The dataset does not have a sufficient number of studies, and the available data were collected using a non-standardized method. The one available study suggests that Pb subacetate may have potential to penetrate into the stratum corneum layers of human skin during a time period of 90 min; however, this study was not conducted using a standard protocol and is not useful for PBPK modeling. Percutaneous absorption parameters could not be calculated based on this study (King et al., 1978).

Pb Orthoarsenate

One study evaluated the dermal penetration of Pb orthoarsenate in rats *in vivo* (Table 1-6) (Kunze and Laug, 1948). Although this study was a controlled study in animals, no statistical analysis was completed to determine whether Pb detected in kidneys after exposures was significantly higher than in control animals. The data are inadequate to provide a conclusion regarding percutaneous absorption. The dataset does not have a sufficient number of studies, and the available data were collected using a non-standardized method. This study did not provide data that may be useful for PBPK modeling (Kunze and

Laug, 1948). Percutaneous absorption parameters could not be calculated based on this study (Kunze and Laug, 1948).

Pb Sulfate

One study was identified that evaluated the dermal penetration of Pb sulfate in rats (Table 1-6) (Sun et al., 2002). Pb concentration in urine was statistically significantly increased compared with controls by dermal dosing over a 12-day period (Sun et al., 2002). The data are inadequate to provide a conclusion regarding percutaneous absorption. The dataset does not have a sufficient number of studies, and these data were collected using a non-standardized method. The available study did not provide data useful for PBPK modeling, because it did not provide a fractional analysis of the dose of Pb applied or tissue dose in other compartments other than urine (Sun et al., 2002).

Discussion

A rapid review methodology was used to evaluate dermal penetration and absorption of iPb compounds. Though rapid reviews are rigorous and transparent, they may provide fewer quality checks compared with systematic reviews due to limited resources (Hempel et al., 2016). Additionally, rapid reviews provide a less rigorous documentation of the a priori search strategy and formulaic documentation of the application of exclusion and evaluation criteria. Lastly, in this rapid review, only one reviewer evaluated all studies identified in the literature search. Because the number of studies on dermal Pb absorption is limited, we do not think these limitations significantly impacted the results of this review. We considered a more formal systematic approach including both quality assessment and evidence integration steps; however, most studies were not guideline-compliant designed and thus, there was no clear value for separating studies based on formal scoring quality and confidence metrics. Rather, an overall evidence integration from the pool of studies, most of which had limited design, was employed.

The studies identified suggest dermal absorption of water-soluble and -insoluble iPb compounds is not only possible, but highly likely. These studies suggest Pb in contact with skin can enter the blood and be distributed more widely in the body. However, the preponderance of studies evaluating route of exposure were not conducted under standard test guideline-compliant methods, and/or did not collect data that were conducive for calculating percutaneous absorption parameters.

Together, K_p and flux define the skin permeability of chemicals (Samhel et al., 2009). K_p is ideally determined under steady-state conditions; however, this is technically challenging to determine for metals because permeation rates are slow (Hostýnek et al., 1993). To be independent of time, flux should be determined under steady-state conditions. If steady state is not achieved, rates of permeation are more simply described as a 'diffusion rate' (Julander et al., 2020). Although flux provides more certainty about the rate of permeation, diffusion rates still provide a rough approximation that could be useful for dermal risk assessment purposes, if better data are not available. Exposure factors including concentration, area of exposure, and time of exposure can be related to absorbed dose using Fick's first law which, when applied to the skin, implicitly assumes that the stratum corneum acts as a homogenous barrier that is independent of time or position (Hostýnek, 2003; Mitragotri et al., 2011).

However, absorption of metals through skin does not always seem to follow 'Fickian' behavior. It has been proposed that protein-metal ion bond in substratum corneum layers of the skin leads to accumulation of metals (i.e., depot effect), which could then act as a reservoir for extended exposure (Hostýnek, 2003; Franken et al., 2015). Data collected by both Julander et al., (2020) and Filon et al., (2006) suggest that a reservoir effect may be occurring with iPb compounds in exposures. This phenomenon has been observed with other metals as well, including chromate ions and mercuric chloride, where increasing dermal doses resulted in lowered permeability coefficients (Friberg et al., 1961; Wahlberg and Skog, 1965; Gammelgaard et al., 1992).

Three mechanisms of dermal chemical absorption have been proposed: transcellular (through cells), intercellular (around cells), and transappendageal (via skin appendages such as hair follicles, sebaceous glands, and sweat glands) (McCarley and Bunge, 2001; Mitragotri et al., 2011). A general mechanism by which metals penetrate into and absorb through skin has been proposed by Hostýnek (2003) and is dependent on several exogenous factors (e.g., dose applied, vehicle, molecular volume, counter ion, etc.) and endogenous factors (e.g., age of skin, anatomical site, homeostatic control, skin layers/shunts). The mechanism(s) that drive(s) iPb absorption is likely related to several of these factors. However, it has been hypothesized that the predominant pathway for diffusion of strong electrolytes (e.g., Pb salts) is through skin appendages such as hair follicles and sweat ducts (Tregear, 1966). The same mechanism, in reverse, is associated with the loss of essential elements in sweat (Cohn and Emmett, 1978). However, other mechanisms may also be important for absorption. Hostýnek et al. (2001) determined that nickel nitrate is the only nickel salt that has been tested, and slowly penetrates through the stratum corneum, suggesting that the relatively higher lipophilicity of this salt may drive transcellular absorption. In a follow-up experiment, it was determined that molecular volume is also playing a substantial role (Hostýnek, 2003).

Despite the lack of data on specific absorption mechanisms, there are absorption parameters of iPb that can inform occupational risk assessment. The K_p and flux in Pb compounds have been previously reviewed, but these evaluations considered fewer studies and have looked at both inorganic and organic forms of Pb (Hostýnek, 2003; Hostýnek and Maibach, 2006; Franken et al., 2015). A summary of calculated and literature-referenced K_p , flux, and diffusion rate values from relevant studies collected in this review is provided in Table 1-2. Most calculated values were available for Pb acetate, with only a few available for Pb nitrate, Pb oxide, and Pb metal. This is not an unexpected finding given Pb acetate's former usage in hair dye, which was once a public health concern given the total number of people potentially exposed (Marzulli et al., 1978; FDA, 2021). The data identified in this paper suggest K_p values

for percutaneous absorption of Pb compounds across both human and animal skin to be in the range of 10^{-5} to 10^{-7} cm/h. The diffusion rates were calculated to be of even broader range from 10^{-4} to 10^{-7} mg/cm²/h, likely reflecting non-steady-state time and model dependencies. K_p estimates for other inorganic metals have also been reviewed and are spread over the same order of magnitudes. K_p and flux values for inorganic copper through human skin are in the range of 10^{-4} to 10^{-6} cm/h (K_p) and 10^{-2} to 10^{-6} mg/cm²/h (flux); chromium compounds range from 10^{-3} to 10^{-6} cm/h (K_p) and 10^{-3} to 10^{-7} mg/cm²/h (flux); and inorganic nickel compounds in the order of 10^{-3} to 10^{-7} cm/h (K_p) and 10^{-5} mg/cm²/h (flux) (Hostýnek et al., 1993; Hostýnek, 2003; Hostýnek and Maibach, 2006; Franken et al., 2015). Flux estimates have been calculated by Hostýnek et al., (1993) and Franken et al., (2015) for some organic Pb compounds including tetrabutyl Pb (2×10^{-2} mg/cm²/h, Pb nuolate (oleate and linoleate) (4.2×10^{-3} mg/cm²/h), and Pb naphthenate (1×10^{-3} to 8×10^{-5} mg/cm²/h) based on the experimental data from Bress and Bidanset, (1991) and Rasetti et al., (1961). A K_p value for Pb naphthenate, based on the data in Rasetti et al., (1961), was estimated to be 2×10^{-3} to 3×10^{-3} cm/h (EPA, 1992; Hostýnek et al., 1993). Overall, the K_p , flux, and diffusion rate values identified and calculated for iPb compounds are within the same order of magnitudes of other inorganic metals and organic Pb compounds.

The wide range of estimated K_p and flux values increases uncertainty in application to risk assessments.

The wide range of K_p values for these different metal compounds likely reflects differences in the exogenous and endogenous factors of both the metal species tested and test systems (e.g., different animal species, total experimental times, and solvents) (Hostýnek et al., 1993; Hostýnek, 2003).

Although it is difficult to rigorously assess absorption kinetics for Pb compounds based on the limited data available, different test species likely contribute to the wide range of absorption metrics reported.

Jung and Maibach, (2015) evaluated dermal absorption and found that rat, rabbit, and guinea pig skin tend to overestimate rates of absorption of chemicals across human skin; whereas, monkey, pig, and hairless guinea pig skin are more predictive of human skin absorption rates. This is attributable to the

phylogenetic similarities (monkeys); similar hair coats, epidermis and dermis structure, follicular structures, stratum corneum protein fractions, and other epidermal/dermal structural similarities (pigs); and similar epidermis structure, stratum corneum thickness, and blood vessel density (hairless guinea pigs) (Jung and Maibach, 2015). Only one Pb compound, Pb acetate, had data available to compare across different animal species and humans in this review (Table 1-2). In this case, human absorption, for both *in vivo* and *in vitro* skin penetration studies suggested greater absorption potential relative to rat, mouse, and guinea pig. This finding is unexpected, since these animal species have lower skin thicknesses and a higher density of hair follicles compared with humans. However, confidence in the magnitude of these differences is relatively low, since these studies were not conducted using standard test guideline-compliant methods. Some investigators have used a subset of these studies to estimate the impact of dermal absorption of Pb on blood Pb levels. Filon et al., (2006) used human skin to estimate percutaneous absorption of Pb oxide and calculated a diffusion rate of $1.21 \times 10^{-7} \mu\text{g}/\text{cm}^2/\text{h}$, which would result in a steady-state increase in blood Pb levels of 2.5 $\mu\text{g}/\text{dl}$ (confidence intervals—0.3, 5.1), if the exposure were to occur on unwashed hands and arms for 250 days/year. Julander et al., (2020) estimated that steady-state blood Pb levels would increase from 3.34 to 6.33 $\mu\text{g}/\text{dl}$ from dermal absorption of Pb through metal cutting fluids based on inhalation, hand-to-mouth, and skin absorption parameters observed in a brass foundry environment using pig skin data. Pounds, (1979) estimated that the total absorbed dose for dermal exposures to Pb acetate occurring 3 times a week for 4 weeks would result in an estimated dose of 7.2 $\mu\text{g}/\text{day}$. The U.S. Food and Drug Administration has currently set an Interim Reference Level for dietary Pb exposure for women of childbearing age and other adults to be 12.5 $\mu\text{g}/\text{day}$, which is estimated to increase blood Pb levels by 0.5 $\mu\text{g}/\text{dl}$ (FDA, 2020; Flannery et al., 2020). In occupational environments where other routes of exposure to Pb may be relevant, these dermal exposure estimates could represent a significant relative source contribution to overall body burden of Pb exposure. Though the methodological issues with these studies may not fully translate to

the occupational environment, nor were two of them conducted according to standard test guideline-compliant methods, the estimated impact on blood Pb levels could be increased by greater than 6 µg/dl, which would represent >100% of blood Pb levels that are associated with adverse health effects in adults, determined by the National Toxicology Program, (2012). Further analysis of these data using PBPK modeling, including the impact of 24-h diffusion rates like Filon et al., (2006) and Julander et al. (2020) compared with multi-dosing studies (Pounds, 1979), may better elucidate whether skin may be serving as a reservoir for exposure, which is an important consideration in the occupational setting.

An alternative way to validate dermal absorption of iPb compounds would be to evaluate high confidence epidemiology data. However, studies where Pb exposure is limited to only skin contact were not identified, since environments where Pb exposure occurs through the dermal route would also likely have exposures through gastrointestinal and inhalation routes. However, several *in vivo* animal pharmacokinetics studies support percutaneous absorption as an important source of systemic Pb exposure (Kunze and Laug, 1948; Rastogi and Clausen, 1976; King et al., 1978; Pounds, 1979; Moore et al., 1980; Bress and Bidanset, 1991; Sun et al., 2002; Pan et al., 2010; Fang et al., 2014). In seven of these studies, the analysis of Pb dermal exposures does not permit the fundamental kinetic rate constants to be determined due to study design limitations. Two studies provided enough information to calculate kinetic values. However, these studies were not concordant with standard test guideline-compliant methods, since they preceded adoption of these methods; and thus, there is uncertainty with the calculated values (Pounds, 1979; Moore et al., 1980). The K_p (10^{-7} to 10^{-5} cm/h) and flux/diffusion rates (10^{-6} to 10^{-4} µg/cm²/h) calculated in these studies were in the same orders of magnitude of the other *in vitro* studies identified in this review (Bress and Bidanset, 1991; Filon et al., 2006; Pan et al., 2010; Julander et al., 2020).

Limitations point to directions for emphasis in future research. These include the absence of statistical analyses of differences between treatment groups, absence of adequate details on controls for oral exposures, and availability of only single timepoint measurements of tissue-dose estimations rather than time course estimates. Furthermore, across all *in vitro* skin penetration studies, mass balance of the applied dose was either not tracked or not provided. Mass balance is an important check of the experimental system to ensure the internal validity of the test system. This includes recovery of the test material from receptor and donor solutions, skin, and skin washes as an integrity check of the experimental system including: conformation of the analytical method, wash collection methods, and skin dissolution and analysis. Emphasis on future research should include conducting studies according to standard test guideline-compliant methods (EPA, 1992, 1998, 2007; OECD, 2004a,b, 2011; EFSA, 2012) and according to recommendations outlined by Franken et al., (2015) and Hostýnek, (2003). Only one study was conducted using a standard test guideline-compliant method (Julander et al., 2020); it is unclear why the other studies identified did not follow standard test guideline-compliant methods. Additionally, future research is needed to better understand the mechanisms of absorption, important exogenous factors that drive absorption, and the potential impact of a reservoir effect to better estimate the impact on blood Pb levels. The results of this review suggest that further efforts to reduce Pb contamination on the skin and Pb removal from skin are needed. Use of soaps and wipes designed for heavy metal removal from skin is important, as handwashing with soap and water does not effectively remove Pb contamination from skin (Filon et al., 2006; Esswein et al., 2011; Guth et al., 2020).

Chapter 2. Dissolution of Inorganic Lead (Pb) Compounds in Synthetic Sweat Related to Dermal Route Risk Assessment

Introduction

Inorganic lead (iPb) continues to be widely used in the U.S. with manufacturing of Pb compounds exceeding 4.53×10^8 kg in 2020 (ATSDR, 2020a). As controls and best practices to reduce inhalation and gastrointestinal exposures to Pb have been implemented, the relative source contribution of dermal exposures has potential to become an important emphasis in the continuing effort to reduce blood lead levels (BLLs) in occupational settings (Julander et al., 2020). Dermal iPb exposures occur in several industries, including waste incineration, automotive repair, battery manufacturing, electricity generation, construction, electronic scrap recycling, and metal refining (NIOSH, 1992, 1996a, 1996b, 1999, 2015; Far et al., 1993; Tharr, 1993; Dykeman et al., 2002; Hughson, 2005; Virji et al., 2009). Dermal loading of iPb on hands in these industries varies widely ranging from 0.005 - $16.1 \mu\text{g}/\text{cm}^2$, with the highest reported exposures in automotive radiator repair shops, battery manufacturing, and lead chemical processing plants (Tharr, 1993; NIOSH 1996a, 1999; Dykeman et al., 2002; Hughson, 2005) (Table 2-1). Virji et al., (2009) collected wipe samples on the hands, faces, necks, and arms of workers and reported geometric mean dermal iPb loading in the construction industry. These values range from 0.01 to $1.23 \mu\text{g}/\text{cm}^2$, with the highest values on hands collected during breaks. Employment projections for these industries (Table 2-2) in the North American Industry Classification System (NAICS) codes, published by the U.S. Bureau of Labor Statistics (BLS, 2021) and the U.S. Census Statistics of U.S. Businesses (SUSB) dataset (USCB, 2018), indicate that there are approximately 1,456,000 U.S. workers with potential for dermal exposure to iPb compounds. In addition, these same workers also have potential airborne and oral aggregate exposures to iPb. Regarding this estimate of potential dermal exposures, since there is a lack of specificity in the less granular estimates in the BLS, this can lead to an overestimation in the number of workers potentially exposed to Pb. To address for this lack of specific,

the U.S. Census Statistics of U.S. Businesses (SUSB) 2018 dataset, which contains lower-level digits in NAICS codes, was used to determine the proportion of the lower-level digit code is for the less granular code identified in using the BLS data (BLS, 2021). The SUSB dataset was not used for overall employment since more recent estimates were obtained from BLS. The sum of each NAICS was calculated to determine the estimate of workers potentially exposed to lead.

Table 2-1. Dermal Loading of Lead Compounds on Hands in Occupational Settings

Industry	Wipe sample result (µg/sample)	Dermal loading* (µg/cm ²)	Lead compound	References
Automotive repair	432–652	0.40- 0.61	Pb solder (likely Pb/Sn alloy)	Tharr, 1993; Dykemann et al., 2002
Battery manufacturing	37–5100	0.03-4.77	Pb oxide	NIOSH, 1996a; NIOSH, 1999
Electricity generation	4.4–35	0.004-0.03	Pb metal (source: fly ash)	NIOSH, 1996b
Refinery	n/a	2.7- 4.6 [†]	Pb red oxide, Pb oxide	Hughson, 2005
Chemical production	n/a	16.1 [†]	Pb red oxide, Pb oxide	Hughson, 2005
Waste incineration	41–480	0.04-0.45	Pb metal and Pb oxide	NIOSH, 1992
Electronic waste recycling	1.5–150	0.001–0.14	Pb metal and Pb oxide	NIOSH, 2015
Construction	Not reported	0.01-1.23 ^{‡,¶}	Pb oxide	Virji et al., 2009

*Surface areas of hands estimated to be 1070 cm² (EPA, 2011).

†Median values based on author’s estimated hand surface areas of 840 cm².

‡Reported as geometric means.

¶Author estimated hand surface area was 970 cm².

Table 2-2. Estimate of Workers Potentially Dermally Exposed to Lead (Pb), 2019 (USCB, 2018; BLS, 2021)

NAICS code*	Industry description	Worker estimate in thousands	Refined NAICS	Refined NAICS & Industry description	Granularity adjustment	Adjusted worker estimate in thousands
221110	Electric power generation	146.6	221112	Fossil fuel electric power generation	0.14	20.524
230000	Construction	7,492.20	237300; 238320	Highway, street, and bridge construction; Painting and wall covering contractors	0.05	374.61
331400	Nonferrous metal (except aluminum) production and processing	62	331410	Nonferrous Metal (except Aluminum)	0.14	8.68
335900	Other electrical equipment and component manufacturing	150.1	335912	Primary Battery Manufacturing	0.05	7.505
423000	Merchant wholesalers, durable goods	3,083.9	423930	Recyclable material merchant wholesalers	0.03	92.517
562200	Waste Treatment and Disposal	101.2	562213	Solid Waste Combustors and Incinerators	0.04	4.048
811110	Automotive Mechanical and Electrical Repair and Maintenance	948.8	NA	NA	NA	948.8
Total		11,984.8				1,456.684

*North American Industry Classification System.

Evidence from *in vitro* skin studies that applied risk assessment estimates suggests that dermal exposures to iPb could increase BLLs by as much as 6.3 µg/dl (Filon et al., 2006, Julander et al., 2020). If correct, this concentration exceeds BLLs identified by the National Toxicology Program (5 µg/dl) associated with increased incidence of adverse effects in humans (NTP, 2012). The fate of metals in contact with skin is a complex process dependent on several factors (Hostýnek, 2003; Franken et al., 2015). Exposure occurs when metals contact the outer layers of the skin, the stratum corneum. Once on

the skin, metals may be physically removed from the skin (e.g., by hand hygiene or brushed off) or remain in contact with the outermost layer of the skin, which is coated with a film of skin surface film liquids (SSFL) composed of sweat and sebum. Metals that remain on the skin can undergo dissolution in SSFL to produce ions. The dermal absorption rate through the stratum corneum to the underlying active epidermis depends on the concentration of these ions dissolved in SSFL (Hillwalker and Anderson, 2014; Stefaniak et al., 2014a; Marin Villegas et al., 2019). Some bioaccessible metal ions can pass through the stratum corneum via passive diffusion and reach the epidermis and viable dermis layers, albeit at rates that are two to three orders of magnitude slower than low molecular weight molecules with lipophilic and nonelectrolyte characteristics (Hostýnek et al., 1993; Hostýnek, 2003). These metal ions likely also pass through skin appendages, like hair follicles and sweat ducts (Hostýnek, 2003). Once absorbed into the underlying layers of the skin, metal ions may be retained in the skin or be available for systemic distribution depending on their disposition within the skin layers (Samhel et al., 2009; Anderson and Meade, 2014). The portion of bioaccessible metal ions that cross the exterior of the upper stratum corneum are referred to as the bioavailable fraction; these metal ions can be deposited throughout the layers of the skin and are potentially available for systemic distribution (EPA, 2007; Van de Sandt et al., 2007; Samhel, 2009; OECD, 2011; Anderson and Meade, 2014).

Sweat is an important dermal modifier of metals bioaccessibility, particularly in occupational environments where, for example, dermal iPb exposures have been reported and high heat loads may be present. Sweat is a aqueous solution, and when iPb powders come into contact, it can result in dissolution and release of Pb ions, which could influence dermal penetration and absorption compared to undissolved powders on the skin (Filon et al., 2006). Pan et al., (2010) reported in an *in vitro* mouse skin study of lead nitrate (PbN) and lead acetate (PbA), dissolved in either a synthetic sweat (containing sodium chloride, urea, and amino acids) or water, that permeation was hindered by the interaction of synthetic sweat and the Pb compounds tested. Stauber et al., (1994) found that both Pb metal and lead

oxide (PbO) had similar dissolution patterns, with the highest dissolution in water alone compared to synthetic sweat and sauna sweat providing further evidence of interactions between sweat components and Pb compounds. Because the mass of a metal (measured in exposure assessments) on the skin may be a poor surrogate for permeation compared with the concentration of metal ions in sweat, understanding the dissolution of compounds in sweat is an important consideration to better estimate the potential for dermal penetration and absorption (Van de Sandt et al., 2007). The rate of iPb dissolution in SSFL describes the potential rate of formation of Pb ions in the sweat film on skin that are available for dermal penetration and absorption. Since dissolution rates of metals are influenced by their interaction with SSFL (Stefaniak et al., 2010a, 2014a), understanding dissolution kinetics is important to inform bioaccessibility as an input for risk assessment. For example, dissolution kinetics data allow for better estimation of the concentration of iPb on skin in occupational environments where skin exposures could be occurring for as long as a work shift (~8–12 h) and have varying periods of deposition and removal. Additionally, this information may provide important practical considerations to inform the impacts of risk mitigation strategies in occupation scenarios with dermal iPb exposures (e.g., frequency of handwashing). The dissolution of metal particles in contact with sweat and sebum under skin surface loading conditions results in formation of soluble metal ions that can penetrate across the outer skin layer and into the body. While data are available on the water solubility of iPb compounds, quantitative data on dissolution in sweat are lacking.

Water solubility of compounds is an equilibrium measurement usually determined by OECD Guideline 105 (OECD, 1995), using either a column elution method for compounds with low water solubility (<0.01 g/l), or the flask method for compounds with higher water solubility (>0.01 g/l). In this study, dissolution is the measurement of Pb ion formation in SSFL that does not necessarily reach equilibrium and can be influenced by both physiochemical interactions of the Pb compounds and components in SSFL (Kanapilly et al., 1973). Though water solubility and dissolution may be related for some

compounds, water solubility does not necessarily predict the dissolution behavior of compounds in sweat. For example, some beryllium compounds that are considered to have poor water solubility will readily undergo dissolution in artificial sweat (Stefaniak et al., 2011). Sweat is a complex mixture that contains variable amounts of primary electrolytes, ionic constituents, amino acids, and vitamins (Stefaniak and Harvey, 2006). Sebum contains a variety of chemical classes including squalene, wax esters, triglycerides, free fatty acids, cholesterol esters, free cholesterol, and Vitamin E (Stefaniak et al., 2010b). It has been hypothesized that some metals, including Pb, Nickel (Ni), Chromium (Cr), and Copper (Cu), are oxidized by fatty acids on the skin surface allowing for penetration of the derivative salts into the stratum corneum (Hostýnek et al., 1993). Metal ion absorption and the chemical milieu present on the skin surface, including the pH of sweat and presence of numerous chemicals (ions, amino acids, proteins, and vitamins), provides many possibilities for interaction with metals on the skin surface that could influence the metal ion concentration on the skin. Thus, understanding the bioaccessibility of metal compounds in sweat is important as it could influence the potential for metal ion penetration through skin.

Synthetic sweat is intended to simulate human sweat and is often used for *in vitro* studies, as it is more cost-effective and obtainable compared with human sweat. One synthetic sweat formulation consists of 61 different constituents including electrolytes, organic acids, carbohydrates, amino acids, nitrogenous substances, vitamins, and other ionic constituents (Harvey et al., 2010). Additionally, an artificial sebum has been developed that approximates the types and concentrations of lipids found in human sebum (Stefaniak et al., 2010b). Although simpler sweat models exist that contain just a few key constituents that are sufficient to estimate metal ion release (Midander et al., 2016), more complex formulations might be more reflective of natural human sweat (Harvey et al., 2010; Callewaert et al., 2014). These more complex sweat formulations are intended to provide more realistic milieu to estimate *in vitro* bioaccessibility (Midander et al., 2016). The combination of synthetic sweat and sebum formulations

(SSFL) together have been used to evaluate dissolution of metals including beryllium, silver nanoparticles, cobalt, nickel, and chromium (Stefaniak et al., 2010a, 2011, 2014a, 2014b; Duling et al., 2012). In addition to its composition, the pH of synthetic sweat is an important consideration when evaluating dissolution, because some metals may dissolve more rapidly or to a greater extent under acidic conditions compared with alkaline conditions and vice versa (Stefaniak and Harvey, 2006). Dissolution of Pb on the skin surface is important, because it enables estimation of dermal bioaccessibility. Knowledge of bioaccessibility obtained from dissolution experiments can be used to calculate ion concentration in sweat, which is needed for modeling bioavailability via dermal absorption. For metals, estimation of dermal bioavailability requires quantification of the concentration of dissolved ions in sweat, and the permeation rate of chemicals through the skin (Stefaniak et al., 2014a, 2014b; Marin Villegas et al., 2019). Skin permeation can be expressed in terms of K_p and dermal flux. K_p represents the rate at which a chemical penetrates through the skin (cm/h) (EPA, 1992). Dermal flux is defined as the amount of chemical absorbed across a defined surface area per unit time ($\text{mg}/\text{cm}^2/\text{h}$) at steady state (EPA, 1992), or as a diffusion rate under non-steady state conditions. Most permeation values in the literature for iPb are not determined or are specified to be at steady state. Niemeier et al., (2021) summarized the diffusion rate of iPb ions, including PbA and PbN across the skin and found these Pb compounds to have diffusion rates 1- to 3-orders of magnitude greater (range- 10^{-6} – 10^{-4} $\text{mg}/\text{cm}^2/\text{h}$) than those found for Pb metal and PbO (1×10^{-7} $\text{mg}/\text{cm}^2/\text{h}$). K_p values were only available for PbA and PbN and ranged from 10^{-7} – 10^{-5} (Niemeier et al., 2021). The lower diffusion rate permeability predicted for iPb metals may be related to a lower water solubility (i.e., the available concentration of iPb ions on the skin). Hence, given the water solubility of metal Pb compounds, we hypothesize that dissolution of water soluble iPb compounds PbA (water solubility 625 g/l @25°C) and PbN (water solubility 597 g/L @25°C) will be higher than poorly water soluble iPb compounds PbO (water solubility 0.017 g/L @ 20°C) and lead red oxide (PbRO) (water solubility- insoluble) (Pubchem, 2022a,b,f,i) in SSFL. Since both PbN

and PbA have diffusion rate values that are roughly equivalent (within one order of magnitude), it is further hypothesized that these observed diffusion rate values reflect the available concentration of iPb ions available on the skin for dermal penetration. Therefore, the dissolution rates of these compounds should be similar, and much greater than the solubilities of PbO and PbRO in SSFL.

Sweat pH is important, because Pb salts dissociate in aqueous solutions to form anionic conjugate bases. PbN releases Pb^{2+} and NO_3^- in solution, with the nitrate anion forming a strong acid (HNO_3) in the presence of H^+ cations ($\text{pK}_a < 1$) and would be fully dissociated at both pHs tested (5.3 and 6.5). PbA dissociates to Pb^{2+} and CH_3COO^- , with the acetate anion forming a weak acid (acetic acid) in the presence of H^+ cations ($\text{pK}_a 4.7$). For PbA, both pH values are greater than the pK_a ; however, since PbA is a weak acid, it is expected that approximately 80% of the compound should be dissociated at pH 5.3 and 98% dissociated at pH 6.5. In accordance with Le Chatelier's principle, the reaction equilibrium shifts towards the products (increased Pb^{2+} ions available) in lower pH conditions with the formation of CH_3COOH . Consistent with this principle, we hypothesize that since CH_3COOH is a weak acid, pH should have a greater influence on the dissolution of PbA compared to PbN. Since both PbO and PbRO are poorly water soluble and are not subject to Le Chatelier's principle, we hypothesize that there will be minimal influence of pH on the solubilities of these compounds, which will be consistent with the null hypothesis. If correct, PbA and PbN in SSFL will rapidly ionize and quickly reach a slow rate of dissolution. Comparatively, PbO and PbRO are expected to undergo slower dissolution because of the low solubility in water and will have limited reactions with other compounds present in SSFL. We evaluated these relationships as the dissolution of four Pb compounds, including PbN, PbA, PbRO, and PbO in National Institute for Occupational Safety and Health (NIOSH) synthetic sweat, using a static dissolution technique (Kanapilly et al., 1973).

Methods

Dissolution Assay

Four laboratory-grade Pb powders were evaluated in this study including lead (II) nitrate (PbN; CAS# 10099-74-8) (Fisher Scientific, Pittsburgh, PA), lead (II) acetate trihydrate (PbA; CAS# 6080-56-4) (Aldrich, St. Louis, MO), lead (II) oxide (PbO; CAS# 1317-36-8) (Acros Organics, Pittsburgh, PA), and lead (II,IV) oxide (PbRO; CAS# 1314-41-6) (containing 2:1 ratio of Pb²⁺ to Pb⁴⁺ ions) (Aldrich, St. Louis, MO). The dissolution of these powders was evaluated in a static dissolution test using a synthetic sweat solution as the solvent, prepared without the addition of Pb (Harvey et al., 2010; Kanapilly et al., 1973; Stefaniak et al., 2005, 2010a). Briefly, a known mass of study powder (approximately 25 mg) was weighed on a sebum-coated, 0.025 µm pore size, 47 mm diameter nitrocellulose filter. Two filters (0.025 µm pore size, 47 mm diameter) were placed on either side of the sebum-coated filter to create a “sandwich” that was loaded and secured in a static dissolution chamber (InTox Products, Moriarity, NM). Chambers were submerged in 80 ml of a synthetic sweat solution in polypropylene plastic cups, and maintained at 36.3°C in an incubator for the entire experiment and were not agitated or stirred. Cups were covered with screw-top lids during the entire experiment, except when changing synthetic sweat. Synthetic sweat solutions were prepared, and pH was adjusted to pH 5.3 or pH 6.5 through the addition of NaOH. The chambers were removed from the incubators at 1, 3, 8, 24, and 72 h, and the synthetic sweat solution was collected and fully replaced with fresh synthetic sweat solution. Sweat solution samples were collected in separate borosilicate jars and frozen until analysis. Sample analysis was performed according to a modified NIOSH method 7302 using yttrium (Y) as an internal standard. Concentrated HNO₃ was added to samples prior to analysis to achieve an acid concentration of 5% v/v in the sample. Inductively coupled plasma-atomic emission spectroscopy (ICP-AES) was performed using a Spectro Arcos EOP (Spectro Ametek, Mahwah, NJ) using spectral line 220.353 nm (limit of quantification= 0.096 µg/ml). The ICP-AES was calibrated according to manufacturer recommendations, and a 3-point

calibration curve including blank and Pb-spiked samples of NIOSH synthetic sweat (1% and 10% Pb concentrations). Concentrated HNO₃ (5% v/v) was also added to calibration samples.

Statistical Analyses

The cumulative fraction of the dissolved Pb mass for each experimental group was determined by: 1) summing the dissolved Pb concentrations determined at each timepoint by ICP-AES; and 2) dividing this total mass by the initial mass of Pb per compound (based on stoichiometry) loaded on the filter using Microsoft Excel (2021).

Values of the average (n = 3 replicates for Pb compound at both pH values) mass of the iPb fraction remaining (M/M₀) (outcome variable) versus time (t) were plotted, and single- or multiple-component negative exponential functions were fitted to the data. Functions were fitted using the proc NLIN non-linear regression models in SAS (version 9.4, SAS Institute Inc., Cary, NC) first with a single component, then with two components.

$$M/M_0 = (\alpha * \exp(\beta_1 * \text{sample time})) \text{ (single component model) [Equation 2-1]}$$

Or

$$M/M_0 = (\alpha * \exp(\beta_1 * \text{sample time})) + ((1-\alpha) * \exp(\beta_2 * \text{sample time})) \text{ (two component model) [Equation 2-2]}$$

Where:

M/M_0 = percent of undissolved metal mass to initial metal mass

α = y intercept

β_1 = slope #1

β_2 = slope #2 (multi-component model)

exp = exponential function

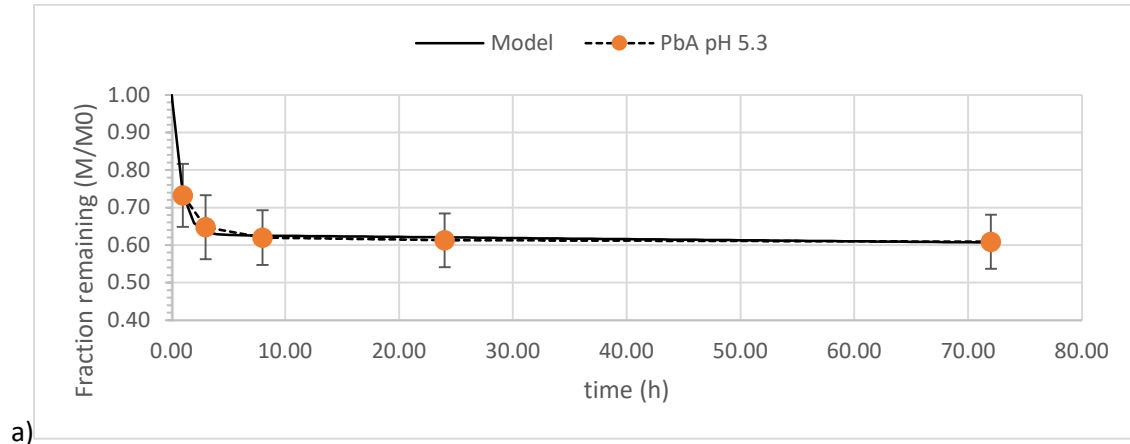
The β estimates and the intercept (α) values that minimized the sum of squared errors (SSE) were obtained using Gauss-Newton iterative methods, until the convergence criteria were met. The number of iterations before convergence was reached varied by Pb compound. The initial estimates for α and β were the slope and intercepts of the average mass fraction of Pb compounds and sample time estimated using Microsoft Excel. Bounds were set to restrict the parameter estimates such that the slopes were negative, and the y intercepts were positive. The optimum number of components for each model was determined by comparing the SSE from the single, $M_{t=0} = (\alpha * \exp(\beta_1 * \text{Sample time}))$, and multi-component models, $M_{t=0} = (\alpha * \exp(\beta_1 * \text{Sample time})) + ((1-\alpha) * \exp(\beta_2 * \text{Sample time}))$, using Analysis of Variance (ANOVA) and the F-ratio test. The model outputs (α and β_1) were used to calculate the percentage of material dissolved ($\alpha \times 100$) and $t_{1/2}$, the dissolution half-time ($-0.693/\beta_1$) for each Pb compound. To assure the model's assumptions were met, residuals versus fitted values were plotted, histograms of residuals were evaluated, and quantile-quantile (Q-Q) plots for comparing probability distributions of residuals were evaluated in SAS 9.4. An analysis of covariance was conducted using the GLM in SAS 9.4 to determine if pH had a significant effect on Pb dissolution within compounds (e.g., PbA at pH 5.3 vs. pH 6.5).

Results

Dissolution Assay

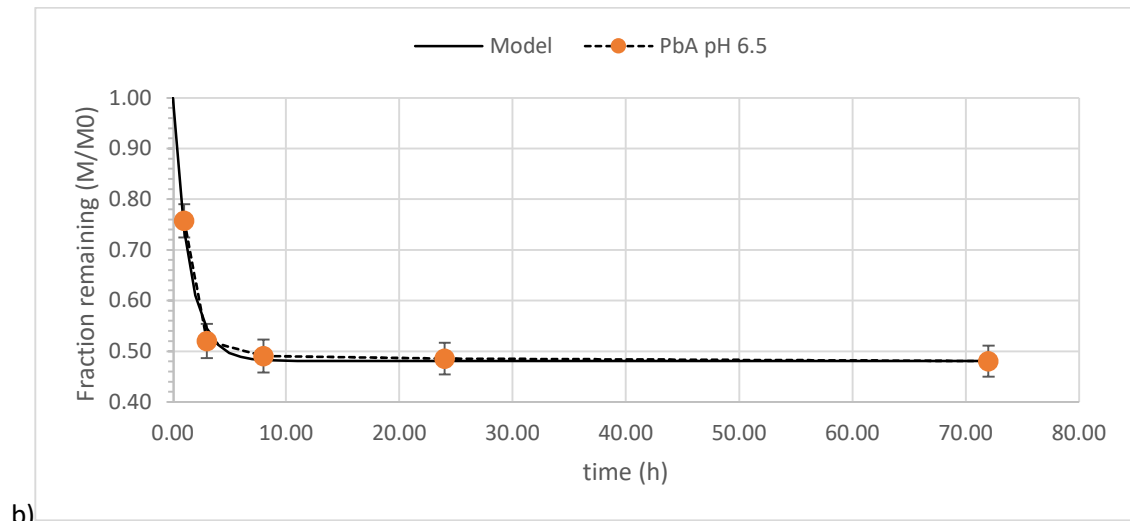
Figures 2-1–2-4 show the dissolution plotted versus time for all tested Pb compounds. These data and model fits are provided at pH 5.3 and 6.5 for PbA (Figure 2-1a and 2-1b), PbN (Figure 2-2a and 2-2b), PbO (Figure 2-3a and 2-3b), and PBRO (Figure 2-4a and 2-4b).

Figure 2-1. Mass Fraction of Lead (Pb) Remaining (\pm SEM*) Versus Time (t) and The Model Fit for PbA in Synthetic Sweat at pH 5.3 (a) and pH 6.5 (b)



a)

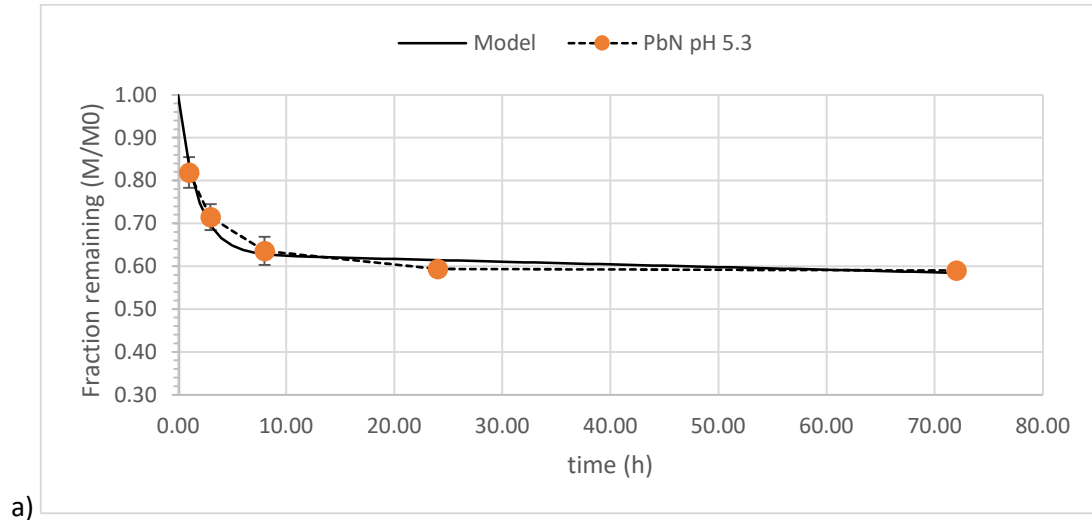
*error bars represent \pm standard error of the mean (SEM).



b)

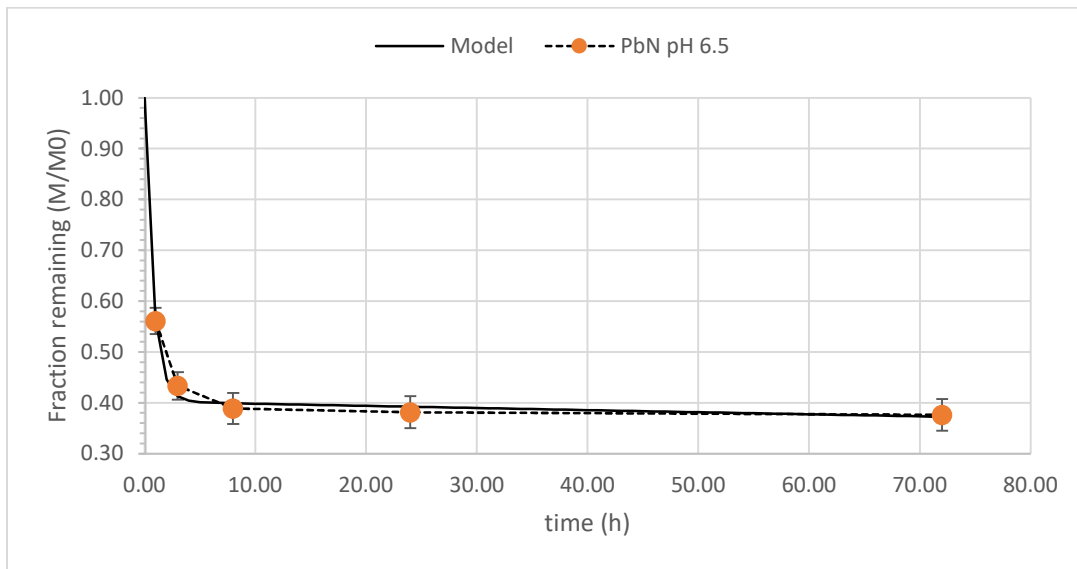
*error bars represent \pm standard error of the mean (SEM).

Figure 2-2. Mass Fraction of Lead (Pb) Remaining (\pm SEM*) Versus Time (t) and the Model Fit for PbN in Synthetic Sweat at pH 5.3 (a) and pH 6.5 (b)



*error bars represent \pm standard error of the mean (SEM).

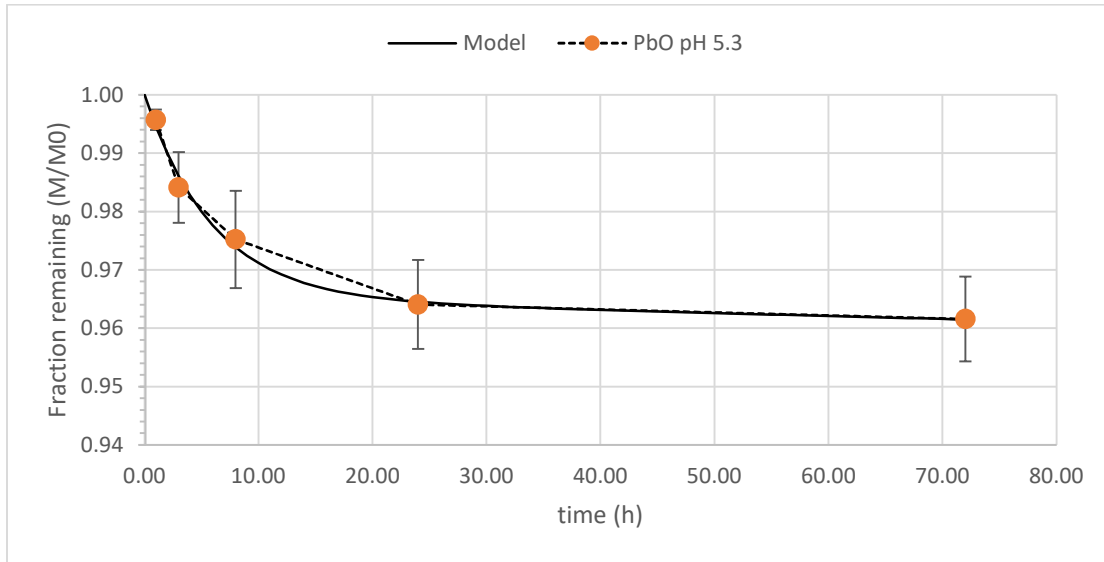
b)



*error bars represent \pm standard error of the mean (SEM).

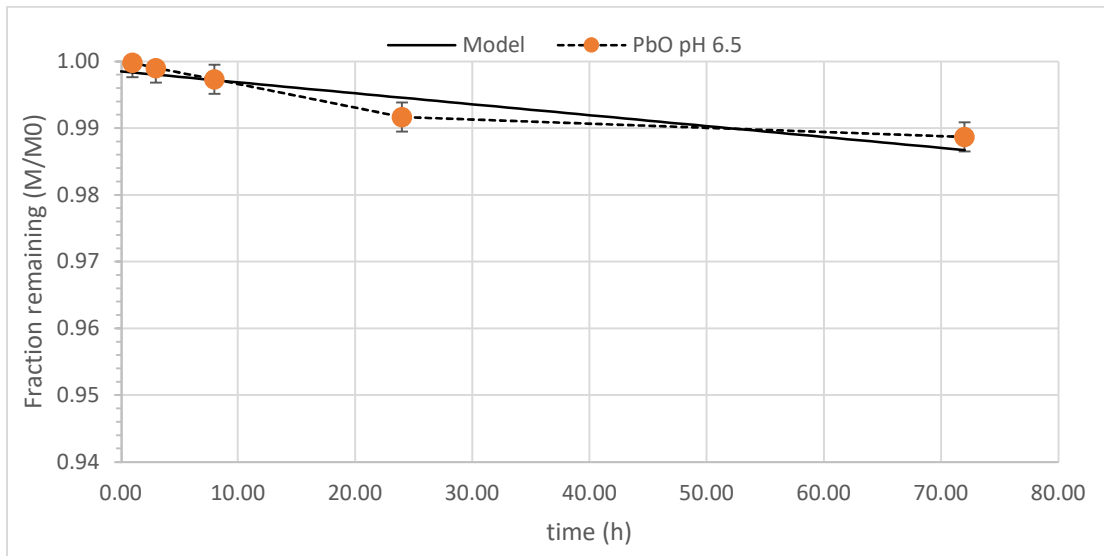
Figure 2-3. Mass Fraction of Lead (Pb) Remaining (\pm SEM*) Versus Time (t) and the Model Fit for PbO in Synthetic Sweat at pH 5.3 (a) and pH 6.5 (b)

a)



*error bars represent \pm standard error of the mean (SEM).

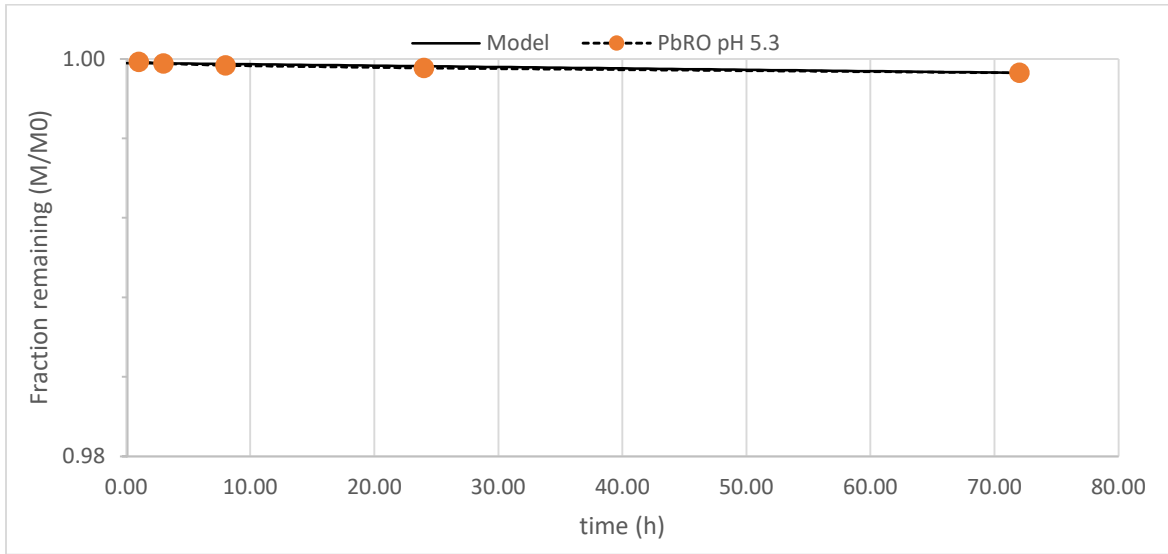
b)



*error bars represent \pm standard error of the mean (SEM).

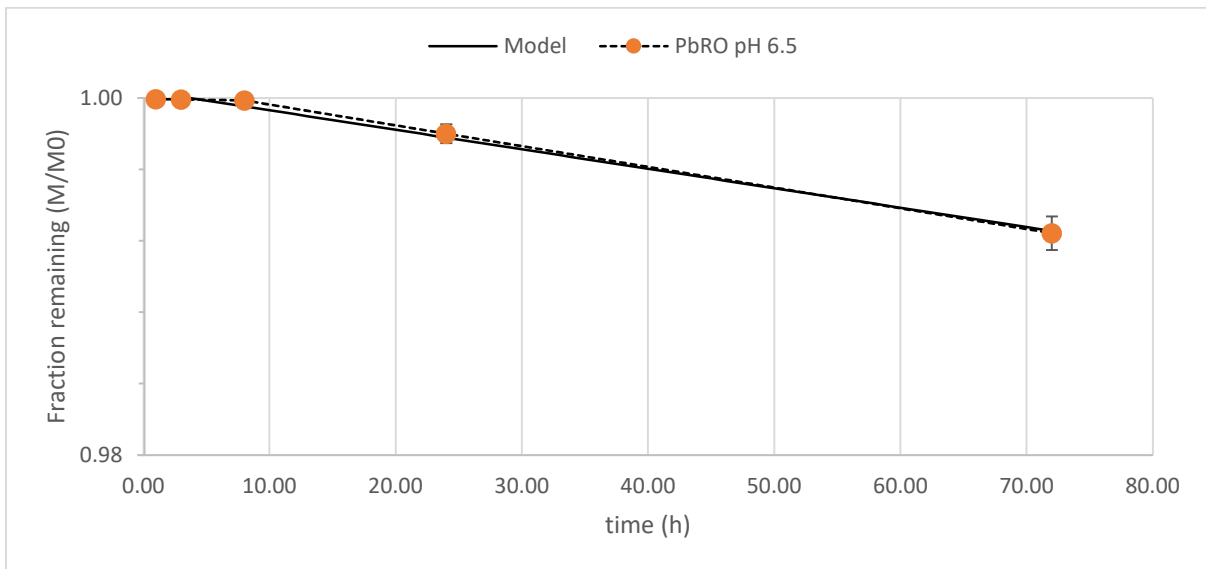
Figure 2-4. Mass Fraction of Lead (Pb) Remaining (\pm SEM*) Versus Time (t) and the Model Fit for PbRO in Synthetic Sweat at pH 5.3 (a) and pH 6.5 (b)

a)



*error bars represent \pm standard error of the mean (SEM).

b)



*error bars represent \pm standard error of the mean (SEM).

The PbA and PbN experimental groups show a similar pattern of dissolution, with rapid dissolution occurring within the first 8 h of the experiment and reaching slower dissolution condition that represents maximum dissolution at approximately 8 h. The best fit models for PbA, PbN are two-compartment models, because these models provide occupationally-relevant measures of dissolution on the initial rapid phase (up to 8 h) (important for occupational environments) and a longer phase dissolution (8–72 h). The visual model fit presented in Figures 2-1 and 2-2 for PbA and PbN, respectively, shows a close approximation to the observed data, with the model fitting within the \pm SEM of the observed data for both compounds.

PbO reaches an approximate slower dissolution between 8–24 h at both pH values (Figure 2-3a and 2-3b). At pH 5.3 (Figure 2a), the dissolution shows similar curvilinear patterns of dissolution as PbA and PbN compounds (Figure 2-1 and 2-2). The best fit model for PbO at pH 5.3 is a two-component model. PbO at pH 6.5 exhibits a more linear dissolution vs. curvilinear and, as expected, the best fit model was a single-component model within the \pm SEM of the observed data, except at the 24h timepoint (Figure 2-2b). PbRO at both pH values does not reach a slower dissolution phase under the test duration, and was best described by a single-component regression model (Figures 2-4a and 2-4b). PbRO at pH 6.5 (Figure 2-4b) also exhibits a pattern of dissolution different from the soluble Pb compounds. At the end of 72 h, this compound appears to continue to slowly release Pb ions into the SSFL; however, it still fits a single component model. Models for PbRO at both pH levels fit the observed data, within \pm SEM, at most of the timepoints.

The calculated initial rapid-phase dissolution $t_{1/2}$ of the iPB compounds with two-component dissolution profiles ranged between 0.54-1.2 h (for PbN and PbA) and 4.2h (for PbO) at pH 5.3. The latter slow-phase dissolution $t_{1/2}$ ranged from 1.3×10^3 – 6.9×10^7 h (for PbN and PbA) and 4×10^4 h (for PbO) at pH 5.3. The single-phase PbRO dissolution $t_{1/2}$ ranged from 7.0×10^3 – 1.1×10^5 h and 4.2×10^3 h for PbO at pH 6.5 (Table 2-3).

Table 2-3. Dissolution Function Parameters for Four Lead (Pb) Compounds

Compound	pH	M ₀ (mg)	ΣM _D (mg)	Total Mass Dissolved at 8 h (%) [*]	Dissolution function parameters (Mean ±SEM)				α	β ₁ β ₂
					Initial Rapid Phase [†]		Latter Long-Term Phase [§]			
					F (%)	t ½ (h)	F (%)	t ½ (h)		
PbO	5.3	24.017±9.40	0.94±0.21	2.5±0.83	60.3±12.9	4.2	39.7±12.9	1.3x10 ⁴	0.035	-0.166 -5.2x10 ⁻⁵
PbN	5.3	15.448±2.54	6.32±0.15	36.4±3.2	88.5±4.8	1.2	11.5±4.8	1.3x10 ³	0.370	-0.567 -1.03x10 ⁻⁴
	6.5	15.608±2.53	9.74±0.59	61.1±3.1	98.0±0.3	0.54	2.0±0.3	1.7x10 ³	0.598	-1.295 1.08x10 ⁻³
PbA	5.3	16.192±9.14	6.35±1.23	38.0±7.3	96.8±1.2	0.56	3.2±1.2	2.8x10 ³	0.373	-1.231 -4.68x10 ⁻⁴
	6.5	15.887±2.17	8.23±0.37	50.9±3.2	98.1±0.4	1.0	1.9±0.4	6.9x10 ⁷	0.521	-0.691 -1.11x10 ⁻⁴
					Single Phase				α	β ₁
					F%	t ½ (h)				
PbO	6.5	22.290±4.61	0.27±0.07	0.29±0.10	100	4.2x10 ³		0.999	1.7x10 ⁻⁴	
PbRO	5.3	24.707±3.46	0.02±0.002	0.03±0.004	100	1.0x10 ⁵		0.999	-7.0x10 ⁻⁶	
	6.5	22.164±5.46	0.17±0.02	0.01±0.01	100	6.3x10 ³		1.000	-1.1x10 ⁻⁵	

M₀= average initial mass of Pb in metal oxide or salt (n=3 replicates); ΣM_D= average sum of the dissolved masses of Pb; F= fraction of total Pb dissolved in each dissolution phase t_{1/2}= dissolution half-time for each dissolution phase; PbO= Lead (II) oxide; PbRO= Lead (II,IV) red oxide; PbN=Lead (II) nitrate; PbA= Lead (II) acetate; Non-linear regression model parameters: α=y intercept; β₁= slope #1; β₂=slope #1 (multicomponent models).

*M₀/ΣM_D *100 at 8 h timepoint (chosen as an occupationally-relevant timepoint).

[†]Initial rapid phase lengths were 0-8 h.

[§]Latter long-term phase lengths: 8-72 h.

The percent total mass of PbN or PbA dissolved ($M_o/\sum M_D$) at 8 h (occupationally-relevant timepoint) across both pH values tested ranged from 36.4–61.1% and 38.0–50.9%, respectively (Table 2-3). The percent total mass of PbO and PbRO dissolved ($M_o/\sum M_D$) at 8 h across both pH values tested ranged from 0.29–2.5% and 0.01–0.03%, respectively (Table 2-3).

The influence of pH on dissolution rate is significant for all four Pb compounds tested based on ANOVA. This includes dissolution of PbN in SSFL at pH 6.5, which is significantly greater cumulative percent dissolution (at 72 h) than at pH 5.3 (40.9% at pH 5.3 vs. 62.4% at pH 6.5) ($p < 0.0001$). A similar finding was observed for PbA at pH 5.3 and pH 6.5 (39.2% at pH 5.3 vs. 51.8% at pH 6.5) ($p < 0.0264$). This is also observed for PbRO (0.08% at pH 5.3 vs. 0.77% at pH 6.5) ($p < 0.0001$). However, for PbO, dissolution in SSFL at a lower pH (5.3) is significantly greater dissolution rate compared to the higher pH (6.5) (3.9% at pH 5.3 vs. 1.2% at pH 6.5) ($p < 0.0001$).

Discussion

To our knowledge, this is the first study to assess the dissolution rate of Pb compounds in SSFL to estimate the potential for Pb ion release and model dermal absorption from bioaccessibility data. Similar studies have previously evaluated dissolution of other metals (Kanapilly et al., 1973; Stefaniak et al., 2005, 2010a, 2011, 2014a, 2014b). The current study demonstrates that PbN and PbA compounds may be more soluble in SSFL over an 8 h period compared to PbO and PbRO compounds with dissolutions ranging from 36.4–61.1% (for PbA and PbN) compared to 0.01–2.5% (for PbO and PbRO). Most of the Pb ions released (88.5–98.1%) by the PbN and PbA compounds occur within the first 8 hours of contact with SSFL. Additionally, dissolution $t_{1/2}$ values ranging from 0.54–1.2 h for PbA and PbN suggests that potential for bioaccessible occupational exposures may be high, even if Pb is removed from the skin during breaks or at the end of a work shift. PbO at pH 5.3, had a dissolution $t_{1/2}$ of 4.2 h, suggesting a potential bioaccessible dose on the skin during a work shift. However, PbO at pH 6.5 and PbRO at both pHs release Pb ions much more slowly over the course of the experiment and may be

more likely to be removed from skin by hygiene practices before becoming bioavailable. However, Pb compounds that come in contact with damaged skin may have much greater penetration and absorption without the need for dissolution in SSFL (Filon et al., 2006).

The percentage range of Pb ions released from these compounds is similar to the dissolution of other metals studied using similar methodologies, including tungsten (W), tungsten carbide (WC), cobalt (Co), beryllium (Be), silver (Ag) nanoparticles, nickel (Ni), and chromium carbide (Cr₃C₂), iron (Fe) and gold (Au) alloy (Hedberg et al., 2010; Stefaniak et al., 2010a, 2011, 2014a,b; Midander et al., 2016). All of these other metals were studied to better understand the mechanism of action for allergic contact dermatitis or sensitization associated with exposure, and the majority of them had total dissolutions of <0.004–4%, which is similar to those observed in the current study for PbO and PbRO (Stefaniak and Harvey, 2006; Stefaniak et al., 2014a,b). One notable exception was with poorly water soluble Be compounds for which dissolution is as high as 40% in SSFL in 8 h, and with faster rates of dissolution at lower pH (5.3) compared to higher pH (6.5) (Stefaniak et al., 2011). This dissolution is much higher than what was observed for PbO and PbRO in this experiment. It should be noted that the studies evaluating other metals (Hedberg et al., 2010; Stefaniak et al., 2010a, 2011, 2014a,b; Midander et al., 2016) were conducted using similar methods to measure metal ion release; however, direct comparisons of results are difficult because of other chemical factors that could influence dissolution, such as differences in the specific surface areas of the particles, which can contribute to dissolution.

Measurements of the pH of human sweat have ranged from 2.1–8.2, with a median value of 5.3 (Stefaniak and Harvey, 2006). An approximate range of healthy human sweat is from pH 5-6 (Stefaniak and Harvey, 2006). The pH of sweat impacts the dissolution of all four iPb compounds evaluated in our experiment. PbA and PbN have significantly higher dissolution rates at pH 6.5 compared to pH 5.3, which is an unexpected finding. The effect of pH is also statistically significant for both PbRO and PbO, although concentrations of Pb ions in sweat are much lower compared to the PbN and PbA compounds.

In this case, our null hypothesis was rejected that pH would not influence the solubilities of PbRO and PbO. Similar influence of sweat pH on dissolution of other metals are reported for beryllium and nickel (Hemingway and Molokhia, 1987; Lidén and Carter, 2001; Stefaniak et al., 2011); however, this influence was not evident for cobalt or tungsten (Stefaniak et al., 2010a).

There are a few potential explanations for the observations in the current study. Le Chatelier's principle did not seem to account for the difference in dissolution for PbA. However, the common ion effect, where the presence of common ions in solution drives the equilibrium towards the reactants, may contribute to the lower dissolution of PbA at lower pH, due to the presence of $\text{-CH}_3\text{OOH}$ anions available from the acetic acid that are present as part of the synthetic sweat solution. However, the dissolution of all four Pb compounds tested is likely also influenced by other biochemical interactions. Inorganic Pb compounds, including PbN, PbA, and Pb chloride, have been reported to interact with proteins in both *in vitro* and *in vivo* test systems (Thier et al., 2003; Pan et al., 2010). Other studies have found that heavy metals (Cu^{2+} , Cd^{2+} , Ni^{2+} , and Zn^{2+}) interact with amino acids such as cysteine and histidine to form metal chelate complexes (Leberman and Rabin, 1959; Demin et al., 2021). These amino acids are present in the SSFL used in the current study and may have promoted a reaction of Pb ions and amino acids, driving the equilibrium towards the products. At neutral to alkaline pH conditions, heavy metals form complexes with amino acids, peptides, and proteins (Demin et al., 2021). We speculate that numerous amino acids, nitrogenous substances, and vitamins in the SSFL contain carbon-carbon bonds that may be reactive to Pb compounds, though this appears to be largely unstudied. Ascorbic acid, a component of both human sweat and the SSFL used in this experiment, has long been known to chelate Pb *in vivo* (Holmes et al., 1939; Marchmont-Robinson, 1941; Goyer and Cherian, 1979; Simon and Hudes, 1999). Holmes et al., (1939) investigated whether a precipitate was formed when mixing Pb acetate and ascorbic acid *in vitro*, but did not detect a visible precipitate; however, the description of experimental

methods lacks important details. Further studies to better understand the potential reactions with Pb compounds and SSFL constituents are needed.

Findings from drinking water chemistry studies may also support some of the observation in the current study. Santucci and Scully, (2020) list several chemical species that affect Pb corrosion and pH in water systems that are also found in SSFL, including calcium (Ca), carbonate (CO_3^{2-}), chloride (Cl^-), magnesium (Mg^{2+}), phosphate (PO_4^{3-}), and sulfate (SO_4^{2-}). In drinking water, several water chemistry factors influence the release of poorly water soluble Pb compounds from water pipes, including pH, temperature, concentration of chlorine residual, and dissolved oxygen content, among others (Kim et al., 2011). Our findings for PbO are supported by research in water systems chemistry that show decreases in pH in water systems from 8 to 7 promotes a significant release of Pb in service lines (Kim et al., 2011). The influence of pH explains the results observed for PbO, which show higher Pb concentration in the lower pH SSFL. Similar results are observed in PbO-contaminated soil studies (Hardison et al., 2007; Cao et al., 2008). However, hydroxyl ion availability does not explain the results observed for PbRO. Higher cumulative dissolutions are observed for PbRO at higher pH levels, while the opposite is true for PbO. The PbRO powder tested in this experiment contained a 2:1 ratio of Pb^{2+} to Pb^{4+} ions, so it is possible that these observations are driven by the Pb^{4+} ions in the mixture. Pb^{4+} compounds are strong electrophiles used in oxidative catalysts for cleavage reaction of 1,2-diols and other carbon-carbon bonds, which results in the formation of Pb^{2+} species (Marken et al., 1997, 1998; Aplin et al., 2002; Buston et al., 2002; Dryer and Korshin, 2007) or the reduction of Pb^{4+} to Pb^{2+} by iodide (present in synthetic sweat formulation), as observed in water systems chemistry (Lin et al., 2008).

The influence of particle size on Pb dissolution is not well understood and is not explicitly evaluated in our study. Particle size has been suggested to be a predictor for metal ion release; smaller particles have increased potential for higher ion exposure on skin due to the increased surface area of the metal (Nowack et al., 2011). To our knowledge, there are no studies that have measured the particle size of

iPb loaded on skin in occupational environments from either direct contact or deposition from the air. However, the size of iPb particulate in air has been previously investigated in some workplace settings, which should provide some indication of the particle sizes of dermally exposed Pb in these environments. Park and Paik, (2002) investigated the airborne particle size range of Pb in secondary smelting, radiator manufacturing, and battery and lead powder manufacturing plants. The average mass median aerodynamic diameters (MMAD) of Pb particles in these workplaces ranges from 1.3–15.1 μm . Samples collected in radiator manufacturing and secondary smelting are highly variable, but Pb particle with an aerodynamic diameter of $<1 \mu\text{m}$ average 41.3% and 24.5%, respectively, of the total samples collected (Park and Paik, 2002). Others have found similar particle size ranges in battery manufacturing plants (MMAD 13.2–32 μm) (Hodgkins et al., 1991; Petito Boyce et al., 2017), and secondary smelters (MMAD 15–25 μm) (Petito Boyce et al., 2017). Liu et al., (1996) found a large range of Pb particle sizes in a battery manufacturing plant, with the majority of particles ($\sim 70\%$) $>10 \mu\text{m}$ in size. The same authors reported a much wider variety of Pb particles sizes in a brass foundry, with as much as 46.7 and 56.8% of Pb particles $<3 \mu\text{m}$ in size, in pouring and furnace operations, respectively. A total of 80% of Pb particles were $>10 \mu\text{m}$ in cutting and grinding operations in the brass foundry (Liu et al., 1996). Aurell et al., (2019) determined that Pb particle sizes generated during small arms weapons firing resulted in 15.8%–82% of Pb particles generated sized $<2.5 \mu\text{m}$. Testing the dissolution of Pb powders collected from industrial settings will further the understanding of the particle size and dissolution characteristics of these production materials.

There are a few limitations of the experimental design. First, we chose to replace the entire volume of SSFL (80 ml) at each timepoint in the experiment (1, 3, 8, 24, 72 h), rather than sampling a small aliquot of SSFL solution, which follows a previously published method (Kanapilly et al., 1973; Stefaniak et al., 2005, 2010a). The impact of the specific volume of SSFL used in this experiment on Pb dissolution was not explicitly evaluated. It is unknown if, at each timepoint, the Pb fraction dissolved in solution

reached a concentration close to the maximum solubility limit saturation concentration of the Pb compounds in solution based on the volume of SSFL used. This influence of the sampling volume could influence the dissolution of iPb compounds used in this study, where less sample volume may lead to a quicker saturation of Pb ion in SSFL. Additionally, the metal mass to SSFL volume ratio may be different in this test system vs. on actual skin. SSFL contains several compounds (discussed above) that likely react with the iPb compounds in this experiment to create less soluble Pb compounds. The dissolution of these compounds and Pb ion availability may differ on skin compared to this test system, depending on the concentration of SSFL and mass of iPb compounds on the skin. Other methodological limitations may also add uncertainty to the dissolution values observed. This study used a static dissolution chamber with two 0.025 μm pore size, 47 mm diameter filters with the iPb metals loaded on a third filter sandwiched in between these filters. In this setup, the dissolving solution (SSFL) needs to diffuse through the filter pores, which adds a mass transfer resistance on the system that could slow the dissolution kinetics. Additionally, there is also a lag time when the filter in the dissolution chamber containing Pb compounds may be surrounded by air during initial submersion in the SSFL, and during each SSFL change. If present, this air pocket could result in a further slowing of the dissolution rate that was measured in the experimental setup compared with *in vivo* conditions, that would likely only have a small impact and influence the initial time points when the static dissolution chambers were initially submerged into the SSFL. Additionally, the influence of particle size on dissolution was not evaluated in this study and could vary across the iPb compounds tested. Finally, the iPb compounds tested in this study were loaded into filters based on total mass (including weight of salt or oxide) instead of Pb mass only. Because of this experimental design, it is difficult to compare dissolution across the different iPb particles tested. However, even with these limitations, the values provided in this paper provide screening level estimates of the concentration of Pb ion that may dissolve on skin in the presence of

sweat. This area of research deserves further study and refinement to better understand the dissolution of Pb compounds on skin.

Chapter 3. Lead (Pb) Nitrate Percutaneous Absorption Pilot Studies Using a Franz Cell Assay

Introduction

Lead (Pb) nitrate (PbN) has an estimated U.S. production rate of 42,500 lbs/year (ATSDR, 2020a). It has several uses in occupational environments including uses in the dyeing, photography, and printing industries as a mordant, oxidizer, and photographic sensitizer. It is used in ore processing for titanium, electrolytic refining of elemental Pb, and in the recovery of precious metals from soils. Pb nitrate is also used in the manufacturing of plastics (rayon delustering, heat stabilization of nylon, and polyester catalyst) and in the production of matches, pyrotechnics, explosives, electroluminescents, and for electrodepositing Pb dioxide on nickel anodes (ATSDR, 2020a; Pubchem, 2022a) (Table 1-1). Though there are numerous occupational uses for PbN, workplace dermal exposures have not been well characterized or understood.

Only a few studies published to date have the potential to provide data necessary to understand the potential for percutaneous absorption of PbN (Pan et al., 2010; Sun et al., 2002). Percutaneous absorption parameters including diffusion rates ranging from 1.9×10^{-5} – 4.3×10^{-5} mg/cm²/h, and K_p values ranging from 5.0×10^{-7} – 1.1×10^{-6} , were calculated from the Pan et al., (2010) mouse skin *in vitro* experiments (Table 1-5). Percutaneous absorption rates could not be calculated from the Sun et al., (2002) or Pan et al., (2010) *in-vivo* studies; however, these studies demonstrated accumulation of Pb in liver, kidneys, or urine, further suggesting percutaneous absorption of PbN. A third study (Stauber et al., 1994), which was not summarized in Chapter 1, because it did not meet the inclusion and exclusion criteria outlined in the rapid review, also suggests an absorption rate as high as 29% of PbN dosed on an occluded patch. However, the Stauber et al., (1994) study is difficult to interpret, since data were only collected on one test subject. Both the Pan et al., (2010) and Sun et al., (2002) studies have several limitations noted in Chapter 1 and by Niemeier et al., (2021). None of these studies were conducted using guideline-compliant methods, leading to low confidence in quantitative percutaneous absorption-

related kinetic parameter estimates (Pan et al., 2010; Sun et al., 2002; Stauber et al., (1994). Two *in vivo* studies (Sun et al., 2002; Stauber et al., 1994) were not adequate for PBPK modeling efforts, because they did not provide a fractional analysis of the dose applied, appropriate statistical analyses, or multiple timepoint collections of tissue dose. Further evaluation of the potential for percutaneous absorption of PbN through human skin is warranted.

The objective of this investigation was to better understand the potential for PbN to penetrate through human skin under occupationally relevant conditions using both de-ionized (DI) water and a synthetic sweat solution (SSFL) to better understand the impact of sweat on percutaneous absorption using a static Franz cell assay (Franz, 1975). Static Franz cells are commonly used to measure *in-vitro* percutaneous absorption across samples of skin or other membranes. These cells are precisely calibrated for diffusion area and volumes, maintain constant temperatures, and are easy to sample and replenish receptor solutions (Hahn, 2011).

This investigation consists of a series of 4 pilot studies to work out methodological issues with Franz cell studies, including use of buffered receptor solution, dosing solutions, and skin dissolution techniques, with the intent to work towards the design of an OECD, (2004a) guideline-compliant study to estimate the percutaneous absorption of PbN through human skin. Both an infinite dosing study (Study 1) and finite dosing studies (Studies 2-4) were completed. Infinite dosing studies are defined as, “*the amount of the test preparation applied to the skin where the maximum absorption rate is achieved and maintained*” (OECD, 2004b). Finite dosing studies are defined as the, “*amount of test preparation applied to the skin where a maximum absorption rate of the test substance may be achieved for a certain time interval but is not maintained*” (OECD, 2004b).

Unfortunately, further studies were delayed due to a lack of funding to purchase human skin. Once the skin was purchased in January 2020, the laboratories used to conduct these studies at the University of

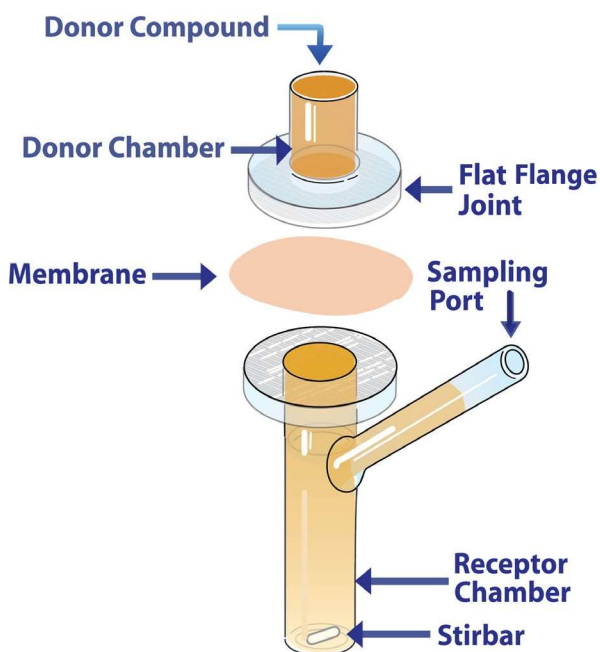
Cincinnati and NIOSH were shut down shortly afterwards due to the COVID-19 pandemic, and further studies were unable to be completed.

Methods

Franz Cell Setup

The Franz cell assay is a commonly used static diffusion assay that measures diffusion of chemicals across human cadaver skin and consists of a donor and receptor compartment (Franz, 1975; OECD 2004b; Ng et al., 2010; Hahn, 2011). This study used unjacketed Franz cells (diameter 0.79 cm²) (Figure 3-1). Receptor compartments were filled with phosphate buffer saline (PBS), and stir bars were added. Human cadaver skin was mounted on top of the receptor compartment, and the donor compartment was secured with a clip. Franz cells were placed in heater blocks at 37°C, to maintain the skin surface at 32°C.

Figure 3-1. Diagram of Unjacketed Franz Diffusion Cell (adapted from Permagear, 2022)



Skin Samples

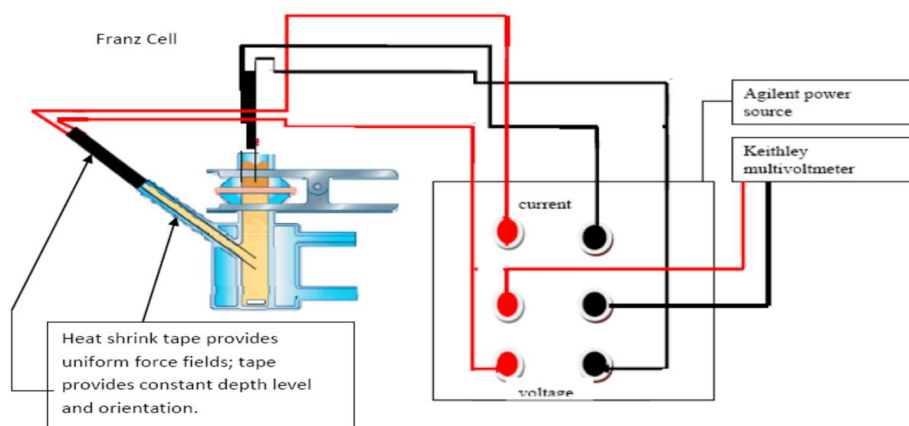
Human cadaver abdominal split-thickness skin, donated by the New York Fire Fighters Skin Bank (New York, NY) was cryopreserved upon collection (less than 24 hours postmortem) and stored at -80°C until time of use. On the morning prior to the study, skin was removed from the freezer and thawed rapidly at room temperature in Millipore water. Skin was cut to roughly $2\text{ cm} \times 2\text{ cm}$ pieces and mounted in Franz diffusion cells with the stratum corneum facing up. Clips secured the skin in the diffusion cells.

Electrical Resistance Testing (Skin Pre-screening)

Electrical resistance testing was conducted on the day prior to the beginning of the dosing. After mounting skin on Franz cells, receptor and donor chambers were filled with 1x Dulbecco's PBS (Sigma Aldrich, 2021) (St. Louis, MO, Cat. 070M8306) with 0.02% (w:v) sodium azide (Fisher Scientific (Pittsburgh, PA, Cat. S227I, LOT # 154398A)). Franz cells were allowed to equilibrate for 1-2 h in heated aluminum blocks at 37°C . Electrodes were placed in donor and receptor chambers to measure the millivolt (mV) drop through the skin (Figure 3-1). The skin samples with the highest specific resistivity were selected (cutoff $<5\text{k}\Omega/\text{cm}^2$).

After screening, the PBS buffer in the receptor chambers was replaced with fresh PBS buffer and stirbar and was allowed to rest until the following day in the heater block at 37°C . Skin samples were randomly assigned in a block randomization schedule by resistivity into 5 blocks.

Figure 3-2. Schematic of Electrical Screening Test to Verify Integrity of Skin Samples Mounted on a Franz Cell



NIOSH SSFL

NIOSH SSFL was donated by A. Stefaniak's laboratory (NIOSH, Morgantown, WV) and prepared according to the protocol outlined by Harvey et al., (2010) at a pH of 5.3. One modification made to the solution is that Pb was not added to the mixture. After preparation, stock SSFL solution was frozen and shipped to the University of Cincinnati where it was stored at -80°C until time of use.

Preparation of Dosing Solutions

Study 1

Two stock solutions were prepared at room temperature. One solution containing 21 mg PbN salt in 43.75 ml SSFL (0.48 mg/ml), which contained 0.30 mg Pb ion/ml. A second was a 50% dilution of the first solution, diluted in DI water and contained 0.15 mg Pb ion/ml.

Note: upon mixing PbN and SSFL for the 0.48 mg/mL stock solution, a precipitate formed in both stock solutions; precipitate remained visible in the 0.24 mg/mL stock. Both stock solutions were vortexed for 30s, and then 1 ml aliquots were transferred to micro centrifuge tubes. These tubes were centrifuged for 1 min, and the supernatant (~ 0.8 ml) was transferred to a new centrifuge tube. These centrifuged-stock solutions were used for dosing of skin in Study 1.

Studies 2–4

A stock solution of PbN in DI water was prepared at a concentration of 25.2 g PbN/L water (0.0158 g Pb ion/ml of water) and mixed with 2% Tween 20 at room temperature. This Pb concentration in water was selected to provide a worst case scenario of Pb ion on skin. The stock solution was vortexed until PbN powder was no longer visible (~1-2 minutes) and no precipitate was observed. Stock solutions were heated to 32°C in a water bath shaker for 15 minutes prior to dosing. Skin was loaded with 20 µl of Pb stock solution (nominal concentration of 316 µg Pb ion) at specific intervals (further described below for each study).

Skin Dissolution

At the end of the studies, skin samples were removed from Franz cells and placed in acid-washed borosilicate glass jars and frozen at -80°C until further processing. The dissolution of skin to determine the concentration of Pb in the skin was initially based on the methodology described by Filon et al., (2006). In this method, skin was dissolved in 5 ml of 70% HNO₃ and agitated for 12 hours. Filon et al., (2006) then centrifuged the samples and analyzed the supernatant. For this experiment, instead of centrifuging the samples, they were filtered using an Acrodisk® 0.45 µm polytetrafluoroethylene (PTFE), 25 mm filter (Waters Corporation, Milford, MA) to remove any remaining undissolved skin particles. Over the course of the different experiments, steps were taken to maximize the amount of skin tissue dissolved. The final methodology included using a modified NIOSH 7303 method, in which skin samples were placed in a 50 ml Falcon tube, dissolved in 5 ml concentrated nitric acid (70%), covered with a watch glass, and heated to 95°C for 15 minutes in an aluminum hot block. Samples were cooled for 5 minutes, then 5 ml of concentrated hydrochloric acid (37%) was added, and the heating protocol was repeated. Samples were then diluted to 5% acid and filtered prior to analysis by ICP-AES at the NIOSH Hamilton Laboratory in Cincinnati, Ohio.

Inductively Coupled Plasma-Atomic Emission Spectroscopy (ICP-AES) and Inductively Coupled Plasma-Mass Spectrometry (ICP-MS)

Sample analysis was performed by a Spectro Arcos EOP inductively coupled plasma-atomic emission spectroscopy (ICP-AES) (Spectro Ametek, Mahwah, NJ) at the NIOSH Hamilton Laboratory in Cincinnati, Ohio. The limit of quantification (LOQ) was 0.096 µg/ml. Samples were analyzed in triplicate and background corrected with known concentrations of Pb in sample media (PBS buffer, water, SSFL). Samples analyzed with ICP-AES included stock Pb dosing solutions, receptor solutions, wash samples, and skin samples. All samples were collected in acid-washed borosilicate jars. Pb dosing solutions, receptor solutions, and wash samples were fixed with concentrated nitric acid (5% v/v final concentration) on the day of collection and stored at room temperature until analysis. A subset of samples was sent to the NIOSH contract laboratory, Maxxam, for inductively coupled plasma-mass spectrometry (ICP-MS) analysis which has a LOQ of 0.0005 ng/ml.

K_p and Diffusion Rate Calculations

In this study, K_p and diffusion rate ranges were calculated based on concentrations of Pb ion found in skin layers from each of the three finite dosing pilot studies conducted using both SSFL and DI water as a wetting agent (Studies 2-4). As a note, K_p and diffusion rate values in Studies 2-3 were calculated based on Pb concentration in full skin samples (epidermis + dermis), whereas Study 4 values were only calculated on epidermis layer Pb concentrations. Calculations were based on formulas provided in Chapter 1.

Statistical Analysis

Wilcoxon rank sum tests

Wilcoxon rank sum tests (Statistics Kingdom, 2021) were used to statistically compare differences of Pb concentrations in skin between experimental groups (SSFL vs. DI water wetted samples) in pilot Studies 2-4. This non-parametric test was chosen since sample sizes were usually small ($n=3-8$ /experimental group) and did not meet assumptions for parametric statistical tests.

Sample size power calculations

Power calculations based on the means and standard deviations observed in pilot Studies 2-3 were estimated to determine the sample size needed to detect a statistical difference between the two treatment groups (SSFL and DI water) for future studies. Assumptions included a two-sided test with an alpha value of 0.05 and power value of 0.8. For these calculations, the mean value of Pb mass detected in skin and the highest standard deviation observed between the two treatment groups was used. An online tool available at <https://www.stat.ubc.ca/~rollin/stats/ssize/n2.html> was used for these calculations.

Specific Study Detail Objectives and Descriptions

Study 1- Infinite dosing study using SSFL as donor solvent

The aim of the first experiment was to develop a pilot protocol for dermal penetration studies with PbN. In this first experiment, PbN was dosed in an infinite dosing study where PbN solutions were prepared in SSFL. This experiment was conducted under an infinite dosing condition using skin from 2 donors. 450 µl of both PbN stock solutions (n=3 replicates for each solution) were pipetted into the donor compartment of the Franz cell at the beginning of the experiment. After loading, the donor compartments were covered with parafilm to reduce evaporation of donor solution. Receptor solution was changed at 2 hours and 8 hours after the beginning of the experiment. At the 2 h receptor solution change, the donor solution was pipetted off the skin, and the receptor solution was collected, and “fresh” solution immediately reapplied. After 8 hours, the donor solution was removed from the skin surface and the surface of the skin was rinsed with 0.5 ml DI water 3 times. After 24 hours, the receptor solutions were collected.

Study 2- Finite dosing study-24 h

The objective of experiment 2 was to evaluate the potential for PbN to penetrate through skin under finite dosing conditions, where the skin was wetted with hourly aliquots of DI water or SSFL. An additional objective of this experiment was to evaluate a wash protocol to determine the amount of Pb

that was washed off the skin at the end of the experiment. This experiment was conducted under a finite dosing condition using skin from two donors. At the start of the experiment, skin was dosed with either 20 μL Pb solution (n=6) or 20 μL DI water (n=4). After one hour, 10 μL SSFL (n=6; 3-lead, 2-controls) or 10 μL DI water (n=6; 3-lead, 2-controls) were dosed to the skin, and reapplied without removal every hour for 8 h (cumulative load- 80 μL SSFL or 80 μL DI water). Receptor solution was replaced at 2 h and 8 h after the beginning of the experiment. After 8 h, the surface of the skin was rinsed four consecutive times with approximately 0.5 ml DI water for each rinse. Each rinse was collected in separate vials for analysis. After 24 h, the receptor solutions and skin samples were collected for analysis.

Study 3- Finite dosing study- 72 h

The objective of experiment 3 was to evaluate the impact of multiple Pb doses applied to the skin over 72 h. This experiment was conducted under a finite dosing condition. 20 μL of PbN solution (n=6 samples) or 20 μL DI water (n=2 samples) was pipetted onto the skin at the beginning of the experiment. After one hour, 10 μL SSFL (n=4; 3-lead, 1-control) or 10 μL DI water (n=4; 3-lead, 1-control) was dosed to the skin and repeated every hour for 8 h. After 8 h, the surface of the skin was rinsed with approximately 0.5 ml Millipore water 4 times by up/down pipetting. After 24 h, the receptor solution was collected and replaced. On the following 2 days, the skin samples were dosed again with 20 μL of Pb solution or 20 μL DI water and hourly aliquots of SSFL or DI water for 8 h and washed at the end of the 8-h period. Receptor fluid samples were collected at 2, 8, 24, 48, and 72 h from the beginning of the experiment. On the morning of the 4th day (~72 h), the skin samples were collected and separated into dermis and epidermis samples. This separation included using a clean tweezer to separate and remove the epidermis layer from the dermis layer for each sample to eliminate the chance of cross contamination between samples.

Study 4- Finite dosing study- 24 h (epidermis only)

The objective of Study 4 was to evaluate the potential for PbN to penetrate through the epidermis layer over 24 h. This experiment was conducted under a finite dosing condition. Prior to the beginning of the experiment, Franz cells were acid washed in a 1% nitric acid solution for 12 h to remove any Pb from previous experiments. To separate and test the epidermis-only layer, the skin was cut into long strips and dipped into 60°C DI water for 30 seconds. Skin was then placed on a glass plate, stretched, and the epidermis layer was removed from the dermis layer. Epidermis layer was cut to approximately 2 cm × 2 cm pieces and mounted on large pore dialysis tubing. Skin/dialysis tubing was then mounted on Franz diffusion cells with the stratum corneum facing up. 20 µL of PbN solution (n=6) or 20 µL DI water (control) (n=2) was pipetted onto the skin at the beginning of the experiment. After one hour, 10 µL SSFL (n=3) or 10 µL DI water (n=3) was dosed to the skin and repeated every hour for 8 hours. Receptor solution was changed after 0.5, 2, 4, 8, and 24 h. Skin was washed 4 times after 8 h to remove Pb from the skin.

Pb recovery studies

The aim of these Pb recovery studies was to evaluate the efficiency of recovering Pb from split-thickness skin samples loaded onto Franz cells. Two studies (Recovery Study 1 and Recovery Study 2) were conducted, with 3 samples collected in each study (N=6). The Franz cells were prepared and handled with the same experimental details described above for Studies 2-4 (e.g., skin screening, receptor fluid, experimental temperature, etc.). Skin was dosed with the same dose, and with the same PbN dosing solution, described for Studies 2 and 4 above (10 µL 0.0158 g Pb ion/ml in DI water (nominal Pb ion mass applied- 316 µg) at the beginning of the experiment. After 8 hours, skin samples were collected and frozen until skin dissolution and Pb analysis was completed. In Recovery Study 1, receptor fluid samples were collected at 2 h and 8 h and analyzed for Pb content. For Recovery Study 2, receptor fluid samples were collected at 0.5 h, 2 h, and 8 h. As a note, the skin in these studies was not wetted with hourly aliquots of SSFL or DI water, and the skin was not washed at the end of the study.

Results

Study 1: Infinite dosing study using SSFL as donor solvent

The aim of Study 1 was to develop a pilot protocol for dermal penetration studies using PbN. Study 1 was conducted under an infinite dosing condition with PbN dissolved in SSFL. The donor solution concentrations, which were taken from the supernatant portion of the mixed PbN/SSFL solution were found to be 12.68 µg Pb ion/ml (nominal concentration- 300 µg Pb ion/ml) and 1.44 µg Pb ion/ml (nominal concentration 150 µg Pb ion/ml (Table 3-1). The skin in each Franz cell was loaded with 450 µl of this solution, resulting in a total of 5.71 µg Pb ion loaded into the Franz cell donor compartment in the high-dose arm, and 0.65 µg Pb ion in the low-dose arm. No Pb was detected in receptor solutions above the LOQ. Pb was detected in washed skin samples in the high-concentration treatments, with an average concentration of 5.98 µg of Pb recovered in wash water, and 0.22 µg recovered in wash water in the low-dose arm (Table 3-1). A total of 8.9% of the Pb dosed on the skin was detected in the washed skin at the end of the experiment. The total recovery of Pb dosed in the system was 113%.

Table 3-1. Study 1 Results - Infinite Dosing of Lead (Pb) Nitrate in a Franz Cell Assay for 24 hours in Split Thickness Human Skin

Pb ion Dose (µg/ml)	Solvent	Replicates	Mass of Pb ion in Skin [µg] (SD)	Mass of Pb ion in wash water [µg] (SD)	Mass of Pb ion in Receptor fluid	Total recovery of Pb Ion (%)
5.71 µg*	SSFL	3	0.51 (0.32)	5.98 (1.47)	<LOQ	113%
0.65 µg**		3	Not analyzed	0.22 (0.23)	<LOQ	Not calculated
Control (DI water)	DI water	3	<LOQ	<LOQ	<LOQ	--

*Calculated dose = 12.68 µg/ml*0.450 ml = 5.71 µg.

**Calculated dose = 1.44 µg/ml*0.450 ml = 0.65 µg.

Study 2: Finite dosing study- 24 h

The second study used a finite dosing protocol where 290.16 µg of Pb ion was dosed on the surface of the skin (Table 3-2). In this study, skin was wetted with hourly aliquots of DI water or SSFL. Additionally, this study evaluated a wash protocol to determine the amount of Pb that was washed off the skin at the end of the experiment.

Washed skin that was dosed with hourly aliquots of SSFL had an average Pb mass of 47.81 µg compared to skin dosed with hourly aliquots of DI water, where the Pb mass was 91.68 µg. The concentration of Pb in the skin dosed with hourly aliquots of SSFL was not statistically different from the skin dosed with hourly aliquots of DI water (p<0.1). Skin dosed with hourly aliquots of SSFL and skin dosed with hourly aliquots of DI water had similar masses of Pb washed off the skin, with 129.05 µg and 114.68 µg washed off in the SSFL and DI water groups, respectively (Table 3-2). Both groups closely followed the same decay pattern of Pb removal from the surface of the skin, including the total concentration of Pb removed during each wash (Figure 3-3a), and the fraction of the total Pb in wash water during each wash (Figure 3-3b). The total recovery of Pb in the SSFL group was 60.9%, and 71.1% in the DI water group.

Table 3-2. Study 2 Results - Finite Dosing of Lead (Pb) Nitrate in a Franz Cell Assay for 24 hours in Split Thickness Human Skin

Pb Dose[µg]	Solvent	Replicates	Skin Pb ion concentrations [µg] (SD)	Wash Pb ion concentration [µg] (SD)	Receptor Pb ion concentration	Total Pb ion recovery (%)
290.16*	SSFL	3	47.81 (5.03)	1 st wash: 74.83 (55.77)	<LOQ	60.9%
				2 nd wash: 27.07 (16.60)		
				3 rd wash: 18.22 (17.5)		
				4 th wash: 8.93 (7.33)		
				Total: 129.05		

	DI water	3	91.68 (36.5)	1 st wash: 64.72 (48.55)	<LOQ	71.1%
				2 nd wash: 23.06 (15.03)		
				3 rd wash: 15.84 (11.68)		
				4 th wash: 11.05 (13.94)		
				Total: 114.68		
Control	SSFL	2	<LOQ	<LOQ***	<LOQ	--
Control	DI water	2	1.5 (2.54)**	<LOQ***	<LOQ	--

*Calculated dose: 14,508 µg/ml*0.020 ml = 290.16 µg.

**Two samples were <LOQ, and one sample was 4.4. Average and SD were calculated using LOQ/SQRT (2) = 0.096/2 = 0.068.

***Only one wash sample collected.

Figure 3-3a. Lead (Pb) Content (µg) (±SD) in Wash Water Collected on Skin Dosed with Pb Nitrate and Hourly Aliquots of Synthetic Sweat (SSFL) or Deionized Water (DI Water) Collected Sequentially at the End of Study 2

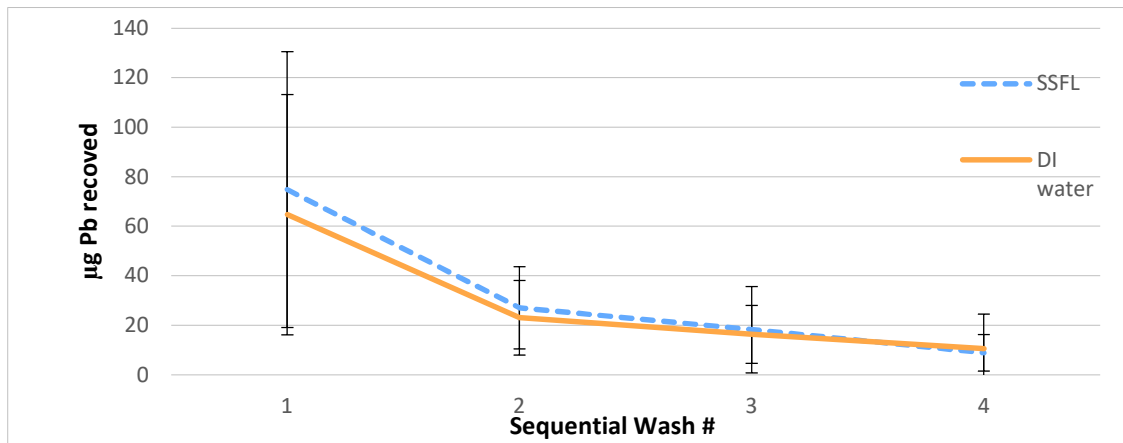
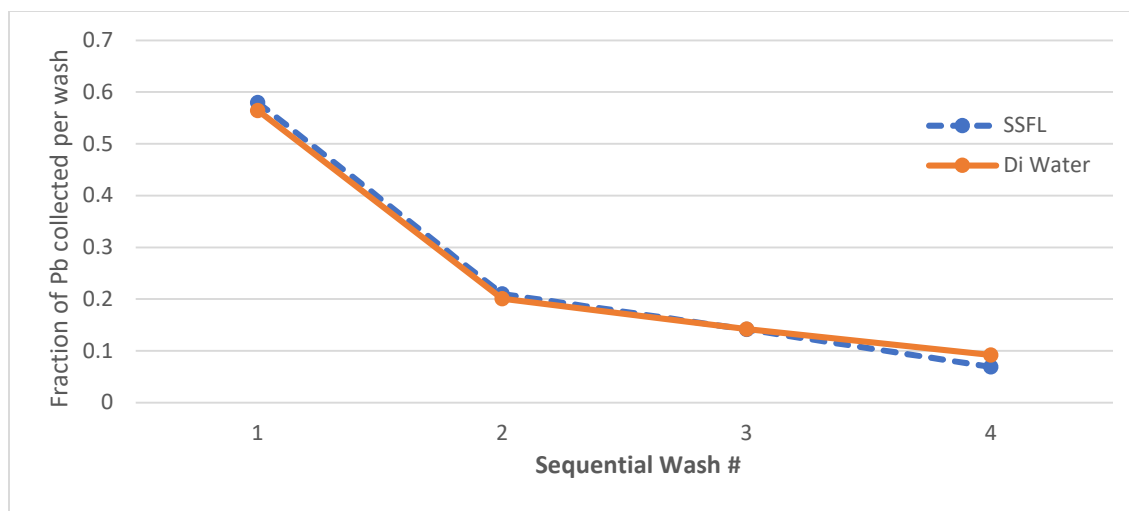


Figure 3-3b. Fraction of Total Lead (Pb) in Wash Water Collected During Each Wash Collected Sequentially at the End of Study 2



Study 3: Finite dosing study- 72 h

The objective of experiment 3 was to evaluate the impact of multiple Pb doses applied to the skin over 72 h. This experiment used a finite dosing protocol to dose a total mass of 1076.88 μg of Pb ion in three applications on the skin over 72 hours (Table 3-3). Pb was detected in both epidermis and dermis skin layers in both experimental groups (hourly aliquots of either SSFL or DI water) after washing. The total mass of Pb in the skin after washing was 194.37 μg and 251.48 μg , for the synthetic sweat and DI water groups, respectively.

For the SSFL group, 53.9% (161.66 $\mu\text{g} \pm 53.69(\text{SD})$) of the Pb mass was detected in the epidermis layer, while 16.8% (32.71 $\mu\text{g} \pm 28.44(\text{SD})$) was detected in the dermis layer. In the DI water group, 28.8% (72.52 $\mu\text{g} \pm 27.02(\text{SD})$) of the Pb mass was found in the epidermis layer, while 71.1% (178.96 $\mu\text{g} \pm 185.53(\text{SD})$) was found in the dermis layer. There was a statistically significant difference ($p < 0.05$) between the mass of Pb ion found in the epidermis layer of the SSFL group compared to the DI water group ($p < 0.0002$). However, the mass of Pb ion found in the dermis layers between SSFL and DI water wetted skin was not significant ($p < 0.19$) due to the large variance across replicates. Receptor samples were below the LOQ. A subset of receptor samples was analyzed using ICP-MS, which has a lower LOQ (0.0005 $\mu\text{g}/\text{ml}$) compared to ICP-AES (96 $\mu\text{g}/\text{ml}$) to determine if ICP-AES was not sensitive enough to detect Pb in receptor fluid. Pb was detected in both the Pb dosed and control samples at very low mass levels

(0.003-0.02 μg). There was no apparent difference in Pb concentrations in receptor fluid samples analyzed by ICP-MS, when comparing experimental groups and controls. Statistical inference testing was not completed due to the low number of samples tested. Wash samples were not analyzed for this study, so total recovery could not be calculated.

Table 3-3. Study 3 Results - Finite Dosing of Lead (Pb) Nitrate in a Franz Cell Assay for 72 hours in Split Thickness Human Skin

Pb ion Dose[μg]	Solvent	Replicates	Skin concentrations of Pb ion [μg] (SD)	Receptor concentration [of Pb ion [μg] (range)
1076.88*	SSFL	8	Epidermis: 161.66 (53.69)	ICP-AES Samples (n=8) <LOQ
			Dermis: 32.71 (28.44)	ICP-AES Samples (n=5) <LOQ ICP-MS Sample (n=3) 0.010 (0.0077-0.0203)
	DI water	8	Epidermis: 72.52 (27.02)	ICP-AES Samples (n=8) <LOQ
			Dermis: 178.96 (185.53)	ICP-AES Samples (n=5) <LOQ ICP-MS Sample (n=2)** 0.007 (0.0054-0.0085)
Control	SSFL	2	<LOQ	ICP-AES Samples (n=8) <LOQ
				ICP-AES Samples (n=7) <LOQ
				ICP-MS Sample (n=1) 0.0054
Control	DI water	2	<LOQ	ICP-AES Samples (n=8) <LOQ
				ICP-AES Samples (n=7) <LOQ
				ICP-MS Sample (n=1) 0.003 (ICP-MS)

*Calculated dose: $17,948 \mu\text{g/ml} \times 0.060 \text{ ml} = 1076.88 \mu\text{g}$.

**One sample removed because result suggested breakthrough (0.5 μg).

Study 4: Finite dosing study- 24 h (epidermis only)

The objective of Study 4 was to evaluate the potential for PbN to penetrate through the epidermis layer only over 24 h. This experiment was conducted under a finite dosing condition where a total of 769.02 μg of Pb ion was dosed on the skin (Table 3-4). Pb was detected in the washed epidermis layer

for both SSFL and DI water-wetted experimental groups, at mass levels of 91.22 µg and 43.28 µg, respectively. No Pb was detected in the receptor fluid samples, and Pb was not analyzed in the wash samples. A Wilcoxon rank-sum test was used to test for a significant difference between the concentration of Pb in SSFL and DI water-wetted groups. There was no statistically significant difference between these two experimental groups.

Table 3-4. Study 4 Results - Finite Dosing of Lead (Pb) Nitrate in a Franz Cell Assay for 24 hours in Epidermis Layer of Human Skin

Pb mass loaded on skin (µg)	Solvent	Replicates	Epidermis Pb ion concentration [µg] (SD)	Receptor Pb ion concentration	Total Pb ion recovery (%)
769.02*	SSFL	8	91.22 (74.7)	<LOQ	11.86*
	DI water	8	43.28 (27.6)	<LOQ	5.62***
Control	SSFL	2	<LOQ	<LOQ	--
Control	DI water	2	<LOQ	<LOQ	--

*Calculated dose based on analytical concentration: 38,451 µg/ml*0.020 ml = 769.02 µg.

Lead (Pb) Recovery Studies

Two Pb recovery studies found the total recovery of Pb on and in skin to be from an average of 21.9%-63.9% of the mass of the Pb dosed across two studies (Table 3-5). In Recovery Study 1, all of the Pb recovered from the experimental system was observed in the skin samples (no Pb was detected in the receptor samples). The mass of Pb in the dosing concentration (290.16 µg) closely matched the calculated nominal concentration (316 µg) in Recovery Study 1.

In Recovery Study 2, Pb was detected in all skin samples. Additionally, Pb was detected in two receptor fluid samples, with 17.99 µg detected in a sample collected at 0.5 h, and 0.5 µg detected in a sample

collected at 2 h. The mass of Pb in the dosing concentration (769.02 µg) did not closely match the calculated nominal concentration (316 µg) in Recovery Study 2.

Table 3-5. Recovery of Lead (Pb) in Skin Samples Collected in Study 2 and Study 4

Dosing concentration (µg)	Replicates	Skin concentrations (SD) (µg/sample)	Wash concentration (SD)	Receptor concentration (µg/sample)	Total recovery (%)
290.16 µg* (Recovery Study 1)	3	185.61 (27.6)	n/a	<LOQ	63.9
769.02** (Recovery Study 2)	3	161.86 (84.6)	n/a	6.25***	21.9

*Calculated dose: 14,508 µg/ml*0.020 ml = 290.16 µg.

**Calculated dose: 38,451 µg/ml*0.020 ml = 769.02 µg.

***Two receptor solution samples collected at 0.5 h and 2 h after the start of the experiment, had Pb in receptor solution at concentrations of 17.99 µg/sample and 0.5 µg/sample, respectively. All other receptor fluid samples from the skin recovery study did not detect Pb above the LOQ (0.096 µg). Receptor fluid concentrations were averaged across all replicates. Non-detects were calculated as LOQ/SQRT(2) = 0.068 µg.

Calculations:

0.5 h timepoint: (17.99 + 0.068 + 0.068)/3 = 6.04 µg.

2 h timepoint: (0.5 + 0.068 + 0.068)/3 = 0.21 µg.

Sample Size Power Calculations

Study 2

Based on the observed combined epidermis and dermis mean mass of Pb in skin for the SSFL treatment group (47.81 µg) and DI water treatment group (91.68 µg) (Table 3-2), 11 samples are needed to determine a statistically significant difference between treatment groups. This was based on sigma value of 36.5 (standard deviation in the DI water treatment group, which was highest standard deviation value observed between the two treatment groups).

Study 3

Based on the observed dermis mean mass of Pb in skin for the SSFL treatment group (32.71 µg) and DI water treatment group (178.96 µg) (Table 3-3), 26 samples are needed to determine a statistically significant difference between treatment groups. This was based on sigma value of 185.53 (standard deviation in the DI water treatment group, which was highest standard deviation value observed between the two treatment groups). A sample size power calculation was not determined for epidermis layered skin since a statistically significant difference between treatment groups was observed in the current study.

K_p and Diffusion Rate Calculations

A K_p value was calculated for Study 1 where SSFL was used as a dosing solution in an infinite dosing design and was determined to be 10⁻³ cm/h (Table 3-6). Diffusion rates in Studies 2-4 in SSFL-wetted skin ranged from 2.52–4.81 µg/cm²/h and 2.28–4.84 µg/cm²/h in DI water-wetted skin (Table 3-6). A diffusion rate of 0.027 µg/cm²/h was calculated for Study 1 (Table 3-6). Calculations for K_p and diffusion rates are provided in Appendix 4, and all are within the range of 10⁻⁴ cm/h in SSFL-wetted skin and 10⁻⁴–10⁻⁵ cm/h for DI water-wetted skin.

Table 3-6. K_p and Diffusion Rate Calculations Based on Lead (Pb) Skin Concentrations Determined in Studies 1–4*

Study		K _p (cm/h)		Diffusion rate (µg/cm ² /h)		
		SSFL	DI water		SSFL	DI water
1	Full skin	2.13x10 ⁻³	--	Full skin	0.027	--
2	Full skin	1.73x10 ⁻⁴	3.33x10 ⁻⁴	Full skin	2.52	4.84
3	Full skin	1.90x10 ⁻⁴	2.46x10 ⁻⁴	Full skin	3.42	4.42
4	Epidermis layer	1.25x10 ⁻⁴	5.94x10 ⁻⁵	Epidermis layer	4.81	2.28

*Calculations for K_p and diffusion rate values are provided in Appendix 4.

Discussion

This set of pilot studies evaluate the potential for penetration and absorption of PbN through human cadaver skin. Overall, the results of these pilot studies show dermal penetration of Pb ions into both washed epidermis and dermis skin layers using a Franz cell methodology. However, penetration of Pb ion into the receptor solution was not observed. One other *in-vitro* dermal penetration study identified in the literature for PbN was conducted using skin harvested from the dorsal section of 8-week-old female nude mice (ICR-Foxn1^{nu} strain) tested under infinite dosing conditions (Pan et al., 2010). Other *in-vitro* dermal penetration studies for other Pb compounds using either a Franz cell methodology or J-diffusion tube have detected Pb in receptor fluid for PbA (Table 1-2), and PbO and Pb Metal (Table 1-4) in human skin, stillborn piglet skin, and guinea pig skin (Bress and Bidanset, 1991; Filon et al., 2006; Pan et al., 2010; Julander et al., 2020). The data from these studies were used to derive percutaneous absorption values published by Niemeier et al., (2021) (Chapter 1) and others (EPA, 1992; Hostýnek et al., 1993, Hostýnek, 2003; Franken et al., 2015; Julander et al., 2020). There is debate as to whether finite or infinite dosing approaches are better for occupational-related exposures. OECD (2011) indicates that finite dose experiments better reflect occupational exposures, since they are more similar to the exposure scenarios that occur within workplaces. In this case, workers are dermally exposed to a limited amount of Pb over the work shift (Table 2-1). However, Franken et al., (2015) argue that for metals, infinite dosing studies are preferable, as they provide more useful data to estimate absorption at steady state conditions to determine K_p values. Though infinite dosing studies are not directly applicable to workplace exposures (i.e., workers' skin is usually not submerged in Pb-containing liquids for their entire work shift), the determination of K_p is critically important for exposure modeling, further discussed in Chapter 5.

This study, as well as two *in vivo* studies conducted by Pan et al., (2010) in mice, and Sun et al., (2002) in rats, where Pb was detected in liver, kidney, and urine (discussed in Chapter 1), demonstrate the

potential for PbN to penetrate through mammalian skin and bioaccumulate as Pb in tissue after short-term exposures (5-12 days). However, an important question is why Pb was not detected in the receptor fluid of the Franz cell studies conducted in the current study.

There are several differences between this study and the Pan et al., (2010) study. One important methodological difference is the type of skin used. Our studies used human cadaver skin; whereas Pan et al. (2010) used mouse skin in previous studies. As discussed in Chapter 1, Jung and Maibach, (2015) determined that animal skin, including rat, rabbit, and guinea pig skin, tends to overestimate the rates of absorption of chemicals across human skin. Mouse skin from hairless mice has also been shown to have higher permeation rates than human skin used in *in-vitro* permeation studies (Seo et al., 2017). EFSA (2012) also suggests that animal models will over-predict human dermal absorption, though Jung and Maibach, (2015) suggest that phylogenetically similar skin from primates, or skin with other dermal structural similarities to human skin, such as that found in pigs or hairless guinea pigs are appropriate alternatives for human skin for *in-vitro* dermal penetration studies.

A second important difference between the current study and the Pan et al., (2010) *in-vitro* study was the dosing regimen used. Pan et al., (2010) evaluated the permeation of PbN using an infinite dosing condition where the donor compartment was loaded with 0.5 ml of a 120 mM solution of PbN ($2.44 \times 10^4 \mu\text{g Pb}^{2+}$ ion/ml available, assuming full dissolution) in either double-distilled water or SSFL and dosed for 10 hours. As a comparison, in the current set of pilot studies, the first study (Study 1) was conducted as an infinite dosing study; however, the concentration of PbN dosed on the skin was much lower than that used by Pan et al., (2010). In this case, the concentration of Pb in the dosing solution in Study 1 was analytically determined (via ICP-AES) to be 12.68 $\mu\text{g/ml}$, which is ~ 4 orders of magnitude lower than the dosing solution used by Pan et al., (2010). The dosing solution in Study 1 was prepared in SSFL and precipitated when mixing PbN powder into the solution (further discussed in Chapter 4). Only the supernatant of the SSFL stock solution was dosed on the skin in this study. At the end of 24 h, the dosing

solution was removed from the donor compartment and the skin was washed. A total recovery of the Pb in the system was calculated to be 113%, with 8.9% of the dosed Pb found within the skin, based on the concentration of Pb determined analytically in the supernatant that was dosed on the skin. Pan et al., (2010) also dosed PbN in a SSFL containing sodium chloride, lactic acid, urea, and five amino acids. The authors reported that skin deposited Pb was statistically significantly less ($p < 0.05$) in skin dosed with SSFL compared to skin dosed with distilled water. Pan et al., (2010) reported Pb concentration in skin as mass of Pb per mass of skin sample, reporting an uptake of 14.38 $\mu\text{g}/\text{mg}$ for PbN in intact skin, $\sim 33 \mu\text{g}/\text{mg}$ for stratum corneum stripped skin, and $\sim 3 \mu\text{g}/\text{mg}$ when PbN was dosed in SSFL in water. However, they did not provide the mass of the skin sample, so direct comparison to the mass of skin in the current study (Study 1) is not possible. Pan et al., (2010) also reported higher total concentrations of Pb ion in receptor in the distilled water dosing arm for intact skin ($0.20 \pm 0.13 \mu\text{g}/\text{cm}^2$) compared to SSFL dosing arm ($0.13 \pm 0.09 \mu\text{g}/\text{cm}^2$), though statistical testing was not reported. An interaction between PbN and SSFL that occurred in Study 1 also occurred in the Pan et al., (2010) study. However, Pan et al., (2010) did not report if a visible precipitate was formed when mixing PbN with SSFL, nor did they provide the analytical concentration of Pb ions in the dosing solution. However, they did indicate that the presence of sodium chloride, urea, and amino acids may hinder the permeation of Pb into the skin (Pan et al., 2010).

A third difference in the Pan et al., (2010) study compared to the dermal penetration studies reported in this chapter was the different use of receptor solutions. A detailed analysis of the interaction of PbN and buffers is described in Chapter 4. However, it is important to note that Pan et al., (2010) used a McIlvaine buffer containing both PBS and citrate buffers (Fang JY, personal communication, March 4, 2019). The current studies used a 1x PBS buffer. As described in Chapter 4, both a PBS and McIlvaine buffers appear to form a similar mass of precipitate when in contact with PbN; however, it is not known

if these buffers would behave similarly as a receptor fluid in Franz cells without directly comparing them in the same study.

In the current studies, though no Pb was detected in receptor fluids, Pb was detected in skin in Studies 1-4. In Study 2, the concentration of Pb in the skin was $47.81 \pm 5.03 \mu\text{g}$ in SSFL-wetted skin (16.5% of Pb mass loaded on skin), compared to $91.68 \pm 36.5 \mu\text{g}$ in DI-wetted skin (31.5% of the mass of Pb loaded on skin). For the SSFL-wetted skin, the concentrations detected in the skin were approximately 5x greater than the Pb detected in the final wash ($47.81 \mu\text{g}$ vs. $8.93 \mu\text{g}$) (Table 3-2). Similarly, wash concentrations in DI water-wetted skin were approximately 8x greater than the Pb detected in the final wash ($91.68 \mu\text{g}$ vs. $11.05 \mu\text{g}$) (Table 3-2). These comparisons suggest that Pb penetrated into the skin layers, though it was not determined whether Pb penetrated into the deeper layers of the skin.

Study 3 evaluated the ability of Pb to penetrate to deeper levels of the skin. In Study 3, skin was dosed with Pb on three consecutive days and washed daily with DI water to better simulate workplace conditions and maximize the amount of Pb dosed to skin for detection in receptor fluid. Similar to Study 2, skin was wetted with SSFL or DI water for 8 h periods over the course of 3 days. At the end of 72 hours, skin samples were separated into epidermis and dermis layers for analysis of Pb concentrations in both skin layers. At the end of the experiment, Pb was not detected in receptor fluid. However, Pb was detected in both epidermis and dermis layers of skin. There was no statistical difference in Pb deposition in total skin (epidermis + dermis) or dermis layer between the SSFL and DI water-wetted groups; however, the content of Pb in the epidermis only was statistically significantly different between SSFL and DI water-wetted skin ($p < 0.0002$). The total percent of Pb deposited in washed skin (percent of total loaded on skin) was 18.5% for SSFL-wetted skin (compared to 16.5% in Study 2), and 23.4% in DI-wetted skin (compared to 31.5%), suggesting a similar trend of deposition of Pb for both SSFL- and DI-wetted skin. The presence of Pb in the dermis layer of skin for both SSFL-wetted

(32.71±28.44 (SD) µg) and DI-wetted skin (178.96±185.53 (SD) µg) provides evidence that Pb is penetrating to deeper layers of the skin and may be available for systemic distribution.

In a follow-up study (Study 4), the epidermis layer was heat-separated from the dermis layer, mounted on Franz cells, and dosed with 769.02 µg Pb for 24 h. This study was designed to test the potential penetration of Pb through just the epidermis layer, where any Pb detected in the receptor solution would represent Pb found in the dermis layer. Similar to Study 3, hourly aliquots of SSFL and DI water were used to wet the skin for 8 hours. Again, no Pb was detected in the receptor solution; however, after skin washing, Pb was detected in the epidermis layer at similar percentages to the epidermis results in Study 3 for both SSFL- and DI water-wetted skin. In this case, Study 4 results show that 11.86% (91.22 µg) of the Pb dosed on the skin was detected in washed epidermis for the SSFL-wetted group, and 5.62% (43.28 µg) in the DI water-wetted group, though these results were not statistically significantly different. This is a similar trend to Study 3 results, where more Pb was detected in the epidermis layer for SSFL-wetted skin- 15.01% (161.66 µg) compared to DI water-wetted skin- 6.73% (72.52 µg). As described above for Study 3, there was a statistically significant difference between the mass of Pb in the epidermis layer for SSFL- vs. DI water-wetted skin ($p < 0.0002$). However, the differences observed in the dermis layer in Study 3 for SSFL vs. DI water did not reach statistical significance. It is intriguing that there are similar percent masses of Pb in the epidermis layer for both SSFL- and DI water-wetted skin for both Studies 3 and 4; however, it is unclear why Pb penetrating through the epidermis layer was not detected in the receptor fluid in Study 4. One major methodological difference between Study 3 and Study 4 was the total length of the studies, where Study 3 was 72 h and Study 4 was 24 h. It could be that Study 4 did not provide enough time for penetration of Pb into the receptor fluid. Unfortunately, further studies were halted because of the COVID-19 pandemic.

Though Pb was detected in the skin in all 4 studies, further methodological development of skin dissolution protocols is needed. The skin dissolution protocol used in these studies was based on the

method published by Filon et al., (2006), where concentrated nitric acid (HNO₃) was used to dissolve skin prior to ICP-AES analysis. Similarly, Pan et al., (2010) also determined skin Pb levels by homogenizing the skin in a 1N hydrochloric acid (HCl) solution for 5 min, centrifuging the solution, and analyzing the supernatant. However, it was observed that in the current studies, the use of both concentrated HNO₃ and HCl did not fully dissolve the skin. Small pieces of tissue were still visible in the dissolution liquid and required filtration prior to ICP-AES analysis. This likely underestimated the concentration of Pb in the skin samples and the total percent recovery of Pb in all of the experiments. This is evidenced by the two skin recovery studies that found that 21.9%–63.9% dosed on skin was recovered (Table 3-5). In these studies, skin was not washed or wetted with DI water or SSFL. At the end of the experiment (24 h), skin was dissolved according to the protocols specified in the Methods section. Additionally, receptor fluid samples were analyzed for Pb determination. In Study 4, only 21.9% of the Pb dosed was recovered in the skin sample, which is substantially less than the results in Study 2 (63.9%). Study 4 evaluated epidermis-only skin layer, while Study 2 evaluated full skin dissolution. In Study 3, dermis and epidermis layer skin samples were collected and analyzed separately. It was visually noted in that study that epidermis samples had larger pieces of undissolved skin and clouded dissolution liquids compared to the dissolution liquids containing dermis layer samples; however, a Pb recovery experimental group was not run as part of Study 3. This suggests that part of the reduced recovery of Pb observed in Study 4 may be related to the fact that these samples were epidermis-only, which may have resulted in a higher percentage of Pb filtered out in undissolved tissue compared to samples in Study 2, which contained both epidermis and dermis layer tissue. Another reason for this discrepancy may be due to an error in calculation of the concentration of Pb applied to the skin in Study 4. The nominal concentration applied to the skin was calculated to be 15,639.75 µg/ml, with 0.020 ml applied for a total skin dose of 312.80 µg of Pb. However, the calculated dose from the ICP-AES analysis of the dosing solution indicated that the Pb concentration was 38,451 µg/ml, with 0.020 ml applied for a total skin dose of 769.02 µg of

Pb. It is likely that the error occurred in the preparation of the dosing solution and not in the analysis of the dosing solution sample by ICP-AES, though it is not fully clear. Further studies on skin recovery were not conducted due to the COVID-19 pandemic. Future studies to further enhance the skin dissolution efficiency should be considered. Alternatively, future studies could be designed to always collect skin recovery samples, which could be used to estimate the recovery efficiency of Pb in skin and applied to the other experimental groups.

An important consideration to understand if Pb is penetrating into the skin is to ensure that Pb on the surface of the skin has been adequately removed from the skin prior to skin dissolution. Study 2 provides evidence that Pb is adequately washed off the skin in 4 washes. Nearly identical percentages of Pb were determined in the wash solutions for both the SSFL hourly-wetted and DI water hourly-wetted experimental groups (Figures 3-2a and 3-2b). By the 4th wash, 8.93 µg of Pb was present in the SSFL-wetted group (6.9% of total Pb determined in all wash water) vs. 11.05 µg in the DI arm (9.6% of total Pb determined in all wash water). This represented an 88% reduction of Pb on the surface of the skin for SSFL-wetted skin after 4 washes, compared to an 84% reduction in the DI water-dosed group. It is an important consideration to compare the wash efficiency of SSFL-wetted skin vs. DI water-wetted skin, as a different milieu of Pb-precipitated compounds may be formed on the skin, particularly with the interaction of SSFL and PbN (described in Chapter 2 and Chapter 4). These potential Pb-precipitated compounds, such as Pb phosphate, could have had different adhesion to skin compared to PbN on skin dissolved in DI water. The results of this study suggest this is not the case, and that this skin washing protocol is equally effective for PbN-dosed skin treated with SSFL or DI water.

The primary observation of this set of studies is that Pb is penetrating into the skin. OECD, (2004b) indicates that test substance found within the skin should be considered as part of the fraction that is absorbed, unless there is a reason that only receptor fluid concentrations should be considered absorbed. In this case, there is no reason that is justified to exclude Pb determined in the skin layers

since: 1) the skin was washed after studies were completed, and 2) Study 3, conducted over a 72 h period, shows that Pb is able to penetrate to the dermis layer of the skin. Both the epidermis layer (excluding the stratum corneum) and the dermis layers of the skin are viable tissue; however, the epidermis layer is not vascularized (Ruela et al., 2016). The dermis layer of the skin is about 1-2 mm thick, embedded with several skin-related structures including blood vessels, sebaceous and sweat glands and nerve endings, provides mechanical support and elasticity, and serves as a water reservoir, which may allow for systemic absorption of xenobiotics in contact with this layer (Ruela et al., 2016; Supe and Takudage, 2021; Savoji et al., 2018). In the current studies, an analysis to determine the concentration of Pb in stratum corneum vs. deeper levels of epidermis was not conducted. Future studies could ascertain this information by tape stripping to better understand the levels of Pb deposition in stratum corneum layers (Lademann et al., 2009).

K_p and diffusion rate values were calculated based on the total concentration of Pb in the skin for all four pilot studies. K_p values determined in this study ranged from 10^{-5} – 10^{-3} cm/h (Table 3-6), based solely on the deposition of Pb in skin, since Pb was not found in receptor fluid. Only one other study was identified where K_p values could be calculated for PbN (Pan et al., 2010), where the K_p through mouse skin was determined to be 10^{-7} – 10^{-6} cm/h. The values calculated in the current study are one to four orders of magnitude greater than Pan et al., (2010), likely because the Pan et al., (2010) values were based on receptor fluid results only. Surveying all of the literature identified in Chapter 1 where K_p values could be calculated, there is a range of 10^{-7} – 10^{-5} cm/h across all species and Pb compounds identified (Table 1-2). For dissolution rate values, the current study determined values ranging from 0.027–4.84 $\mu\text{g}/\text{cm}^2/\text{h}$ (Table 3-6) compared to diffusion rate values for PbN calculated from Pan et al., (2010) in receptor fluid, which were 0.019–0.043 $\mu\text{g}/\text{cm}^2/\text{h}$. K_p and diffusion rate calculations for skin-deposited Pb in the Pan et al., (2010) study could not be directly compared to values calculated in the current studies, since Pan et al., (2010) reported Pb concentration in skin as mass of Pb per mass of skin

sample and did not provide values for the mass of the skin. Therefore, the total mass of Pb in the skin could not be estimated from their data. The diffusion rate results for all Pb studies identified in receptor fluid ranged from 2.1×10^{-4} - $0.3 \mu\text{g}/\text{cm}^2/\text{h}$ (Table 1-2). Both the K_p values and diffusion rate values calculated in the current study overlap with values identified in the literature; however, they are not directly comparable, since all of the literature values are based on identification of Pb in the receptor fluid. The K_p and diffusion rate values calculated from Studies 1-4 likely represent maximum values since they are based on skin concentrations only, and serve best as a screening level assessment for the penetration of PbN through human skin. Future studies, conducted under guideline-compliant methods (EPA, 1992, 1998, 2007; OECD, 2004a,b, 2011; EFSA, 2012) should be further conducted in human skin to better refine K_p and dissolution rate values for PbN (see Chapter 6 for further discussion).

Chapter 4. Analysis of Interaction between Lead (Pb) Nitrate and Buffers Used as Franz Cell Receptor Fluids

Introduction

The dermal absorption pathway for iPb as a contributor to body burden continues to be uncertain (ATSDR, 2020a), however, our recent review of evidence suggests that dermal exposures could result in meaningful dermal uptake (Chapter 1- Niemeier et al., 2021). Of the studies identified by Niemeier et al., (2021), four were *in vitro* absorption studies that used either a Franz cell or J-diffusion tube assay to estimate Pb penetration through human or animal skin for 4 different iPb compounds including Pb acetate, Pb oxide (PbO), Pb metal, and Pb nitrate (PbN) (Pan et al., 2010; Bress and Bidanset, 1991; Filon et al., 2006; Julander et al., 2020). Franz cell studies can provide valuable data to estimate dermal penetration of compounds, including the permeability coefficients of diffusion rate and steady state flux. Here we define the amount of chemical absorbed across a defined surface area of the skin ($\text{mg}/\text{cm}^2/\text{h}$) at steady state as flux, or as diffusion rate when steady state is not achieved (EPA, 1992; Niemeier et al., 2021). In the Pb studies identified, Pb was detected in receptor fluid and dissolution rates were estimated to be 1.21×10^{-7} – 1.6×10^{-4} $\text{mg}/\text{cm}^2/\text{h}$ for the four Pb compounds (Bress and Bidanset, 1991; Filon et al., 2006; Julander et al., 2020; Pan et al., 2010; Hostýnek et al., 1993; Franken et al., 2015).

Of the Pb compounds examined above, PbN has the highest water solubility of 5.2×10^5 – 5.97×10^5 $\mu\text{g}/\text{ml}$ @20-25°C, which may allow for the availability of Pb ions on the surface of the skin in the presence of water (or sweat), and thus having a potential for penetration into the skin via ion/counter ion-driven penetration (Hostýnek, 2003; Pubchem, 2022a). A few studies, both *in vivo* and *in vitro*, have evaluated the potential for dermal penetration of PbN, and have shown measurable absorption of Pb through the skin (Pan et al., 2010; Stauber et al., 1994; Sun et al., 2002; Lilley et al., 1988). However, these studies were of limited use for occupational risk assessment, since they were not guideline-compliant (EPA, 1992, 1998, 2007; OECD, 2004a,b, 2011; EFSA, 2012), were anecdotal case studies, or had other study

design limitations discussed in Chapter 1. Despite these limitations, the results of the studies above suggest that dermal exposure to PbN could result in systemic uptake of Pb.

The aim of this chapter is to provide observational experimental data about the interaction of buffers and SSFL with PbN for use in Franz cell studies. These studies stemmed from observations in four Franz cell studies conducted to evaluate the potential for PbN to penetrate through human cadaver skin (Chapter 3). None of these pilot studies resulted in the detection of Pb in receptor fluid, potentially due to precipitate formation between Pb and buffer solution at the receptor/skin interface. Two of the buffers that were evaluated in this current set of experiments PBS and McIlvaine buffer have been previously used in Franz cell studies to evaluate dermal penetration of PbO and PbN (Filon et al., 2006; Pan et al., 2010). To our knowledge, the citrate buffer and SSFL (same formulation used in experiments described in Chapters 2 and 3) that were tested in this set of experiments have not been previously used in Franz cell studies to evaluate the potential for Pb dermal penetration.

Methods:

Three separate studies were conducted to evaluate the potential interaction of Pb compounds with buffers and a synthetic sweat solution.

Study 1: Pb nitrate/PBS and McIlvaine buffer interaction

Three buffer solutions were evaluated for the potential to precipitate PbN. The three buffer solutions included:

- Dulbecco's PBS (non-magnesium salt) 2X (prepared in house)- 0.2 g (0.001 M) KCL, 0.2 g (0.003 M) KH_2PO_4 , 8 g (0.27 M) NaCl, 1.15 g (0.02 M) Na_2HPO_4 (anhydrous) in 500 ml of double-distilled (DI) water (Sigma Aldrich, 2021)
- McIlvaine Buffer 2X ((prepared according to directions by Fang JY, personal communication, March 4, 2019) - 0.258 g (0.02 M) of Na_2HPO_4 and 0.351 g (0.02 M) citric acid in 90 ml double-distilled water

- Dulbecco's PBS 20X One packet of Dulbecco's buffer powder (D5773-10x1L, Sigma-Aldrich, St. Louis, MO) (0.2 g (0.01 M) KCL, 0.2 g (0.03 M) KH₂PO₄, 8 g (2.7 M)- NaCl, 1.15 g (0.2 M) Na₂HPO₄ (anhydrous) in 50 ml of water (Sigma Aldrich, 2021)

A laboratory grade Pb (II) nitrate (CAS# 10099-74-8) (Fisher Scientific, Pittsburgh, PA) was used to prepare a 0.4 g/ml PbN stock solution in Millipore deionized water. This was prepared by mixing:

- 20 g PbN (containing 12.51g Pb and 7.49 mg nitrate) in 50 ml water (Stock solution).

2 serial dilutions of the PbN stock solution were prepared by mixing:

- 0.4 g/ml PbN stock solution in 9 ml water (0.04 g/L) (Dilution #1)
- 0.04 g/ml PbN stock solution in 9 ml water (0.004 g/L) (Dilution #2)

The three concentrations of PbN solution (Stock solution, Dilution #1, and Dilution #2) were added to samples of the three buffer solutions in a 1:1 ratio to create PbN concentrations of 0.2 g/ml (0.6 M), 0.02 g/ml (0.06 M), and 0.002 g/ml (0.006 M) and a dilution of each of the buffer solutions by half. For example, 5 ml of the 0.4 g/ml PbN solution was added to 5 ml of Dulbecco's PBS (2x) to create a final concentration of 0.2 g/ml in 10 ml of Dulbecco's PBS (1x). This was repeated for each Pb solution and for each buffer, so that the final buffer concentrations were 1x PBS, 1x McIlvaine, and 10X PBS, with a total of 9 samples tested. Samples were visually analyzed for precipitate by centrifuging test solutions at 3000 RPM for 30 minutes. Samples were then re-homogenized, and total precipitate was collected on pre- and post-weighed (dry weight) filter paper (0.025 µm pore size 47 mm diameter, Sigma-Aldrich, St. Louis, MO) to determine the mass of precipitate formed for each solution.

Study 2: Pb nitrate and Pb oxide/citrate buffer interaction

Two laboratory grade Pb powders were evaluated including Pb (II) nitrate (CAS# 10099-74-8) (Fisher Scientific, Pittsburgh, PA), and Pb (II) oxide (CAS# 1317-36-8) (Acros Organics, Pittsburgh, PA). The Pb (II) oxide served as comparator group as a Pb compound with low reported water solubility (17.0–70.2 µg/ml @20-25°C) compared to the water solubility of Pb (II) nitrate (5.2x10⁵–5.97x10⁵ µg/ml at 20-25°C)

(Pubchem, 2022 a,f). The dissolution of these powders was evaluated in a static dissolution test using a 0.1M citrate buffer solution prepared to the specifications outlined by AAT Bioquest, Inc. (2021), including the addition of both 12.044 g (0.082M) sodium citrate ($\text{Na}_3\text{C}_6\text{H}_5\text{O}_7$) and 1.736 g (0.018 M) citric acid ($\text{C}_6\text{H}_8\text{O}_7$) adjusted to pH 6.0 with NaOH.

The dissolution assay method was previously described (Kanapilly et al., 1973; Stefaniak et al., 2005; Stefaniak et al., 2010a). Briefly, a known mass of each powder (approximately 20 mg each) was weighed on a 0.025 μm pore size, 47 mm diameter nitrocellulose filter. The percent mass of Pb in PbN is 62.559%; the percent mass of Pb in PbO is 92.832%. Two additional 0.025 μm pore size, 47 mm diameter filters were placed on either side of the filter to create a “sandwich” that was loaded and secured in a static dissolution chamber (InTox Products, Moriarity, NM). Chambers were placed in polypropylene plastic cups and submerged in 80 ml of the citrate buffer solution maintained at 36.3°C in an incubator for the entire experiment. The chambers were removed from the incubators at 1, 6, and 24 hours, and the citrate buffer solution was collected and fully replaced with fresh citrate buffer solution. Citrate buffer solutions were collected in separate borosilicate jars and frozen until analysis.

Sample analysis

Inductively coupled plasma-atomic emission spectroscopy (ICP-AES) was done using a Spectro Arcos EOP (Spectro Ametek, Mahwah, NJ) using spectral line 220.353 nm (limit of quantification= 0.096 $\mu\text{g}/\text{ml}$). The ICP-AES was calibrated according to manufacturer recommendations, and a 3-point calibration curve including blank and Pb-spiked samples of citrate buffer (1% and 10% Pb concentrations). Concentrated HNO_3 (5% v/v) was also added to the calibration samples.

Statistical analysis

The cumulative fraction of the dissolved Pb mass for each experimental group was determined by: 1) summing the Pb concentrations determined at each timepoint by ICP-AES, and 2) dividing this total mass by the initial mass of Pb compound loaded on the filter using Microsoft Excel (2021). The fraction of

solid remaining (1 minus the cumulative fraction of dissolved mass) was then plotted versus time (t) for each sample. The average of the fraction of solid remaining was calculated across three replicates for each of the compounds (PbN and PbO), and the SEM was calculated.

Study 3: Pb nitrate/synthetic sweat interaction

Laboratory grade Pb (II) nitrate powder (CAS# 10099-74-8) (Fisher Scientific, Pittsburgh, PA) was mixed with SSFL prepared according to the formulation outlined by Harvey et al., (2010) in a concentration of 48 mg/100 ml at room temperature. Precipitate was analyzed by the NIOSH Morgantown, WV

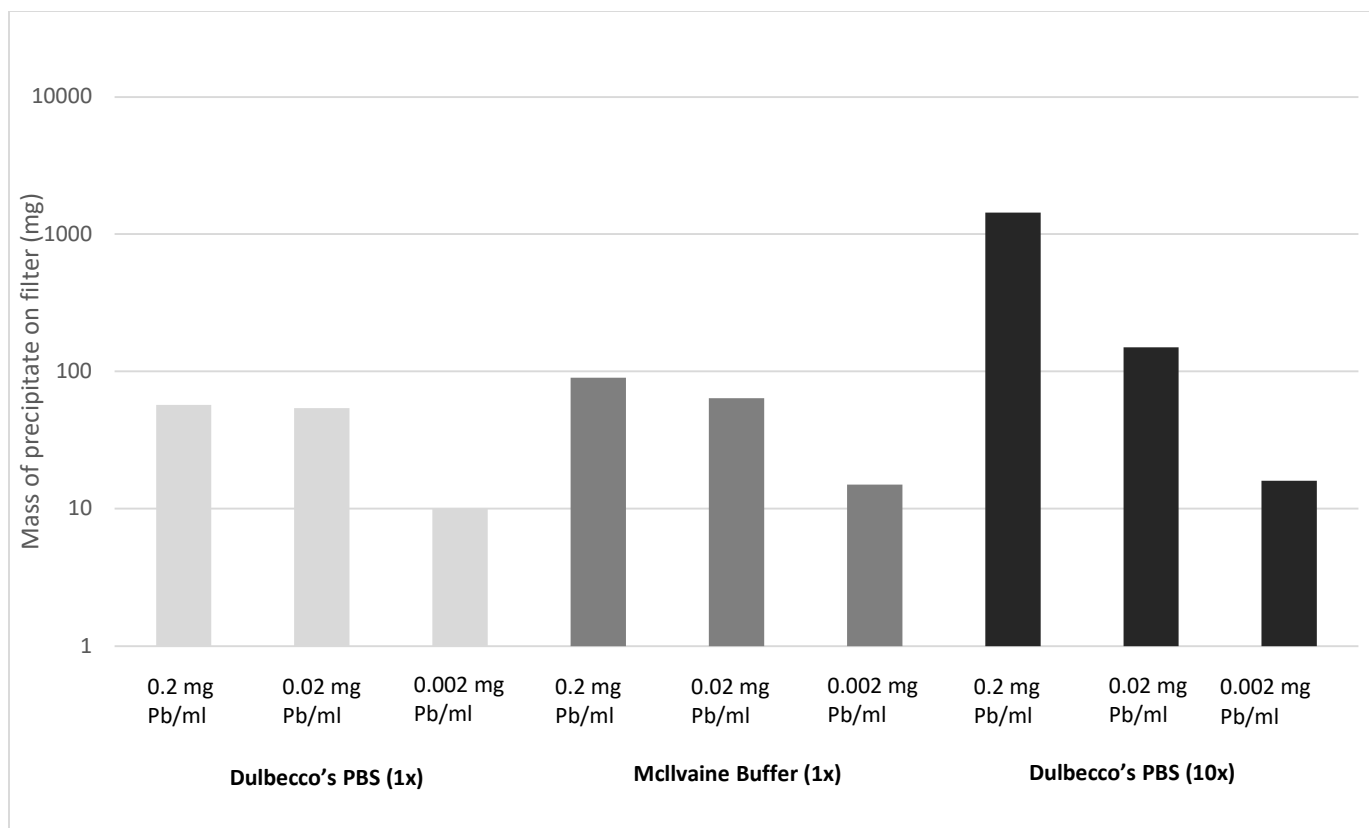
Laboratory using scanning electron microscopy and energy dispersive x-ray analysis (EDX) to identify the precipitate formed.

Results

Study 1: Lead (Pb) nitrate/PBS and McIlvaine buffer interaction

Lead precipitates were observed at all three concentrations of PbN for each of the three buffers that were tested. Each series of buffer/PbN solutions exhibited dose-dependent precipitate formation, with the highest formation of precipitate formed at the highest concentrations of PbN (0.2 mg/ml) for each buffer (Figure 4-1). The lowest overall precipitate formation occurred in the 1X PBS buffers; however, similar masses of precipitate were observed for 1X PBS Buffer and 1X McIlvaine buffer B at all three concentrations tested. It is noted that filter breakthrough occurred for the lowest concentration of PbN (0.002 mg/ml) tested with Buffer A (Sample A3), so the sample result is estimated. Buffer C, which was tested at a 10x concentration of PBS buffer, exhibited a precipitation mass that was 8.8-10.9 times greater than the precipitate mass formed for Buffers A and B at the highest Pb concentration. However, at the lowest concentration of PbN tested, Buffer C formed a similar precipitate mass (16 mg) compared to Buffers A (10 mg) and B (15 mg).

Figure 4-1. Mass (mg) of Precipitate Formed with Three Buffers Mixed with Three Concentrations of Lead (Pb) Nitrate in Water



Study 2: Pb nitrate and Pb oxide/citrate buffer interaction

Both PbN and PbO showed similar patterns of dissolution with faster dissolution occurring within the first 6 hours, and slower rates of dissolution occurring after that until the end of the experiment at 24 h (Figure 4-2). For PbN, the M/M_0 was 9% for PbN and 10.9% for PbO at 6 h. From hours 6-24, an additional M/M_0 of 1.7% was observed for PbN and 0.4% for PbO (Figure 4.2). This shows the rate of dissolution slowing down for both Pb compounds. Over the 24-hour test period, the cumulative dissolution (in 240 ml of SSFL) of PbO was 9.1 $\mu\text{g/ml}$, and 5.9 $\mu\text{g/ml}$ for PbN (Table 4-1).

Table 4-1. Dissolution of Lead Nitrate (PbN) and Lead Oxide (PbO) in 0.1M Citrate Buffer @36.3°C Over a 24-hour Period in a Dissolution Assay

	PbN		PbO	
	Mass dissolved (µg) [SD]	Dissolution (µg/ml)	Mass dissolved (µg) [SD]	Dissolution (µg/ml)
1 hour	761.2 [17.4]	9.5*	1,522.0 [145.8]	19.0*
6 hours	423.8 [8.6]	5.3*	582.3[25.1]	7.3*
24 hours	236.8 [83.0]	3.0*	88.4 [59.8]	1.1*
<i>Cumulative</i>	<i>1,421.9 [61.9]</i>	<i>5.9[†]</i>	<i>2,192.6 [164.6]</i>	<i>9.1[†]</i>
Maximum theoretical Dissolution based on filter load	Mass PbN loaded on filter (µg) [SD] (mass of Pb ion available[§])	Maximum Theoretical Dissolution (µg/ml)	Mass PbO loaded on filter (µg) [SD] (mass of Pb ion available[¶])	Maximum Theoretical Dissolution (µg/ml)
	21,306.7 [866.6] (13,337.9)	166.7** 55.6 ^{††}	20,833.3 [1327.6] (19,400.6)	242.5 ^{§§} 80.8 ^{¶¶}
Reported water solubility	5.2x10 ⁻⁵ –5.97x10 ⁻⁵ µg/ml @20-25°C (Pubchem, 2022a)		17.0–70.2 µg/ml @20-25°C (Pubchem, 2022i; Thermo Fisher Scientific, 2021)	

*In 80 ml.

†In 240 ml.

§Mass % of Pb in PbN = 62.6%. 21,306.7 µg*0.626 = 13,337.9 µg.

¶Mass % of Pb in PbO = 92.9%. 20,833.3 µg*0.929 = 19,400.6 µg.

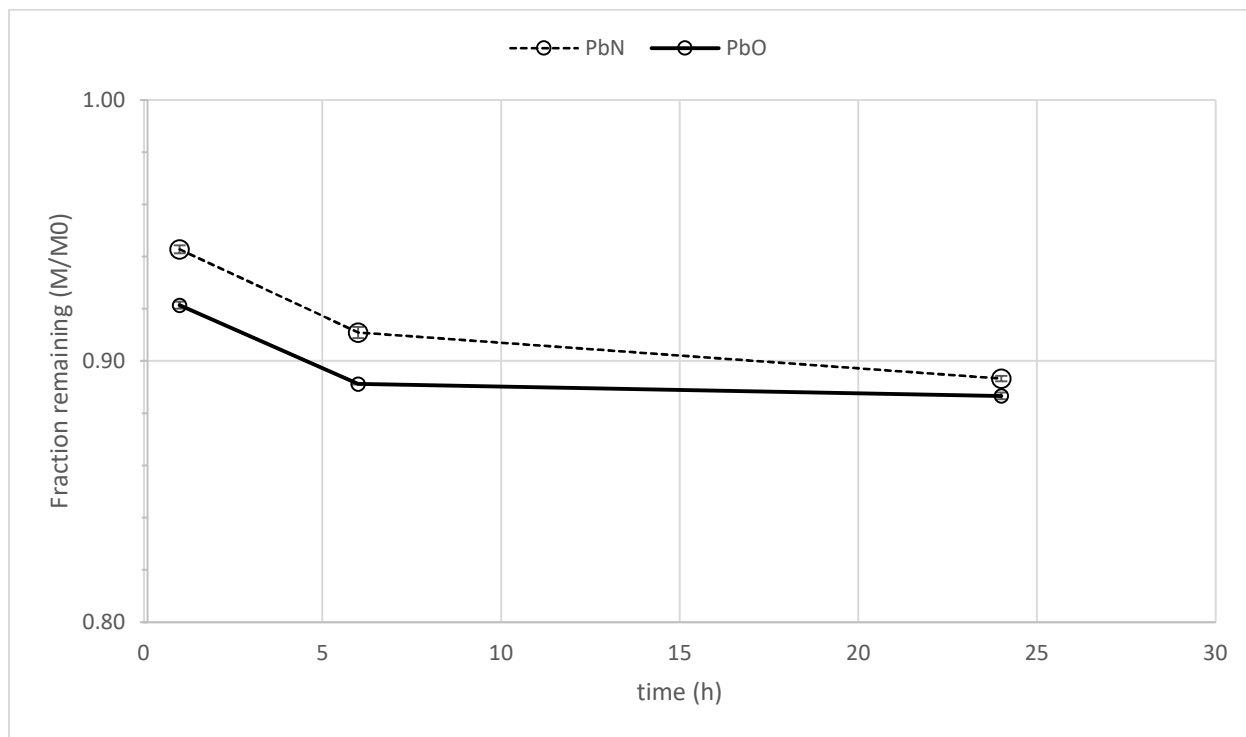
**Calculation for maximum theoretical dissolution in 80 ml- 13,337.9 µg/80 ml = 166.7 µg/ml.

††Calculation for maximum theoretical dissolution in 240 ml- 13,337.9 µg/240 ml = 55.6 µg/ml.

§§Calculation for maximum theoretical dissolution in 80 ml- 19,400.6 µg/80 ml = 242.5 µg/ml.

¶¶Calculation for maximum theoretical dissolution in 240 ml- 19,400.6 µg/240 ml = 80.8 µg/ml.

Figure 4-2. Dissolution (1 minus the cumulative fraction of dissolved mass) (\pm SEM*) Plotted Versus Time (t) for Pb Nitrate (PbN) and Pb Oxide (PbO) Dissolved in 0.1 M Citrate Buffer Solution Over 24 Hours

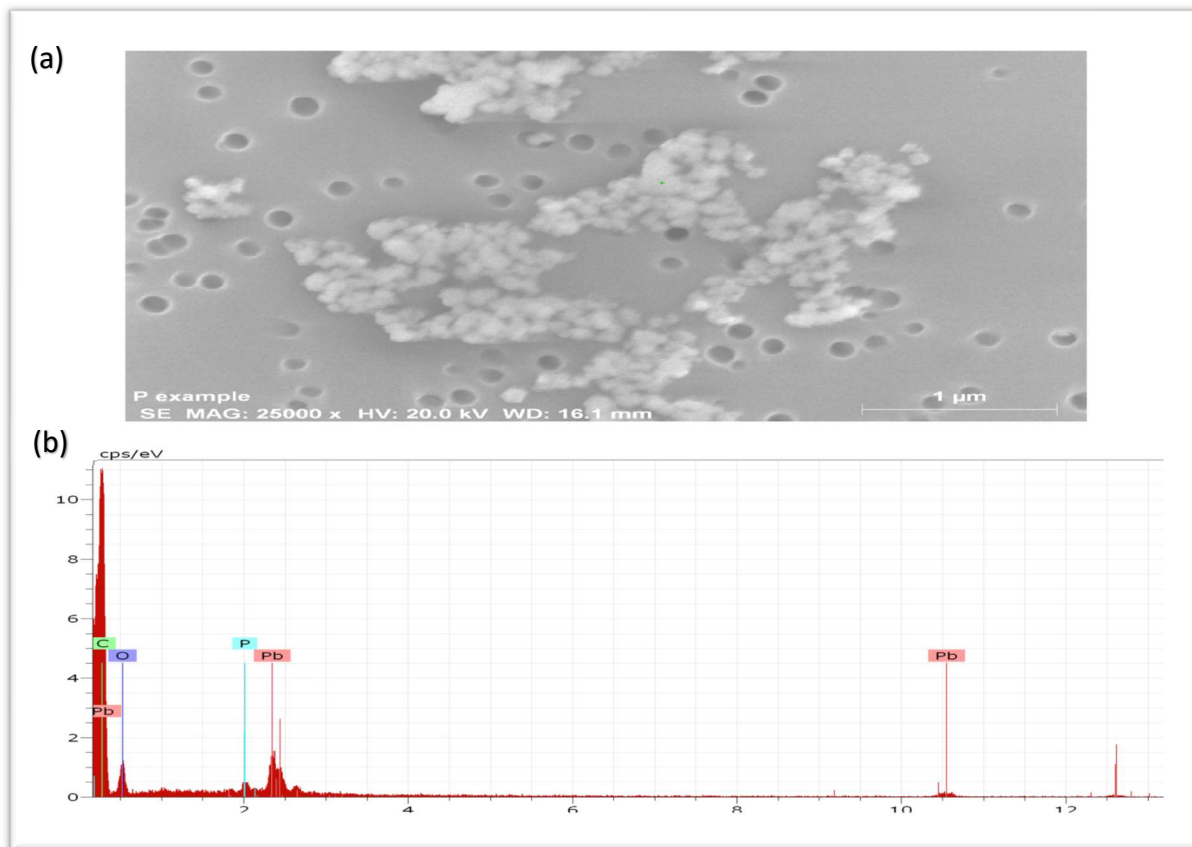


*error bars represent \pm standard error of the mean (SEM).

Study 3: Pb nitrate/synthetic sweat interaction

PbN in contact with SSFL readily forms clusters of insoluble particles generally $<1 \mu\text{m}$ in size (Figure 4-3a). These clusters of particles were determined to be insoluble Pb phosphate particles using EDX spectral analysis (Figure 4-3b).

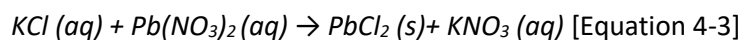
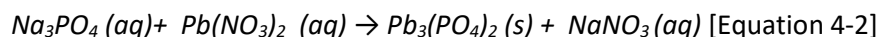
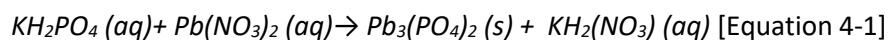
Figure 4-3. (a) Scanning Electron Micrograph, and (b) Energy Dispersive X-ray (EDX) Spectra Analysis of Lead (Pb) Phosphate Particles Formed by Mixing NIOSH Synthetic Sweat with Pb Nitrate



Discussion

PBS and McIlvaine solutions have been used in *in vitro* dermal penetration studies as receptor fluids (Pan et al., 2010; Filon et al., 2006; Julander et al., 2020) to estimate the potential for Pb compounds to diffuse across the skin. All three of these studies demonstrated that Pb does cross the skin barrier in appreciable amounts that, if applied to blood Pb models, suggest these dermal exposures may increase blood Pb levels (Filon et al., 2006; Julander et al., 2020; Niemeier et al., 2021). However, results of the current study suggest that the use of PBS, McIlvaine, and citrate buffers may not be appropriate for use as receptor solutions for *in-vitro* dermal penetration studies for PbN, because precipitate formation may result in an underestimation of Pb in receptor fluid, or on the skin in the case of SSFL.

A few mechanisms may account for the insolubility of PbN in PBS buffer, McIlvaine buffer, or SSFL. Both buffers and SSFL contain potassium phosphate, sodium phosphate, and potassium chloride. These compounds are known to react with PbN to form Pb phosphate or Pb chloride with the following reactions:



These reactions explain the visible precipitate observed when mixing PbN with PBS buffer, McIlvaine buffer or SSFL and demonstrated by the analysis of the precipitate (Pb phosphate) observed by EDX and SEM analysis (Figure 4-3).

PbN is also known to interact with sodium citrate to form an insoluble Pb citrate compound at pH<12 (Reynolds, 1963):



The results of the first experiment suggest that the concentration of phosphate or potassium in the buffer solution is driving the precipitate formation. At lower buffer concentrations (1X PBS and 1X McIlvaine), it appears that the reaction is rate limited by the concentration of buffer in the solution, since at higher concentration of PBS buffer (10x), there was approximately a 100-fold increase in the mass of precipitate formed (Figure 4-1). The mass of precipitate formed in the 1X PBS and 1X McIlvaine were roughly the same (Figure 4-1); however, the precipitate formed were not analyzed to determine if they were comprised of Pb phosphate, Pb citrate, or both.

The reaction of PbN and citrate buffer shown above (Equation 4-4) explains the reduced dissolution of PbN in citrate buffer in the dissolution experiment (Study 2) (Figure 4-3). In this experiment, the overall

dissolution of PbN in citrate buffer at the end of 24 hours was 5.9 µg/ml (Table 4-1). The maximum theoretical dissolution that could be achieved if all of the PbN powder loaded in the dissolution cell was fully dissolved ranged from 55.6 µg/ml (in 240 ml) to 166.7 µg/ml (in 80 ml) (Table 4-1). This maximum theoretical dissolution for this study is more than four orders of magnitude less than the reported solubility range of PbN in water @ 5.2×10^5 – 5.97×10^5 µg/ml @20-25°C; thus, the mass loaded on the filters would be expected to be fully dissolved in water. The dissolution of PbO in citrate buffer at the end of 24 hours was 9.1 µg/ml. The maximum theoretical dissolution for PbO ranged from 80.8 µg/ml (in 240 ml) to 242.5 µg/ml (in 80 ml) (Table 4-1). These theoretical values exceed the reported solubility of PbO in water (17.0–70.2 µg/ml @20-25°C). In this experiment, the dissolution of PbO at 1 h @36°C (19 µg/ml) is within the range of the published water solubility for PbO of 17.0–70.2 µg/ml @20-25°C (Pubchem, 2022i; Thermo Fisher Scientific, 2021) (Table 4-1). Further, the cumulative dissolution of PbO over 24 h was 9.1 µg/ml, which is within the same order of magnitude as its reported water solubility (17.0–70.2 µg/ml @20-25°C) (Pubchem, 2022i; Thermo Fisher Scientific, 2021). This suggests that the dissolution of PbO in citrate buffer is likely driven by its water solubility, and not impeded by precipitate formation.

Water solubilities are usually determined by OECD Guideline 105 (OECD, 1995) using either a column elution method for compounds with low water solubility (<0.01 g/l), or the flask method for compounds with higher water solubility (>0.01 g/l). These methods are different than the methodology used in this experiment to determine dissolution of these compounds in citrate buffer. However, using the water solubility of these compounds as a comparison to their dissolution in other solvents (e.g., citrate buffer) provides a useful benchmark to determine the suitability of buffers for skin penetration studies. The dissolution of these compounds in citrate buffer should roughly match their reported water solubilities if they are soluble in citrate buffer. It is important to note that in drinking water, several water chemistry factors influence the release of poorly water soluble Pb compounds, like PbO, from water pipes. These

include factors such as pH, temperature, concentration of chlorine residual, and dissolved oxygen content, among others (Kim et al., 2011).

In Guideline Method 28, the OECD has indicated for dermal *in-vitro* studies that, “the receptor fluid must have an adequate capacity to solubilize the test substance” (OECD, 2004a). The data presented in this paper have demonstrated that PBS, McIlvaine, and citrate buffers do not meet this criterion for PbN. Ferreira et al., (2015) published a review of interactions of buffers with metal ions, including Pb. They concluded that traditional buffers such as phosphate and citrate buffers are not ideal for use in biological systems, due to formation of complexes with cations, among other issues. They recommend that either 2-(N-morpholino)ethanesulfonic acid (MES) or 3-(N-morpholino)propanesulfonic acid (MOPS) buffers should be used for testing Pb compounds in biological systems (Ferreira et al., 2015). However, neither of these buffers were compatible with the available ICP-AES analytical methods available as part of this study. Further work to understand the incompatibilities of the components of these buffers with ICP-AES, and potentially exploring precipitation of these incompatible components prior to analytical analysis could be explored to determine if these buffers could be utilized for Pb-related skin penetration studies.

Although the ideal buffer for receptor solutions in *in-vitro* dermal penetration studies should allow for solubilization of the penetrant of interest, examination of the buffer’s physiological properties, namely an understanding of the components which may influence dermal penetration and absorption should also be considered. An observation in the current study was the almost immediate formation of a precipitate, determined to be Pb phosphate, when mixing PbN with SSFL (Figure 4-3). The synthetic sweat used in this study was a complex mixture developed by Harvey et al., (2010) consisting of 61 different constituents including electrolytes, organic acids, carbohydrates, amino acids, nitrogenous substances, vitamins, and other ionic constituents.

Though SSFL is likely not an appropriate receptor solution, it may offer some hints to the physiological processes that occur when PbN comes in contact with phosphate ion in blood plasma. Numerous factors contribute to the potential for percutaneous absorption of metals through skin. Hostýnek, (2003) describes several exogenous (e.g., dose, molecular volume, counter ion, etc.) and endogenous (e.g., skin factors, homeostatic controls, skin shunts, etc.) that influence the behavior of metals on skin. One factor is ion-counter-ion behavior of metal salts. Hostýnek et al., (2001) compared the dermal penetration of four nickel salts (chloride, sulfate, nitrate, and acetate) at 1% concentrations through stratum corneum in human volunteers. They found through tape stripping that the specific counter ions predicted penetration potential in the following order: acetate>nitrate>sulfate>chloride. In this case, it was surmised that the anion-pairing with Ni⁺ ion drives this passive diffusion effect (Hostýnek et al., 2001). This ion-counter-ion effect has also been proposed for the penetration mechanism of nickel chloride by Fullerton et al., (1986). The role of the nitrate counter ion in PbN penetration may be driven by the same effect. In the case of nickel salts, the primary effect is allergic skin reactions in sensitized individuals, with <2% of soluble nickel compounds and <0.2% of insoluble nickel compounds absorbed through dermal exposure (Buxton et al., 2019; Fullerton et al., 1986; Tanojo et al., 2001).

There are some limitations to the studies presented in this chapter. Study 1 was designed as a quick screening tool to evaluate the formation of precipitates when combining PbN and different buffers. Only one sample was collected per experimental group, so measurements of error or statistical analysis could not be conducted as part of this study. Also, as similarly discussed in Chapter 2, there are some limitations to this dissolution assay study design in Study 2. The entire volume of SSFL (80 ml) was replaced at each timepoint in the experiment (1, 6, 24 h), rather than sampling a small aliquot of SSFL solution, which follows a previously published method (Kanapilly et al., 1973; Stefaniak et al., 2005; Stefaniak, et al., 2010a). The impact of the specific volume of SSFL used in this experiment on Pb dissolution was not explicitly evaluated. It is unknown if, at each timepoint, the Pb fraction dissolved in

solution reached a concentration close to the maximum solubility limit of the Pb compounds in solution based on the volume of SSFL used. This influence is likely more pronounced in the dissolution of PbN compared to PbO, since there appeared to be an interaction between citrate buffer and PbN. Another limitation that could impact both PbN and PbO is that this study used a static dissolution chamber with two 0.025 μm pore size, 47 mm diameter filters with the Pb metals loaded on a third filter sandwiched in between these filters. In this setup, the dissolving solution (SSFL) needs to diffuse through the filter pores, which adds a mass transfer resistance on the system that could slow the dissolution kinetics. Additionally, there is a lag time when the dissolution chamber containing the Pb compounds may be surrounded by air. This could occur when the dissolution chamber is initially submerged in the SSFL and during each SSFL change. This could result in a further slowing of the dissolution rate that was measured. Additionally, the influence of particle size on dissolution was not evaluated in this study and could impact dissolution kinetics. Lastly, since both Pb compounds tested in this study were loaded into filters based on total mass (including weight of salt or oxide) instead of Pb mass only, it is difficult to compare dissolution rates between these metals. However, even with these limitations, the values provided in this paper provide screening level estimates of the concentration of Pb ion that may dissolve on skin in the presence of sweat. This area of research deserves further study and refinement to better understand the dissolution of Pb compounds on skin.

Chapter 5. Screening Dermal Absorption Modeling Using Key Percutaneous Absorption and Dissolution Parameters

Introduction

One of the primary aims of this dissertation work is to better understand the potential impact of dermal iPb exposure on BLLs. As described in Chapter 2, dermal loading of iPb compounds with values as high as 16.1 $\mu\text{g}/\text{cm}^2$ on hands have been measured in workplace environments (Table 2-1). Additionally, data from Chapter 2 suggest that Pb compounds (PbN, PbA, PbO, and PbRO) ionize in the presence of synthetic sweat, which suggest the availability of Pb ions on skin in the presence of sweat. Data presented in Chapters 1 and 3 also suggest *in vitro* iPb compounds penetrate into the skin and receptor fluids (Bress and Bidanset, 1991; Filon et al., 2006; Pan et al., 2010; Julander et al., 2020). Additionally, *in-vivo* experiments of dermal exposures conducted in humans and other animals have demonstrated systemic distribution of Pb into other organ systems (Pounds, 1979; Moore et al., 1980; Bress and Bidanset, 1991; Pan et al., 2010). Previous estimates of the potential impact of Pb percutaneous absorption have been published by Filon et al., (2006), Julander et al., (2020) and Pounds, (1979) for iPb compounds (discussed in Chapter 1). Filon et al., (2006) estimated a steady-state increase in blood Pb levels of 2.5 $\mu\text{g}/\text{dl}$ (confidence intervals—0.3, 5.1) for PbO, if the exposure were to occur on unwashed hands and arms for 250 days/year. Julander et al., (2020) estimated that steady-state blood Pb levels would increase from 3.34 to 6.33 $\mu\text{g}/\text{dl}$ from dermal absorption of Pb through metal cutting fluids estimated in pig skin. Both the BLL estimates by Filon et al., (2006) and Julander et al., (2020) were based on diffusion rates of 1.2×10^{-4} $\mu\text{g}/\text{cm}^2/\text{h}$ for Pb through skin and using the US EPA adult Pb model (EPA, 2003). Pounds, (1979) estimated that the total absorbed dose for dermal exposures to PbA in hair dye in rats occurring 3 times a week for 4 weeks would result in an estimated 1.2×10^{-2} $\mu\text{g}/\text{cm}^2$ in humans, with the assumption that 80% of the Pb in the hair dye would be bound to hair, though this assumption may underestimate the absorption of PbA through skin when not used as a hair dye.

It is also possible to provide a screening level estimate of the impact of dermal exposures on BLLs with data collected as part of this dissertation work that is different than the methodologies used by Filon et al., (2006), Julander et al., (2020), and Pounds, (1979). Based on feedback from Dr. Annette Bunge, a method of estimation of dermal bioavailability can be derived from the dissolution data in Chapter 2, as well as K_p estimates identified in Chapter 1. In this case, the α and β_1 values from Table 2-3 can be used with a permeation rate estimate (K_p) (Table 1-2), to estimate the amount of ion absorbed per area of skin (M_{abs}/A).

The primary objective of calculating this screening level estimate is to determine if the potential impact on BLLs is greater than a *de minimus* additional exposure (defined as an increase of BLL >1 $\mu\text{g}/\text{dL}$). This value is based on the typical LOD for graphite furnace atomic absorption spectrometry for detecting Pb in blood (WHO, 2011). Screening level estimates >1 $\mu\text{g}/\text{dL}$ suggest that a more comprehensive assessment of the impact of dermal exposures on BLLs should be conducted.

Method

The M_{abs}/A was calculated by the following formula for the four Pb compounds evaluated in the dissolution assay in Chapter 2 (PbA, PbN, PbO, PbRO):

$$M_{abs}/A (\mu\text{g}/\text{cm}^2) = K_p (\text{cm}/\text{h}) * C_{dis,skin} (\mu\text{g}/\text{cm}^3) * \text{time (h)} \text{ [Equation 5-1]}$$

Two K_p values were used to provide a range of estimated impact to BLLs. The K_p values chosen for this modeling exercise were 3×10^{-5} and 1×10^{-4} cm/h for all Pb compounds. The K_p estimate of 3×10^{-5} cm/h is the highest K_p value identified in Chapter 1 (Table 1-2) for PbA absorption through rat skin, based on the *in-vivo* percutaneous absorption study by Pounds, (1979). The K_p estimate of 1×10^{-4} cm/h is a general estimate similar to several ionized chemicals and other inorganic chemicals and provides a worst-case estimate of percutaneous absorption (Vecchia and Bunge, 2002). Though this value is higher than experimental values summarized in Chapter 1 (Table 1-2) for iPb compounds, most of the dermal

penetration data identified for iPb compounds were not collected using standard test guideline-compliant methods (EPA, 1992, 1998, 2007; OECD, 2004a,b, 2011; EFSA, 2012), thus their accuracy is unknown. Using this K_p estimate (1×10^{-4} cm/h) provides a worst case estimate for the impact of the exposures in this model.

$C_{dis,skin}$ is the dissolved concentration ($\mu\text{g/ml}$) of Pb ions available on the skin at time (t) (assumed to be 8h for typical occupational exposures).

$$C_{dis,skin} = C_{high} (1 - \exp(-\beta_{1skin} * t)) \text{ [Equation 5-2]}$$

Where C_{high} is equal to the maximum dissolved concentration ($\mu\text{g/ml}$) of Pb ion in sweat in the experiment

$$C_{high} = (M_{o(exp)}/V_{exp}) * \alpha \text{ [Equation 5-3]}$$

As discussed in Chapter 2, the concentration of Pb ion in SSFL is dependent on volume of SSFL. A ratio was calculated to determine the mass of Pb loaded onto filters in the volume of SSFL in the experiment ($M_{o(exp)}/V_{exp}$) to the maximum observed Pb loaded onto skin in occupational environments in an estimated volume of sweat on the skin surface ($M_{o(skin)}/V_{skin}$). This value was multiplied by β_1 to determine an estimate of β_1 on the skin for an estimated Pb dermal load (β_{1skin}).

$$\beta_{1skin} = \beta_1 (M_{o(skin)}/V_{skin}) / (M_{o(exp)}/V_{exp}) \text{ [Equation 5-4]}$$

The $M_{o(skin)}$ was assumed to be $16.1 \mu\text{g/cm}^2$, which is the highest estimated dermal loading value identified in the literature (Table 2-1).

V_{skin} was assumed to be $5 \mu\text{l/cm}^2$ (5×10^{-3} cm), which is based on the film thickness of water on skin after immersion (EPA, 2011).

The resulting M_{abs}/A ($\mu\text{g}/\text{cm}^2$) provides an estimate of absorbed Pb ion into skin. A biokinetic slope factor calculated by EPA, (2003) to estimate the impact of daily Pb absorption on BLLs was used. In this case, a steady-state blood level of 0.4 $\mu\text{g}/\text{dL}$ for each μg of Pb absorbed per day was used. This EPA, (2003) biokinetic slope factor was previously used by Filon et al., (2006) and Julander et al., (2020) to estimate BLLs based on the percutaneous absorption data in those studies. Pb absorbed per day was calculated for hands with an estimated surface area of 1070 cm^2 (EPA, 2011).

Results

Table 5-1 provides the model outputs to determine M_{abs}/A and application of these values to approximate total absorption of Pb through hand skin, estimated to have surface area of 1070 cm^2 (EPA, 2011) for 8 h of exposure and assuming a skin loading value of $16.1 \mu\text{g}/\text{cm}^2$ of PbO identified in occupational settings (Table 2-1). The predicted M_{abs}/A estimates range from 3.0×10^{-5} – $1.9 \times 10^{-2} \mu\text{g}/\text{cm}^2$ across all four Pb compounds, with PbO and PbRO having lower absorption compared to PbN and PbA compounds (Table 5-1). The M_{abs}/A values applied to the surface of hands result in estimated absorption for PbRO of 4×10^{-2} – $1.7 \mu\text{g}/\text{hands}/8 \text{ h}$ and 0.5 – $2.8 \mu\text{g}/\text{hands}/8 \text{ h}$ for PbO. The estimated impact on BLL for the PbO and PbRO compounds, based on a projected steady-state increase of $0.4 \mu\text{g}/\text{dL}$ for each μg of lead absorbed per day (Filon et al., 2006; EPA, 2003), ranged from 0.01 – $0.7 \mu\text{g}/\text{dl}$ of blood if exposures were limited to hands only (Table 5-1).

For the PbN and PbA compounds, the M_{abs}/A values range from 3.4×10^{-3} – $1.9 \times 10^{-2} \mu\text{g}/\text{cm}^2$ for PbN and 3.6×10^{-3} – $1.6 \times 10^{-2} \mu\text{g}/\text{cm}^2$ for PbA (Table 5-1). The M_{abs}/A values applied to the surface of hands result in estimated absorption for PbN of 3.67 – $19.99 \mu\text{g}/\text{hands}/8 \text{ h}$ and 3.86 – $17.60 \mu\text{g}/\text{hands}/8 \text{ h}$ for PbA (Table 5-1). The estimated impact on BLL for the PbN and PbA compounds based on a projected steady-state increase of $0.4 \mu\text{g}/\text{dL}$ for each μg of Pb absorbed per day (Filon et al., 2006; EPA, 2003) ranged from 1.5 – $8.0 \mu\text{g}/\text{dl}$ of blood if exposures were limited to hands only (Table 5-1).

Table 5-1. Estimates of the Concentration of Lead (Pb) Ion Available on Skin to Estimate the Amount of Pb Absorbed Through the Hands and Impact on Blood Lead Levels

Compound	pH	$M_{o(skin)}/V_{skin}$ ($\mu\text{g}/\mu\text{l}$) [*]	$M_{o(exp)}/V_{exp}$ ($\mu\text{g}/\mu\text{l}$) [†]	β_{1skin} [§]	C_{high} ($\mu\text{g}/\mu\text{l}$) [¶]	$C_{dis,skin}$ ($\mu\text{g}/\mu\text{l}$) ^{**}	M_{abs}/A ($\mu\text{g}/\text{cm}^2$) ^{††}	Pb absorbed by hands per working day (8 h) ($\mu\text{g}/\text{hands}$) ^{§§, ¶¶}	Screening estimated increase to blood lead level for Pb exposure on hands ($\mu\text{g}/\text{dL}$) ^{¶¶, ***}
PbO	5.3	2.5	0.060	7.00	2.1	2.1	5.0×10^{-4} - 1.7×10^{-3}	0.5-1.8	0.2-0.7
	6.5	2.5	0.056	7.5×10^{-3}	55.60	3.2	7.7×10^{-4} - 2.6×10^{-3}	0.8- 2.8	0.3-1.1
PbRO	5.3	2.5	0.059	3.0×10^{-4}	58.9	0.14	3.0×10^{-5} - 1.0×10^{-4}	4×10^{-2} -0.1	0.01-0.05
	6.5	2.5	0.053	4.8×10^{-3}	52.9	2.0	4.7×10^{-4} - 1.6×10^{-3}	0.5-1.7	0.2-0.7
PbN	5.3	2.5	0.039	37.1	14.3	14.3	3.4×10^{-3} - 1.1×10^{-2}	3.7-12.2	1.5-5.0
	6.5	2.5	0.039	83.8	23.4	23.4	5.6×10^{-3} - 1.9×10^{-2}	6.0-20.0	2.4-8.0
PbA	5.3	2.5	0.040	76.9	15.0	15.0	3.6×10^{-3} - 1.2×10^{-2}	3.9-12.9	1.5-5.1
	6.5	2.5	0.040	44.2	20.6	20.6	4.9×10^{-3} - 1.7×10^{-2}	5.3-17.6	2.1-7.0

* $M_{o(skin)} = 16.1 \mu\text{g}/\text{cm}^2$ (Table 1- highest estimated dermal loading of PbO). This value was adjusted $12.6 \mu\text{g}/\text{cm}^2$ based on a hand surface area of 1070 cm^2 ($(16.1 \mu\text{g}/\text{cm}^2 * 840\text{cm}^2)/1070\text{cm}^2 = 12.6 \mu\text{g}/\text{cm}^2$); V_{skin} = estimated to be $5 \mu\text{l}/\text{cm}^2$ ($5 \times 10^{-3} \text{ cm}$)- based on film thickness of water on skin after immersion (EPA, 2011)

† $M_{o(exp)}$ = see Table 3; V_{exp} = 240 ml

§ Equation 5-4

¶ Equation 5-3

** Equation 5-2

†† Equation 5-1

§§ Surface areas of hands estimated to be 1070 cm^2 (EPA, 2011).

¶¶ Ranges reflect calculations based on Kp values of $3 \times 10^{-5} \text{ cm}/\text{h}$ (Table 1-2, Pound, 1979) and $1 \times 10^{-4} \text{ cm}/\text{h}$ (Vecchia and Bunge, 2002)

*** Filon et al., (2006) and Julander et al., (2020) cited an increase in the steady-state blood level of $0.4 \mu\text{g}/\text{dL}$ for each μg of Pb absorbed per day, based on a biokinetic slope factor developed by EPA, (2003).

Discussion

The modeling approach discussed in this chapter provides a screening tool to better understand whether dermal exposures to iPb compounds result in increased absorption of Pb and impact BLLs. The results of the model suggest that the M_{abs}/A varied by approximately 3 orders of magnitude (3.0×10^{-5} – 1.9×10^{-2} $\mu\text{g}/\text{cm}^2$) across the four Pb compounds evaluated, with PbRO exhibiting the lowest amount of potential absorption, and PbN and PbA exhibiting the highest potential absorption (Table 5-1). These absorption values, applied to the surface area of hands (1070 cm^2) (EPA, 2011), suggest daily dermal absorptions ranging from 1×10^{-2} to $20 \text{ ug Pb /workday}$ (assuming 8 h of exposure).

For PbO, which is the iPb compound with the most dermal exposure data identified in occupational settings (Table 2-1), the model suggests daily dermal absorption rates ranged from 0.5 – $2.7 \text{ }\mu\text{g Pb /workday}$. The American Conference of Governmental Industrial Hygienists (ACGIH, 2021) provides estimates of daily intake of Pb in the general U.S. population of 2 – $9 \text{ }\mu\text{g/day}$, with an additional $6 \text{ }\mu\text{g/day}$ of daily Pb intake for smokers. Additionally, the U.S. Food and Drug Administration (FDA) has set an Interim Reference Level (IRL) for dietary Pb exposure for women of childbearing age and other adults to be $12.5 \text{ }\mu\text{g/day}$, which this amount of Pb in food a person would need to consume daily that would result in an estimated BLL of $5 \text{ }\mu\text{g/dl}$ (FDA, 2020).. This suggests PbO occupational dermal exposure on hands represents a minimal addition to the daily Pb intake compared to non-occupational sources. The model output suggests that the impact to steady-state BLLs for PbO ranges from 0.2 – $1.1 \text{ }\mu\text{g/dL}$ (Table 5-1). In the context of occupational exposure limits, ACGIH has a Biological Exposure Index (BEI®) of $20 \text{ }\mu\text{g/dL}$ for iPb compounds (ACGIH, 2017). The impact of the estimated exposures in this screening model would represent $\sim 0.1\%$ – 6% of this BEI for exposure to PbO. For PbRO, daily absorption rate estimates were 4×10^{-2} – $0.7 \text{ }\mu\text{g Pb/workday}$, which is less than the estimates for PbO. The BLL impact of PbRO exposures ranged from 0.01 – $0.7 \text{ }\mu\text{g/dL}$, representing 0.05% – 3.5% of the ACGIH BEI for iPb compounds (ACGIH, 2017).

For PbN and PbA, the model suggests that dermal absorption rates are substantially higher, ranging from 3.7-20 $\mu\text{g Pb/workday}$ (Table 5-1). The high end of this range exceeds the estimated daily intake of Pb by the U.S. general population, including for smokers (2–15 $\mu\text{g/day}$) (ACGIH 2017), and the FDA IRL of 12.5 $\mu\text{g/day}$ (FDA, 2020). Additionally, the estimated steady-state BLLs, based on the model for exposures to PbA and PbN ranged from 1.5–8.0 $\mu\text{g/dL}$, representing 7.5%–40% of the ACGIH BEI for iPb compounds (20 $\mu\text{g/dL}$) (ACGIH, 2017, 2021). In occupational environments where other routes of exposure to iPb may be relevant, these dermal exposure estimates could represent a significant relative source contribution to overall body burden of Pb exposure. Additionally, these model-estimated BLLs exceed BLLs associated with adverse health effects in adults, determined by the National Toxicology Program, (2012) (<5 $\mu\text{g/dL}$).

Interestingly, for PbO at pH 5.3, and PbA and PbN at both pH's (5.3 and 6.5), the estimated C_{high} and C_{dis} values did not change at the assumed skin loading concentration of 12.6 $\mu\text{g/cm}^2$ identified in the literature (Table 2-1). It is estimated that real-world skin loading concentrations as low as 0.9 $\mu\text{g/cm}^2$ for PbO would result in the same estimated BLL increase, based on the model outputs. For PbA and PbN, real world skin load concentrations of 0.1–0.2 $\mu\text{g/cm}^2$ would result in the same estimated BLL as higher skin loading concentrations, based on model outputs. This suggests that dissolution of these compounds is high, with the maximum concentration of Pb ions available on the skin, even at lower skin loading conditions.

There are some important limitations of this model. First, K_p values of 3×10^{-5} – 1×10^{-4} cm/h, which are based on a range taken from both the scientific literature (Niemeier et al, 2021; Pounds, 1979) and approximations for other inorganic and ionized chemicals were used in the model assumption (Vecchia and Bunge, 2002). As discussed in Chapter 1, the K_p values available for iPb compounds were not collected using standard test guideline-compliant methods and their accuracy is unknown (EPA, 1992, 1998, 2007; OECD, 2004a,b, 2011; EFSA, 2012). The impact of the K_p value used for model selection has

a substantial impact on the estimated mass of Pb absorbed through the skin. Further work to generate K_p values based on standard test guideline-compliant methods is critical. Second, as discussed in the limitations section of Chapter 2, the influence of particle size on dissolution of Pb compounds in SSFL was not evaluated and accounted for in this model. Third, this model assumes exposures to the hands only. Data from Hughson, (2005) suggest Pb dermal loading in Pb refinery, Pb/Zn refinery, and Pb chemical processing environments that dermal load across hands, arms, face, neck, and chest all exceed a median value of $2.1 \mu\text{g}/\text{cm}^2$ for each of these body parts. This suggests that at least in refinery settings, dermal exposures occurred on other surface areas of the body, which could increase estimated Pb dermal absorption. Lastly, the model does not account for several workplace variables such as handwashing through the day, longer work durations (>8h), or the potential for increased absorption through damaged skin, as discussed by Filon et al., 2006. These variables could also impact model outputs.

The screening level estimates based on this model suggest that the impact on BLLs is greater than a *de minimus* additional exposure (defined as $>1 \mu\text{g}/\text{dL}$) for PbO, PbN, and PbA. This suggests that a more comprehensive assessment of the impact of Pb dermal exposures on BLLs is needed. In occupational environments where other routes of exposure to Pb may be relevant, these dermal exposure estimates could represent a significant relative source contribution to overall body burden of Pb exposure. Further examination of the impact of dermal exposures on BLLs could also be incorporated into PBPK modeling efforts to further understand the impact of these exposures on BLLs.

Chapter 6. Conclusions and Future Directions

Conclusions

This dissertation work identifies percutaneous absorption data for four iPb compounds (PbA, PbN, PbO, and Pb metal) from the published literature that may inform PBPK models for the purpose of better understanding the systemic dose resulting from dermal exposures. These data included the calculation of average diffusion rate values across animal and human skin ranging from 10^{-7} – 10^{-4} mg/cm²/h, and K_p values ranging from 10^{-7} – 10^{-5} cm/h. These values are within the same order of magnitudes of other inorganic metals and organic Pb compounds where dermal absorption is of concern (Hostýnek et al., 1993; Hostýnek, 2003; Hostýnek and Maibach, 2006; Franken et al., 2015).

Several lines of evidence suggest that dermal exposure to iPb compounds is an important exposure pathway for absorption of Pb into the body, but the majority of these studies are difficult to interpret or use to estimate the body burden of Pb exposure using PBPK modeling. However, the estimates identified in this review may permit screening assessments that support the need for data collection using standard test guideline-compliant methods that can then be used for quantitative risk assessments. The data yielded estimates of high variability over orders of magnitude and need refinement for generating an assessment with reasonable degree of confidence. Nevertheless, the calculated values and limited *in vivo* data all strongly support that a significant contribution of dose from the dermal route cannot be excluded.

In Chapter 2 this dissertation presents the first known study to quantitatively evaluate the bioaccessibility of Pb compounds in SSFL. All iPb compounds (PbA, PbN, PbO, and PbRO) evaluated are bioaccessible in SSFL, though PbN and PbA appeared to have higher dissolution (36.4%–61.1%) compared to PbO and PbRO (0.01%–2.5%) at an occupationally-relevant timepoint of 8 h. Additionally, pH has a statistically significant effect on bioaccessibility for all four compounds tested, although the directionality of this relationship varied by iPb compound. Using these data along with dermal loading

estimates of Pb compounds in workplace settings provides a starting estimate for the concentration of Pb ions in the sweat layer on skin, which can be used along with K_p to provide more robust understanding for the potential for dermal penetration and absorption of these compounds.

Four *in vitro* Franz cell pilot studies were presented (Chapter 3), including one infinite and three finite dosing studies, to examine the percutaneous absorption potential for PbN through human skin. None of the studies resulted in the detection of Pb in receptor fluid; however, Pb was detected in washed skin in all four studies. In one study, Pb was detected in both the epidermis and dermis layers after a 72-h exposure study. Roughly estimated K_p values of $10^{-3} - 10^{-4}$ cm/h and diffusion rates of $10^{-2} - 5$ $\mu\text{g}/\text{cm}^2/\text{h}$ across these studies were estimated based on concentration of Pb observed in the skin. These values were within the ranges of percutaneous absorption values identified for Pb compounds in Chapter 1. These experiments also demonstrate that a 4-wash protocol removes Pb from the surface of the skin, which is an important consideration when determining Pb content in the skin. Lastly, Pb recovery from the skin ranged from 22%–64% across two studies. It was observed during the skin dissolution process with concentrated acids that the skin was not fully dissolving, and filtering was required before analysis with ICP-AES. It is likely that Pb was still bound up in undissolved skin, reducing recovery of Pb from the experimental system.

An evaluation of the potential interactions of PbN in PBS, McIlvaine, and citrate buffer, as well as in SSFL were presented in Chapter 4. This chapter also presents data to evaluate the potential interaction of PbO in McIlvaine buffer. The results suggest that PbN interacts with PBS, McIlvaine, and citrate buffers, and SSFL, to form poorly water-soluble precipitates (Pb phosphate or Pb citrate). These buffers are not suitable as receptor fluids for PbN Franz cell studies. PbO does not appear to interact with citrate buffer to form precipitates and thus would be a suitable option for Franz cell studies for this Pb compound. It is important to evaluate the type of receptor fluid used for skin penetration studies. Further testing to identify a suitable buffer for PbN Franz cell studies is needed. Additionally, further testing is needed to

determine if other buffers, such as PBS, are suitable for PbO-related Franz cell studies. The methodologies presented in this Chapter may also be useful for screening the applicability of buffers for use as Franz cell receptor fluids for other Pb compounds.

A screening model for dermal exposures to predict a range of steady-state BLLs for four iPb compounds (PbO, PbRO, PbA, PbN), based on two K_p values and estimates of bioaccessible Pb ions in SSFL was presented in Chapter 5. These screening estimates suggest that dermal exposures identified in the literature may increase BLLs by as much as 1.1 $\mu\text{g}/\text{dL}$ for PbO, 0.7 $\mu\text{g}/\text{dL}$ for PbRO, and 4–8 $\mu\text{g}/\text{dL}$ for PbN and PbA. The screening estimates for PbO, PbA, and PbN exceed 1 $\mu\text{g}/\text{dL}$, which is the typical LOD for graphite furnace atomic absorption spectrometry for detecting Pb in blood (WHO, 2011). These results suggest that the impact of dermal exposures to some iPb compounds may impact BLLs beyond a *de minimus* additional exposure, suggesting the need for a more comprehensive evaluation of the impact of dermal exposures on BLLs. This includes understanding the impact of potential exposures on other body surfaces (e.g. neck, torso, arms) a, understanding the potential influence of particle size on absorption, and additional research to determine K_p values based on standard test guideline-compliant methods (EPA, 1992, 1998, 2007; OECD, 2004a,b, 2011; EFSA, 2012). Importantly, these results suggest a need to reduce Pb exposure on skin. Exposure reduction strategies could include such measures as wearing skin protection when working with Pb materials, and using lead removal soap frequently during periods with potential skin deposition of lead compounds when leaving the manufacturing areas before breaks, lunch, and at the end of the shift. Additionally, the use of colormetric wipe indicators, like the Full Disclosure® Lead Detection sampling kit (SKC, 2022) can provide quick results to modify worker cleaning behavior to ensure that Pb was adequately removed from the skin.

Future Directions

Based on NAICS code and BLS estimates, there are at least 1,456,000 workers in industries with dermal exposures to Pb compounds (Table 2-2). Additional research on the measurement and impact of

percutaneous absorption of Pb compounds is needed to better understand the relative source contribution of dermal exposures on Pb internal dose. The following areas of future directions are recommended:

Percutaneous Absorption Studies

There is a critical need for additional *in-vitro* percutaneous absorption studies to better understand the potential for dermal penetration of iPb compounds. Future percutaneous absorption studies should be conducted according to standard test guideline-compliant methods (EPA, 1992, 1998, 2007; OECD, 2004a,b, 2011; EFSA, 2012) and other recommendations on *in vitro* permeation studies provided in the scientific literature (Hostýnek, 2003; Franken et al., 2015). Studies that evaluate Pb absorption in both finite and infinite dosing regimens are important; however, it is recommended that the priority is to derive K_p values for Pb compounds, conducted using infinite dosing studies. K_p values derived from studies using standard test guideline-compliant methods would provide more reliable data for model assumptions to estimate the systemic impact of dermal exposure to Pb compounds. Future finite studies conducted under realistic exposure conditions will also help further refine an understanding of the percutaneous absorption potential of Pb compounds. This would include continuing studies like those presented in Chapter 3 to examine realistic exposure conditions, such as the influence of SSFL and multiple exposures, to determine flux and diffusion rates for Pb compounds.

Some specific considerations for future percutaneous absorption studies may include the following:

Selection of appropriate receptor solutions for Franz cell studies

PBS, McIlvaine, and citrate buffer solutions are not appropriate receptor solutions for Franz cell studies examining the percutaneous absorption of PbN, as discussed in Chapters 3 and 4. Further studies are necessary to identify a buffer solution that: 1) does not precipitate when in contact with PbN, and 2) is conducive to available analytical analyses. Dissolution assays, like those presented in Chapter 4 may serve as a good screening test to determine an appropriate receptor fluid for Pb compounds.

Alternatively, OECD, (2004b) suggests that for non-viable skin preparations, a saline solution at pH 7.4 can be used. However, since this is not a buffered solution, the potential impact of changing pH of the receptor solution, particularly if in contact with NO_3^- , in the case of PbN studies, should be evaluated.

Analytical determination of Pb content in skin

Further work is needed to maximize the recovery of Pb in skin. In studies presented in Chapter 3, the recovery of Pb from skin using concentrated and heated acids (HNO_3 and HCl), in a modified NIOSH 7303 method only resulted in recoveries of 21.9%-63.9% of the mass of the Pb dosed on the skin. These acids were unable to fully dissolve skin samples, and skin sample solutions required filtration before ICP-AES analysis. It is likely that Pb content in undissolved skin reduced the recovery of Pb in the experimental system. Future empirical work is needed to maximize the dissolution of skin using these acids. This could include techniques such as: 1) increasing the contact time with each acid, and 2) cutting skin samples into smaller pieces to increase the surface area contact with acids. If these method improvements do not increase recoveries of Pb from skin samples to an acceptable value (~90%-100% of dosed Pb), an alternative option would be to develop a correction factor for Pb recovery in the skin for Franz cell experiments. In this case, a set of Pb recovery samples could be run in each Franz cell experiment (similar to methods for "Pb Recovery Studies- Chapter 3"), and the efficiency of the recovery of Pb in these samples (correction factor) could be applied to other samples in the experiment.

Determination of Pb through stratum corneum

Further work to better understand the kinetics of Pb penetration through the stratum corneum is needed. Methods to determine how quickly Pb is penetrating through the stratum corneum using tape stripping methodologies have been outlined by OECD, (2004b) and Trebilcock et al., (1994).

Dissolution of Pb Compounds in SSFL

Impact of specific volume of SSFL on dissolution

In the Pb dissolution studies presented in Chapter 2, the impact of the specific volume of SSFL to the mass of Pb loaded on the filters was not evaluated. It is unknown if, at each timepoint, the Pb fraction

dissolved in solution reached a concentration close to the maximum solubility limit saturation concentration of the Pb compounds in solution, based on the volume of SSFL used. This influence of the sampling volume could influence the dissolution of iPb compounds used and should be further evaluated. An additional experiment that could be conducted would be to repeat the experiments presented in Chapter 2, but instead of replacing the entire volume of SSFL at each sampled timepoint, collect only a small aliquot of SSFL from the experimental system. This experimental change would provide additional information on if the maximum dissolution of these Pb compounds was occurring, based on the volumes of SSFL used in the experiment. Additionally, future experiments to vary the mass-to-volume ratio of Pb compounds to SSFL to more closely match conditions found in occupational environments should be considered.

Impact of particle size on dissolution

In the Pb dissolution studies presented in Chapter 2, the impact of particle size on dissolution was not evaluated. Particle size could influence dissolution and has been suggested as a predictor for metal ion release. Specifically, smaller particle sizes may have increased potential for increased ion exposure on skin, due to the increased surface area of the metal in contact with sweat (Nowack et al., 2011). It is recommended that future dissolution studies evaluate the influence of particle size of Pb compounds in the study designs. Ideally, future Pb dissolution studies should be conducted with powders collected from industrial settings, which will provide more occupationally-relevant estimates of dissolution, which could then be used to update dermal absorption models.

Dermal Absorption Modeling Refinement

The dermal absorption model presented in Chapter 5 presents a screening approach to better understand the potential impact of dermal exposures to iPb compounds. Additional occupational exposure data are needed to better understand dermal load of Pb compounds, particularly for PbA and PbN, for which no dermal exposure data were identified. Additionally, the model could be further

updated to account for skin loading of Pb across different body parts to better assess the impact of Pb absorption on BLLs. Lastly, dermal absorption models, like the one presented in Chapter 5, should be incorporated into PBPK models to better understand the influence of the dermal absorption route, along with along with co-exposures via gastrointestinal and inhalation routes, to determine the impact on BLLs.

Bibliography

- AAT Bioquest, Inc. (2021). *Citrate Buffer (pH 3.0 to 6.2).* Webpage: <https://www.aatbio.com/resources/buffer-preparations-and-recipes/citrate-buffer-ph-3-to-6-2>. Accessed January 2022
- American Conference of Governmental Industrial Hygienists (ACGIH®) (2017). Lead and Inorganic Compounds BEI®, ACGIH, Cincinnati, OH.
- American Conference of Governmental Industrial Hygienists (ACGIH®) (2021). 2021 TLVs® and BEIs® with 9th edition documentation, ACGIH, Cincinnati, OH.
- Anderson SE, Meade BJ. (2014). Potential health effects associated with dermal exposure to occupational chemicals. *Environ Health Insights*; **8**: 51-62.
- Aplin RT, Buston JEH, Moloney MG. (2002). Detection of aryllead (IV) carboxylates and their solvent adducts by ESI-mass spectrometry. *Journal of Organometallic Chemistry*; **645**: 176-82.
- ATSDR (Agency for Toxic Substances and Disease Registry). (2020a) ATSDR toxzine-lead. Atlanta, GA: U.S. Department of Health and Human Services, Public Health Service. Available at https://www.atsdr.cdc.gov/sites/toxzine/lead_toxzine.html#information. Accessed September 2021.
- ATSDR (Agency for Toxic Substances and Disease Registry). (2020b) *Toxicological profile for lead*. Atlanta, GA: U.S. Department of Health and Human Services, Public Health Service.
- Aurell J, Holder AL, Gullett BK, McNesby K, Weinstein JP. (2019). Characterization of M4 carbine rifle emissions with three ammunition types. *Environ Pollut*; **254**: 112982.
- BLS (U.S. Bureau of Labor Statistics). 2021. Databases, tables and calculators by subject. Website: [Databases, Tables & Calculators by Subject \(bls.gov\)](https://www.bls.gov/databases-tables-calculators-by-subject/). Date accessed: September 2021.
- Bress WC, Bidanset JH. (1991) Percutaneous *in vivo* and *in vitro* absorption of lead. *Vet Hum Toxicol*; **33**: 212-4.
- Buston JEH, Moloney MG, Parry AVL, Wood P. (2002). Rate enhancing ligands for lead (IV)-mediated arylations. *Tetrahedron Letters*; **43**: 3407-09.
- Buxton et al. (2019). Concise Review of Nickel Human Health Toxicology and Ecotoxicology. *Inorganics*, **7**, 89; doi:10.3390/inorganics7070089
- Callewaert C, Buyschaert B, Vossen E, Fievez V, Van de Wiele T, Boon N. (2014). Artificial sweat composition to grow and sustain a mixed human axillary microbiome. *Journal of Microbiological Methods*; **103**: 6-8.
- Cao X, Singh S, Zhou Q. (2008) Phosphate-induced lead immobilization from different lead minerals in soils under varying pH conditions. *Environmental pollution* (Barking, Essex : 1987); **152**: 184-92.
- ChemIDPlus. (2021) U.S. National Library of Medicine. Available at <https://chem.nlm.nih.gov/chemidplus/chemidlite.jsp>. Accessed April 2021.
- Clemons DJ and Seeman JL. (2011) Chapter 1: Important biological features. In Clemons DJ, Seeman JL, editor. *The laboratory guinea pig*, 2nd edn. Boca Raton, FL: CRC Press. ISBN: 9780429105739.
- Cohn JR, Emmett EA. (1978) The excretion of trace metals in human sweat. *Ann Clin Lab Sci*; **8**: 270-5.

Demin DV, Aladin DY, Sevostyanov SM. (2021). Assessment of the stability of amino acid complexes of heavy metals to biodegradation in the aquatic environment. *Journal of Physics: Conference Series*; **1942**: 1-8.

Dryer DJ, Korshin GV. (2007). Investigation of the Reduction of Lead Dioxide by Natural Organic Matter. *Environ Sci Technol*; **41**: 5510-14.

Duling MG, Stefaniak AB, Lawrence RB, Chipera SJ, Virji MA. (2012). Release of beryllium from mineral ores in artificial lung and skin surface fluids. *Environ Geochem Health*; **34**: 313-22.

Dykeman R, Aguilar-Madrid G, Smith T, Juárez-Pérez CA, Piacitelli GM, Hu H, Hernandez-Avila M. (2002). Lead exposure in Mexican radiator repair workers. *Am J Ind Med*; **41**: 179-87.

EFSA (European Food Safety Authority). (2012) Scientific opinion, guidance on dermal absorption, EFSA panel on plant protection products and their residues (PPR). *EFSA J*; **10**: 2665. Available at <https://efsa.onlinelibrary.wiley.com/doi/pdf/10.2903/j.efsa.2012.2665>.

EPA (U.S. Environmental Protection Agency). (1992) Dermal exposure assessment: principles and applications. Washington DC: Office of Research and Development, Office of Health and Environmental Assessment, EPA Publication No. EPA/600/8-91/001b, January 1992, Interim Report.

EPA (U.S. Environmental Protection Agency). (1998) Health effects test guidelines, OPPTS 870.7600 dermal penetration. Washington DC: Office of Prevention, Pesticides, and Toxic Substances, EPA Publication No. EPA 712-C-98-350, August 1998.

EPA. U.S. Environmental Protection Agency (2003) Recommendations of the technical review workgroup for lead for an approach to assessing risks associated with adult exposures to lead in soil. EPA 540-R-03-001, January 2003, Washington DC.

EPA (U.S. Environmental Protection Agency). (2007) Dermal exposure assessment: a summary of EPA approaches. Washington DC: National Center for Environmental Assessment, Office of Research and Development, EPA 600/R-07/040F, September 2007.

EPA . U.S. Environmental Protection Agency. (2011) Exposure Factors Handbook: 2011 Edition. National Center for Environmental Assessment, Washington, DC; EPA/600/R-09/052F. Available from the National Technical Information Service, Springfield, VA, and online at <http://www.epa.gov/ncea/efh>.

Esswein E, Boeniger M, Ashley K. (2011) Hand wipe method for removing lead from skin. In Michael B, Kevin A, editors. *Surface and dermal sampling*. West Conshohocken: ASTM International. pp. 67–84.

Fang JY, Wang PW, Huang CH et al. (2014) Evaluation of the hepatotoxic risk caused by lead acetate via skin exposure using a proteomic approach. *Proteomics*; **14**: 2588–99.

Far HS, Pin NT, Kong CY, Fong KS, Kian CW, Yan CK. (1993). An evaluation of the significance of mouth and hand contamination for lead absorption in lead-acid battery workers. *Int Arch Occup Environ Health*; **64**: 439-43.

Ferreira CMH, Pinto ISS, Soares EV, Soares HMVM (2015) (Un)suitability of the use of pH buffers in biological, biochemical and environmental studies and their interaction with metal ions- a review. *RSC Advances*, **5**, 30989-31003.

FDA (U.S. Food and Drug Administration). (2020) Lead in food, foodwares, and dietary supplements. Available at <https://www.fda.gov/food/metals-and-your-food/lead-food-foodwares-and-dietary->

[supplements#:~:text=The%20FDA%20calculated%20the%20current,the%20CDC%27s%20blood%20reference%20level](#) Accessed June 2021.

FDA (U.S. Food and Drug Administration). (2021) Lead acetate in “progressive” hair dye products. Available at <https://www.fda.gov/cosmetics/cosmetic-products/lead-acetate-progressive-hair-dye-products> Accessed September 2021.

Filon FL, Boeniger M, Maina G *et al.* (2006) Skin absorption of inorganic lead (PbO) and the effect of skin cleansers. *J Occup Environ Med*; **48**: 692–9.

Flannery BM, Dolan LC, Hoffman-Pennesi D *et al.* (2020) U.S. Food and Drug Administration’s interim reference levels for dietary lead exposure in children and women of childbearing age. *Regul Toxicol Pharmacol*; **110**: 104516.

Franken A, Eloff FC, Du Plessis J *et al.* (2015) *In vitro* permeation of metals through human skin: a review and recommendations. *Chem Res Toxicol*; **28**: 2237–49.

Franz TJ. (1975) Percutaneous absorption on the relevance of *in vitro* data. *J Invest Dermatol* **64**:190-195.

Friberg L, Skog E, Wahlberg JE. (1961) Resorption of mercuric chloride and methyl mercury dicyandiamide in guinea-pigs through normal skin and through skin pretreated with acetone, alkylaryl-sulphonate and soap. *Acta Derm Venereol*; **41**: 40–52.

Fullerton *et al.* (1986). Permeation of nickel salts through human skin *in vitro*. *Contact Dermatitis*; **15**:173-177.

Gammelgaard B, Fullerton A, Avnstorp C *et al.* (1992) Permeation of chromium salts through human skin *in vitro*. *Contact Dermatitis*; **27**: 302–10.

Goyer RA, Cherian MG. (1979). Ascorbic acid and EDTA treatment of lead toxicity in rats. *Life Sciences*; **24**: 433-38.

Guth K, Bourgeois M, Johnson G *et al.* (2020) Evaluation of the effectiveness of Hygenall© Leadoff™ foaming soap in reducing lead on workers’ hands and the update of lead on bridge painting projects. *Occup Dis Environ Med*; **27**: 123–34.

Hahn T (2011). Evaluation of finite dose skin absorption experiments with respect to experimental setup and mathematical modeling. Dissertation, Chemie, Pharmazie, Bio- und Werkstoffwissenschaften der Universität des Saarlandes.

Hardison D, Harris W, Cao X, Zhou Q. (2007). Effects of Soil Property and Soil Amendment on Weathering of Abraded Metallic Pb in Shooting Ranges. *Water, Air, and Soil Pollution*; **178**: 297-307.

Harvey CJ, LeBouf RF, Stefaniak AB. (2010). Formulation and stability of a novel artificial human sweat under conditions of storage and use. *Toxicology in Vitro*; **24**: 1790-96.

Hedberg Y, Midander K, Odnevall Wallinder I. (2010). Particles, sweat, and tears: A comparative study on bioaccessibility of ferrochromium alloy and stainless steel particles, the pure metals and their metal oxides, in simulated skin and eye contact. *Integrated Environmental Assessment and Management*; **6**: 456-68.

- Hemingway JD, Molokhia MM. (1987). The dissolution of metallic nickel in artificial sweat. *Contact Dermatitis*; **16**: 99-105.
- Hempel S, Lea Xenakis L, Danz M. (2016) *Systematic reviews for occupational safety and health questions: resources for evidence synthesis*. Santa Monica, CA: RAND Corporation.
- Hillwalker WE, Anderson KA. (2014). Bioaccessibility of metals in alloys: evaluation of three surrogate biofluids. *Environ Pollut*; **185**: 52-8.
- Hodgkins DG, Robins TG, Hinkamp DL, Schork MA, Levine SP, Krebs WH. (1991). The effect of airborne lead particle size on worker blood-lead levels: an empirical study of battery workers. *J Occup Med*; **33**: 1265-73.
- Holmes HN, Campbell K, Amberg EJ. (1939). The effect of vitamin C on lead poisoning. *J Lab Clin Med*; **24**: 1119-27.
- Hostýnek JJ. (2003) Factors determining percutaneous metal absorption. *Food Chem Toxicol*; **41**: 327–45.
- Hostýnek JJ, Dreher F, Nakada T, Schwindt D, Anigbogu A, Maibach HI . (2001) Human stratum corneum adsorption of nickel salts. Investigation of depth profiles by tape stripping *in vivo*. *Acta Derm Venereol*; Suppl 212: 11–8.
- Hostýnek JJ, Hinz RS, Lorence CR, Price M, Guy RH. (1993) Metals and the skin. *Crit Rev Toxicol*; **23**: 171–235.
- Hostynek JJ, Maibach HI. (2006) Skin penetration by metal compounds with special reference to copper. *Toxicol Mech Methods*; **16**: 245–65.
- Hughson G. 2005. An occupational hygiene assessment of dermal inorganic lead exposures in primary and intermediate user industries. Research Report TM/04/06. Institute of Occupational Medicine.
- Julander A, Midander K, Garcia-Garcia S, Vilborg P, Graff P. (2020) A case study of brass foundry workers' estimated lead (Pb) body burden from different exposure routes. *Ann Work Expo Health*; **64**: 970–81.
- Jung EC, Maibach HI. (2015) Animal models for percutaneous absorption. *J Appl Toxicol*; **35**: 1–10.
- Kanapilly GM, Raabe OG, Goh CH, Chimenti RA. (1973). Measurement of *in vitro* dissolution of aerosol particles for comparison to *in vivo* dissolution in the lower respiratory tract after inhalation. *Health Phys*; **24**: 497-507.
- Kehoe RA. (1987) Studies of lead administration and elimination in adult volunteers under natural and experimentally induced condition over extended periods of time. *Food Chem Toxicol*; **25**: i–iv, 425–53.
- Kim EJ, Herrera JE, Huggins D, Braam J, Koshowski S. (2011). Effect of pH on the concentrations of lead and trace contaminants in drinking water: a combined batch, pipe loop and sentinel home study. *Water Res*; **45**: 2763-74.
- King CS, Moore N, Marks R, Nicholls S. (1978) Preliminary studies into percorneal penetration and elemental content of the stratum corneum using X-ray microanalysis. *Arch Dermatol Res*; **263**: 257–65.

Kunze FM, Laug EP. (1948) The penetration of lead through the skin of the rat. *Fed Proc*; **7**(1 Pt 1): 256–9.

Lanphear BP, Rauch S, Auinger P *et al.* (2018) Low-level lead exposure and mortality in US adults: a population-based cohort study. *Lancet Public Health*; **3**: e177–84.

Lademann J, Jacobi U, Surber C, Weigmann HJ, Fluhr JW. (2009) The tape stripping procedure--evaluation of some critical parameters. *Eur J Pharm Biopharm*; **72**: 317-23.

Leberman R, Rabin BR. (1959). Metal complexes of histidine. *Transactions of the Faraday Society*; **55**: 1660-70.

Leggett RW. (1993) An age-specific kinetic model of lead metabolism in humans. *Environ Health Perspect*; **101**: 598–616.

Lidén C, Carter S. (2001). Nickel release from coins. *Contact Dermatitis*; **44**: 160-5.

Marzulli FN, Watlington PM, Maibach HI. (1978) Exploratory skin penetration findings relating to the use of lead acetate hair dyes. Hair as a test tissue for monitoring uptake of systemic lead. *Curr Probl Dermatol*; **7**: 196–204.

Lilley SG, Florence TM, Stauber JL. (1988) The use of sweat to monitor lead absorption through the skin. *Sci Total Environ*; **76**: 267-78.

Lin Y-P, Washburn MP, Valentine RL. (2008) Reduction of Lead Oxide (PbO₂) by Iodide and Formation of Iodoform in the PbO₂/I⁻/NOM System. *Environ Sci Technol*; **42**: 2919-24.

Liu WV, Froines JR, Hinds WC, D. C. (1996). Particle size distribution of lead aerosol in a brass foundry and a battery manufacturing plant. *Occup Hyg*; **3**: 213-28.

Marchmont-Robinson S. (1941). Effect of vitamin C on workers exposed to lead dust. *Journal of Laboratory and Clinical Medicine*; **26**: 1478-81.

Marin Villegas CA, Guney M, Zagury GJ. (2019). Comparison of five artificial skin surface film liquids for assessing dermal bioaccessibility of metals in certified reference soils. *Sci Total Environ*; **692**: 595-601.

Marken F, Compton RG, Buston JEH, Moloney MG. (1998). Sonoelectrochemically Enhanced Electrocatalytic Processes: The Pb(IV) Catalyzed Cleavage of 1,2-cis-Cyclopentanediol at Graphite and Glassy Carbon Electrodes. *Electroanalysis*; **10**: 1188-92.

Marken F, Leslie WM, Compton RG, Moloney MG, Sanders E, Davies SG, Bull SD. (1997). Homogeneous and heterogeneous catalytic redox processes: solution and solid state voltammetry of lead complexes at carbon electrodes. *Journal of Electroanalytical Chemistry*; **424**: 25-34.

McCarley KD, Bunge AL. (2001) Pharmacokinetic models of dermal absorption. *J Pharm Sci*; **90**: 1699–719.

Midander K, Julander A, Kettelarij J, Lidén C. (2016). Testing in artificial sweat - Is less more? Comparison of metal release in two different artificial sweat solutions. *Regul Toxicol Pharmacol*; **81**: 381-86.

Mitragotri S, Anissimov YG, Bunge AL *et al.* (2011) Mathematical models of skin permeability: an overview. *Int J Pharm*; **418**: 115–29.

Moore MR, Meredith PA, Watson WS *et al.* (1980) The percutaneous absorption of lead-203 in humans from cosmetic preparations containing lead acetate, as assessed by whole-body counting and other techniques. *Food Cosmet Toxicol*; **18**: 399–405.

Niemeier RT, Maier A, Reichard JF. (2021). Rapid Review of Dermal Penetration and Absorption for Inorganic Lead Compounds for Occupational Risk Assessment. *Annal of Work Exposure and Health* wxab097, <https://doi.org/10.1093/annweh/wxab097>.

NIOSH (National Institute for Occupational Safety and Health). (1992). Health Hazard Evaluation Report: Delaware County Resource Recovery Facility, Chester, Pennsylvania. By: Esswein E.J., Tepper A. Cincinnati, OH: US Department of Health and Human Services, Centers for Disease Control and Prevention, National Institute for Occupational Safety and Health. NIOSH HHE Report No. 91-0366-2453.

NIOSH (National Institute for Occupational Safety and Health). (1996a). Health Hazard Evaluation Report: Standard Industries, San Antonio Texas. By: Esswein E., Boeniger M., Hall R., Meade K. Cincinnati, OH: US Department of Health and Human Services, Centers for Disease Control and Prevention, National Institute for Occupational Safety and Health. NIOSH HHE Report No. 1994-0268-2618.

NIOSH (National Institute for Occupational Safety and Health). (1996b). Health Hazard Evaluation Report, Bruce Mansfield Power Station. Shippingport, Pennsylvania. By: Mattorano D.A. Cincinnati, OH: US Department of Health and Human Services, Centers for Disease Control and Prevention, National Institute for Occupational Safety and Health. NIOSH HHE Report No. 1994- 0273-2556.

NIOSH (National Institute for Occupational Safety and Health). (1999). Interim Health Hazard Evaluation Report: Yuasa Inc., Sumpter, South Carolina. By: Burr G, Nemhauser J., Tubbs R., Habes D. Cincinnati, OH: US Department of Health and Human Services, Centers for Disease Control and Prevention, National Institute for Occupational Safety and Health. NIOSH HHE Report No. 1999-0188.

NIOSH (National Institute for Occupational Safety and Health). (2015). Health hazard evaluation report: Metal exposures in an electronic scrap recycling facility. By: Page E., Ceballos D., Oza A., Gong W., & Mueller C. Cincinnati, OH: U.S. Department of Health and Human Services, Centers for Disease Control and Prevention, National Institute for Occupational Safety and Health, NIOSH HHE Report No. 2013-0067-3228.

NIOSH (2016). Jacklitsch B, Williams WJ, Musolin K, Coca A, Kim J-H, Turner N. NIOSH criteria for a recommended standard: occupational exposure to heat and hot environments. Cincinnati, OH: U.S. Department of Health and Human Services, Centers for Disease Control and Prevention, National Institute for Occupational Safety and Health, DHHS (NIOSH) Publication 2016-106.

NIOSH (2022). Adult Blood Lead Epidemiology and Surveillance (ABLES). Available at: [Adult Blood Lead Epidemiology and Surveillance \(ABLES\) | NIOSH | CDC](#). Date accessed: March 2022.

Nowack B, Krug HF, Height M. (2011). 120 years of nanosilver history: implications for policy makers. *Environ Sci Technol*; **45**: 1177-83.

NTP (National Toxicology Program). (2012) NTP monograph: health effects of low-Pb levels. Available at [NTP Monograph on Health Effects of Low-Level Lead \(nih.gov\)](#) Accessed February 2021.

Ng, S. F., Rouse, J. J., Sanderson, F. D., Meidan, V., & Eccleston, G. M. (2010). Validation of a static Franz diffusion cell system for *in vitro* permeation studies. *AAPS PharmSciTech*, **11**(3), 1432–1441. <https://doi.org/10.1208/s12249-010-9522-9>

OECD (Organisation for Economic Cooperation and Development) Guideline No.105.(1995). *OECD guideline for the testing of chemicals. Water solubility*. Paris: OECD.

OECD (Organisation for Economic Cooperation and Development) Guideline No. 428. (2004a) *OECD guideline for the testing of chemicals. Skin absorption: in vitro test*. Paris: OECD.

OECD (Organisation for Economic Cooperation and Development) Guidance Document for the Conduct of Skin Absorption Studies. (2004b) *OECD series on testing and assessment, number 28*. Paris: OECD.

OECD (Organisation for Economic Cooperation and Development) Guidance Notes on Dermal Absorption. (2011) *Series on testing and assessment, number 156*. Paris: OECD.

O’Flaherty EJ. (1993) Physiologically based models for bone-seeking elements. IV. Kinetics of lead disposition in humans. *Toxicol Appl Pharmacol*; **118**: 16–29.

OSHA (Occupational Safety and Health Administration). (1978) Lead—1910.1025. Washington DC: Department of Labor, Occupational Safety and Health Administration. Available at <https://www.osha.gov/laws-regs/regulations/standardnumber/1910/1910.1025>. Accessed April 2021.

Pan TL, Wang PW, Al-Suwayeh SA *et al.* (2010) Skin toxicology of lead species evaluated by their permeability and proteomic profiles: a comparison of organic and inorganic lead. *Toxicol Lett*; **197**: 19–28.

Park DU, Paik NW. (2002). Effect on blood lead of airborne lead particles characterized by size. *Ann Occup Hyg*; **46**: 237-43.

Permeagear (2022). Franz cell (image). Website: <https://permeagear.com/wp-content/uploads/2019/11/Cell-Selection-Guide.pdf> Date accessed: February 2022.

Petito Boyce C, Sax SN, Cohen JM. (2017). Particle size distributions of lead measured in battery manufacturing and secondary smelter facilities and implications in setting workplace lead exposure limits. *J Occup Environ Hyg*; **14**: 594-608.

Pounds JG. (1979) *Percutaneous absorption of lead*. Jefferson, Arkansas: Food and Drug Administration, National Center for Toxicological Research. Report number FDA/NCTR-86/28, December 1979.

Pubchem. (2022a) Lead nitrate. National Institutes of Health, National Library of Medicine. Available at <https://pubchem.ncbi.nlm.nih.gov/compound/24924>. Accessed February 2022.

Pubchem. (2022b) Lead acetate. National Institutes of Health, National Library of Medicine. Available at <https://pubchem.ncbi.nlm.nih.gov/compound/9317v>. Accessed February 2022.

Pubchem. (2022c) Lead acetate trihydrate. National Institutes of Health, National Library of Medicine. Available at <https://pubchem.ncbi.nlm.nih.gov/compound/22456>. Accessed February 2022.

Pubchem. (2022d) Lead subacetate. National Institutes of Health, National Library of Medicine. Available at <https://pubchem.ncbi.nlm.nih.gov/compound/5284406>. Accessed February 2022.

Pubchem. (2022e) Lead sulfate. National Institutes of Health, National Library of Medicine. Available at <https://pubchem.ncbi.nlm.nih.gov/compound/24008>. Accessed February 2022.

Pubchem. (2022f) Lead oxide. National Institutes of Health, National Library of Medicine. Available at <https://pubchem.ncbi.nlm.nih.gov/compound/14827>. Accessed February 2022.

Pubchem. (2022g) Lead ortho-arsenate. National Institutes of Health, National Library of Medicine. Available at <https://pubchem.ncbi.nlm.nih.gov/compound/24572>. Accessed February 2022.

Pubchem. (2022h) Lead metal. National Institutes of Health, National Library of Medicine. Available at <https://pubchem.ncbi.nlm.nih.gov/compound/5352425>. Accessed February 2022.

PubChem (2022i) Lead tetroxide. . National Institutes of Health, National Library of Medicine. Available at <https://pubchem.ncbi.nlm.nih.gov/compound/16685188>. Accessed February 2022.

Rasetti L, Cappellaro F, Gaido P. (1961) Contribution to the study of lead poisoning caused by lubricating oil additives. *Rass Med Ind Ig Lav*; **30**: 71–5.

Rastogi SC, Clausen J. (1976) Absorption of lead through the skin. *Toxicology*; **6**: 371–6.

Reynolds, ES. (1963) The use of lead citrate at high pH as an electron-opaque stain for electron microscopy, *J. Cell Biol.*, **17**, 208.

Ruela ALM, Perissinato AG, Lino MEdS, Mudrik PS, Pereira GR. (2016) Evaluation of skin absorption of drugs from topical and transdermal formulations. *Brazilian Journal of Pharmaceutical Sciences*; **52**: 527-44. <https://doi.org/10.1590/S1984-82502016000300018>

Samhel J, Boeniger M, Knutsen J *et al.* (2009) Dermal exposure modeling (chapter 13). In American Industrial Hygiene Association, editor. *Mathematical models for estimating occupational exposure to chemicals*. 2nd ed. Fairfax, VA: AIHA (American Industrial Hygiene Association).

Santucci RJ, Jr., Scully JR. (2020) The pervasive threat of lead (Pb) in drinking water: Unmasking and pursuing scientific factors that govern lead release. *Proc Natl Acad Sci U S A*; **117**: 23211-18.

Savoji H, Godau B, Hassani MS, Akbari M. (2018) Skin Tissue Substitutes and Biomaterial Risk Assessment and Testing. *Front Bioeng Biotechnol*; **6**: 86.

Seo, JE., Kim, S. & Kim, BH. (2017) *In vitro* skin absorption tests of three types of parabens using a Franz diffusion cell. *J Expo Sci Environ Epidemiol* **27**, 320–325. <https://doi.org/10.1038/jes.2016.33>

Sigma Aldrich, (2021). Dulbecco's Phosphate Buffered Saline. Website: [Dulbecco's Phosphate Buffered Saline \(DPBS\) Modified, without CaCl₂ and MgCl₂, sterile-filtered Sigma-Aldrich \(sigmaaldrich.com\)](https://www.sigmaaldrich.com/US/en/products/cell-culture/media/dulbeccos-phosphate-buffered-saline). Date accessed: January 2021.

Simon JA, Hudes ES. (1999). Relationship of Ascorbic Acid to Blood Lead Levels. *JAMA*; **281**: 2289-93.

SKC (2022). Full Disclosure® Lead Detection. Website: [Full Disclosure® Lead Detection | View Our Full Disclosure® Lead Detection at SKC, Inc. \(skinc.com\)](https://www.skinc.com/lead-detection). Date Accessed: February 2022.

Statistics Kingdom (2021). Mann Whitney U test calculator (Wilcoxon rank-sum) non-parametric test. Website: [Mann-Whitney U test \(statskingdom.com\)](https://www.statskingdom.com/mann-whitney-u-test-calculator.html). Accessed: December 2021.

- Stauber JL, Florence TM, Gulson BL, Dale LS. 1994. Percutaneous absorption of inorganic lead compounds. *Sci Total Environ* 145:55-70.
- Stefaniak AB, Guilmette RA, Day GA, Hoover MD, Breyse PN, Scripsick RC. 2005. Characterization of phagolysosomal simulant fluid for study of beryllium aerosol particle dissolution. *Toxicol In Vitro*; 19: 123-34.
- Stefaniak AB, Harvey CJ. (2006). Dissolution of materials in artificial skin surface film liquids. *Toxicol In Vitro*; 20: 1265-83.
- Stefaniak AB, Harvey CJ, Virji MA, Day GA. (2010a). Dissolution of cemented carbide powders in artificial sweat: implications for cobalt sensitization and contact dermatitis. *J Environ Monit*; 12: 1815-22.
- Stefaniak AB, Harvey CJ, Wertz PW. (2010b). Formulation and stability of a novel artificial sebum under conditions of storage and use. *International Journal of Cosmetic Science*; 32: 347-55.
- Stefaniak AB, Virji MA, Day GA. (2011). Release of beryllium from beryllium-containing materials in artificial skin surface film liquids. *Ann Occup Hyg*; 55: 57-69.
- Stefaniak AB, Duling MG, Lawrence RB, Thomas TA, LeBouf RF, Wade EE, Virji MA. (2014a). Dermal exposure potential from textiles that contain silver nanoparticles. *Int J Occup Environ Health*; 20: 220-34.
- Stefaniak AB, Duling MG, Geer L, Virji MA. (2014b). Dissolution of the metal sensitizers Ni, Be, Cr in artificial sweat to improve estimates of dermal bioaccessibility. *Environ Sci Process Impacts*; 16: 341-51.
- Sun CC, Wong TT, Hwang YH *et al.* (2002) Percutaneous absorption of inorganic lead compounds. *AIHA J*; 63: 641–6.
- Supé S, Takudage P. (2021) Methods for evaluating penetration of drug into the skin: A review. *Skin Res Technol*; 27: 299-308. DOI: 10.1111/srt.12968
- Sweeney LM. (2021) Probabilistic pharmacokinetic modeling of airborne lead corresponding to toxicologically relevant blood lead levels in workers. *Regul Toxicol Pharmacol*; 122: 104894.
- Tanojo H, Hostýnek JJ, Mountford HS, Maibach HI (2001). *In vitro* permeation of nickel salts through human stratum corneum. *Acta Derm Venereol Suppl* (Stockh). 212:19-23. doi: 10.1080/000155501753279596.
- Tharr D. (1993). Case Studies. *Applied Occupational and Environmental Hygiene*; 8: 434-38.
- Thermo Fisher Scientific, 2021. Lead (II) oxide, 99.9+%, (trace metal basis), <10 microns, powder, Thermo Scientific™. Webpage: [Lead\(II\) oxide, 99.9+%, \(trace metal basis\), <10 microns, powder, Thermo Scientific™ 100g; Glass bottle Lead\(II\) oxide, 99.9+%, \(trace metal basis\), <10 microns, powder, Thermo Scientific™ | Fisher Scientific](#). Date accessed: December 2021.
- Tregear RT. (1966) The permeability of mammalian skin to ions. *J Invest Dermatol*; 46: 16–23.
- Thier R, Bonacker D, Stoiber T, Böhm KJ, Wang M, Unger E, Bolt HM, Degen G. (2003). Interaction of metal salts with cytoskeletal motor protein systems. *Toxicol. Lett.* 140–141: 75–81.

- Trebilcock KL, Heylings JR, Wilks MF (1994). In vitro tape stripping as a model for in vivo skin stripping. *Toxicol In vitro* 8 665.
- USCB (U.S. Census Bureau). (2018). 2018 SUSB Annual data tables by establishment industry. Website: [2018 SUSB Annual Data Tables by Establishment Industry \(census.gov\)](https://www.census.gov/data/tables/2018/susb/annual.html). Date accessed: September 2021.
- Van de Sandt JJ, Dellarco M, Van Hemmen JJ. (2007). From dermal exposure to internal dose. *J Expo Sci Environ Epidemiol*; **17** Suppl 1: S38-47.
- Vecchia and Bunge (Skin absorption databases and predictive equations, In: J. Hadgraft, R.H. Guy (Eds.) *Transdermal Drug Delivery*, Marcel Dekker, New York, 2002, pp. 57-141.
- Virji MA, Woskie SR, Pepper LD. (2009). Skin and surface lead contamination, hygiene programs, and work practices of bridge surface preparation and painting contractors. *J Occup Environ Hyg*; **6**: 131-42.
- Vork KL, Carlisle JC. (2020) Evaluation and updates to the Leggett model for pharmacokinetic modeling of exposure to lead in the workplace—Part I adjustments to the adult systemic model. *J Occup Environ Hyg*; **17**: 283–300.
- Wahlberg JE, Skog E. (1965) Percutaneous absorption of trivalent and hexavalent chromium: a comparative investigation in the guinea pig by means of ⁵¹Cr. *Arch Dermatol*; **92**: 315–8.
- Wallace BC, Small K, Brodley CE *et al.* (2012) Deploying an interactive machine learning system in an evidence-based practice center: abstract. In *Proc. of the IHI '12: ACM International Health Informatics Symposium*, Miami, FL, USA, January 28–30. pp. 819–24. Available at <https://dl.acm.org/doi/proceedings/10.1145/2110363>.
- Wang Y, Xie Y, Li W *et al.* (2010) Formation of lead(IV) oxides from lead(II) compounds. *Environ Sci Technol*; **44**: 8950–6.
- World Health Organization (WHO) (2011). Brief guide to analytical methods for measuring lead in blood. Available at: [Analytical methods for measuring lead in blood \(who.int\)](https://www.who.int/publications/i/item/9789241548214). Date accessed: February 2022.

Appendices

Appendix 1. Lead (Pb) Compounds and Search Strategy

Table A1. Inorganic Lead names and Chemical Abstract System identification numbers (CAS#s)

Name	CAS#
Lead bromide	10031-22-8
Lead nitrate	10099-74-8
Lead monosilicate	10099-76-0
Lead vanadate(V)	10099-79-3
Lead iodide	10101-63-0
Lead molybdate(VI)	10190-55-3
Lead metaborate monohydrate	10214-39-8
Lead chlorate	10294-47-0
Lead hypophosphite	10294-58-3
Lead silicate	11120-22-2
Iron lead oxide ($\text{Fe}_{12}\text{PbO}_{19}$)	12023-90-4
Plumbate (PbO_{22}), sodium (1:2)	12034-30-9
Lead niobium oxide	12034-88-7
Lead tin oxide	12036-31-6
Lead oxide sulfate ($\text{Pb}_2\text{O}(\text{SO}_4)$)	12036-76-9
Bismuth lead	12048-28-1
Lead oxide (Pb_2O)	12059-89-1
Lead titanium oxide	12060-00-3
Lead zirconium oxide	12060-01-4
Lead tantalum oxide	12065-68-8
Lead oxide sulfate ($\text{Pb}_5\text{O}_4(\text{SO}_4)$)	12065-90-6
Lead selenide	12069-00-0
Lead disulphide	12137-74-5
Lead oxide phosphonate ($\text{Pb}_3\text{O}_2(\text{HPO}_3)$)	12141-20-7
Lead chloride phosphate	12157-93-6
Lead oxide sulfate ($\text{Pb}_4\text{O}_3(\text{SO}_4)$)	12202-17-4
Lead chloride oxide	12205-72-0
Lead hydroxide phosphate	12207-55-5
Antimony, compound with lead (1:1)	12266-38-5
Lead hydroxide nitrate	12268-84-7

Lead germanate	12435-47-1
Hydroxylapatite, lead	12530-18-6
Lead titanate zirconate	12626-81-2
Lead silicate sulfate	12687-78-4
Lead-molybdenum chromate	12709-98-7
Lead tungsten oxide	12737-98-3
Lead oxide sulfate	12765-51-4
Lead dioxide	1309-60-0
Lead sesquioxide	1314-27-8
Lead tetroxide	1314-41-6
Lead sulfide	1314-87-0
Lead telluride	1314-91-6
Lead oxide	1317-36-8
Lead hydroxide carbonate	1319-46-6
Lead subacetate	1335-32-6
Lead azide	13424-46-9
Carbonic acid, lead salt	13427-42-4
Lead oxide phosphonate, hemihydrate	1344-40-7
Diphosphoric acid, lead ⁽²⁺⁾ salt (1:2)	13453-66-2
Lead tetrachloride	13463-30-4
Lead(II) thiosulfate	13478-50-7
Perchloric acid, lead ⁽²⁺⁾ salt (2:1)	13637-76-8
Lead disulphamidate	13767-78-7
Lead bromide chloride	13778-36-4
Lead iodide	13779-98-1
Lead fluoroborate	13814-96-5
Nitrous acid, lead ⁽²⁺⁾ salt (2:1)	13826-65-8
Lead(II) tellurate	13845-35-7
Lead, isotope of mass 206	13966-27-3
Lead, ion (Pb ²⁺)	14280-50-3
Lead ion (1)	14701-27-0
Lead metaborate	14720-53-7
Lead cation Pb ⁴⁺	15158-12-0
Sulfuric acid, lead salt (1:2)	15739-80-7
Chromic acid (H ₂ CrO ₄), lead ⁽²⁺⁾ salt	15804-54-3

Dibasic lead phosphate	15845-52-0
Telluric acid (H ₂ TeO ₃), lead ⁽²⁺⁾ salt (1:1)	15851-47-5
Plumbane	15875-18-0
Lead chloride hydroxide	15887-88-4
Silicic acid (H ₄ SiO ₄), lead salt	15906-71-5
Phosphonic acid, lead salt	16038-76-9
Lead phosphate	16040-38-3
Lead bromide hydroxide	16651-91-5
Lead chromate oxide	18454-12-1
Lead hydroxide	19783-14-3
Cyanamide, lead ⁽²⁺⁾ salt (1:1)	20837-86-9
Lead cyanamide	20890-10-2
Lead silicate	22569-74-0
Carbonic acid, lead ⁽²⁺⁾ salt	25510-11-6
Iodic acid (HIO ₃), lead ⁽²⁺⁾ salt (2:1)	25659-31-8
Lead hexafluorosilicate	25808-74-6
Lead thiosulfate	26265-65-6
Lead acetate	301-04-2
Lead bromate	34018-28-5
Lead cyanamide	35112-70-0
Lead arsenate	3687-31-8
Lead sulfide	39377-56-5
Lead chloride silicate	39390-00-6
Lead chromate sulfate	51899-02-6
Sulfuric acid, lead salt, tetrabasic	52732-72-6
Lead fluoride	53096-04-1
Lead tetraacetate	546-67-8
Lead(II)cyanide	592-05-2
Lead thiocyanate	592-87-0

Lead carbonate	598-63-0
Lead acetate trihydrate	6080-56-4
Lead naphthenate	61790-14-5
Lead potassium thiocyanate	63916-97-2
Lead chloride oxide	65722-61-4
Lead silicate sulfate	67711-86-8
Silicic acid, lead nickel salt	68130-19-8
Hexanoic acid, dimethyl-, lead(2+) salt, basic	68442-95-5
Resin acids and Rosin acids, calcium lead salts	68952-91-0
Benzoic acid, 2,4-dihydroxy-, lead salt, basic	68954-05-2
Lead chromate silicate	69011-07-0
Lead powder	7439-92-1
Lead sulphite	7446-10-8
Lead sulfate	7446-14-2
Lead selenate	7446-15-3
Lead phosphate	7446-27-7
Lead selenite	7488-51-9
Lead chloride	7758-95-4
Lead chromate	7758-97-6
Lead tungstate	7759-01-5
Lead difluoride	7783-46-2
Lead tetrafluoride	7783-59-777
Lead formate	811-54-1
Lead uranate pigment	85536-79-4
Lead fluoride hydroxide	97889-90-2

Table A2- Dermal search terms

"Skin"[MeSH] OR "Skin Irritancy Tests"[MeSH] OR "Skin Tests"[MeSH] OR "Skin Diseases"[MeSH] OR "Skin Physiological Phenomena"[MeSH] OR Acne* OR Apocrine OR Argyria OR Atopic OR 'Blister* OR Callosit* OR Corrositex OR Cutaneous OR Cutis OR Cyst OR Cystic OR Cysts OR Dermal* OR Dermatitis OR Dermato* OR Dermis OR Eccrine OR Ectoderm* OR Eczema* OR Epicutaneous OR Epiderm* OR Episkin OR Erythema* OR Exanthema OR Exfoliat* OR Fingernail* OR Follicul* OR Gangren* OR Granuloma* OR Hirsut* OR Hyperhidrosis OR Hyperpigment* OR Hypertricho* OR Hypopigment* OR Hypotricho* OR Intertrigo OR Intradermal* OR Irritat* OR Jaundice OR Keloid* OR Keratoacanthoma OR Keratoderma OR Keratosis OR Lichenoid OR Miliaria OR Mucocutaneous OR Neurodermat* OR Onychomyco* OR Pallor OR Panniculit* OR Papulosquamous OR Paronychia OR Photosensitiv* OR

Porphyria* OR Prurigo OR Prurit* OR Psoriasis OR Purpura OR QSAR OR Radiodermatitis OR Rash* OR Sebaceous OR Skin OR "Stratum Corneum" OR "Structure Activity Relationship" OR Sunburn OR Sweat OR Urticaria OR Vacciniforme OR Vesiculobullous OR Xeroderma OR transdermal* OR epidermis[MESH] OR "epidermal layer" OR transdermal* OR epidermis [MESH] OR epidermal layer

Appendix 2. K_p and Diffusion Rate Calculation in Chapter 1

Pb acetate

Calculation from Moore et al. (1980)

Concentration of Pb applied: 6 mM/liter of colloidal lotion, radiolabeled with Pb^{203} acetate (0.74mBq) (0.1 ml applied)

6mM Pb acetate= 1.95 mg/ml= 1.95 mg/cm³

Surface area of skin treated: 8 cm²

Applied dose: (load): 2.44x10⁻² mg/ cm²

Application time: 12 hrs (0.5 days)

1.95 mg/ml * 0.1ml= 0.195mg

0.195mg/8cm²= 2.44x10⁻² mg/ cm²

Diffusion rate calculations:

Calculated K_p values from literature: 4x10⁻⁶ cm/h (EPA, 1992); 5x10⁻⁷ cm/h (Hostynek 2003)

Diffusion rate= 4x10⁻⁶ cm/h* 1.95 mg/cm³= 8x10⁻⁶ mg/cm²/h

Diffusion rate= 5x10⁻⁷ cm/h*1.95 mg/cm³= 1x10⁻⁶ mg/cm²/h

Other results:

The mean absorption (\pm standard deviation) in whole body count was 0.058 \pm 0.081%. The authors estimated that 0.355 μ g of a 612 μ g Pb dose was absorbed during the experiment.

Calculations from Pounds (1979)

Concentration of Pb applied: 5mg in 500 μ l solution (Grecian formula or distilled water or 70% ethanol)

Surface area of skin treated: 10 cm²

Applied dose: (load): 0.5 mg/cm²

7 day

Time weighted average diffusion rate calculations:

1.69% percutaneous absorption at 7 days (Grecian Formula)

5 mg* 0.0169/7= 0.01 mg/day

0.012 mg/10cm²/day= 0.0012 mg/cm²/day

= 0.0012/24 hr= 5x10⁻⁵ mg/ cm²/h

1.51% percutaneous absorption at 7 days (ethanol)

5 mg* 0.0151/7= 0.01mg/day

0.011 mg/10 cm²/day= 0.0011 mg/ cm²/day

= 0.0011/24 hr= 4 x10⁻⁵ mg/ cm²/h

2.99% percutaneous absorption at 7 days (distilled water)

$$5 \text{ mg} * 0.0299/7 = 0.02 \text{ mg/day}$$

$$0.021 \text{ mg}/10 \text{ cm}^2/\text{day} = 0.0021 \text{ mg}/\text{cm}^2/\text{day}$$

$$= 0.0021/24 \text{ hr} = 9 \times 10^{-5} \text{ mg}/\text{cm}^2/\text{h}$$

K_p calculations

$$\text{Applied concentration } 5 \text{ mg}/500 \mu\text{l} = 0.01 \text{ mg}/\mu\text{l} = 10 \text{ mg}/\text{ml} = 10 \text{ mg}/\text{cm}^3$$

$$= 5.0 \times 10^{-5} \text{ mg}/\text{cm}^2/\text{h} / 10 \text{ mg}/\text{cm}^3 = 5.0 \times 10^{-6} \text{ cm}^2/\text{h}$$

$$= 4.5 \times 10^{-5} \text{ mg}/\text{cm}^2/\text{h} / 10 \text{ mg}/\text{cm}^3 = 4.5 \times 10^{-6} \text{ cm}^2/\text{h}$$

$$= 8.9 \times 10^{-5} \text{ mg}/\text{cm}^2/\text{h} / 10 \text{ mg}/\text{cm}^3 = 8.9 \times 10^{-6} \text{ cm}^2/\text{h}$$

Time weighted average diffusion rate calculations based on Hostynek et al. (1993)

Reported Flux (Hostynek et al. 1993): $0.7 \mu\text{g}/\text{cm}^2/\text{day}$

$$0.7 \mu\text{g}/\text{cm}^2/\text{day}/24 \text{ hrs}$$

$$= 0.029 \mu\text{g}/\text{cm}^2/\text{h}$$

$$= 3 \times 10^{-5} \text{ mg}/\text{cm}^2/\text{h}$$

Reported Flux (Hostynek et al. 1993): $1.4 \mu\text{g}/\text{cm}^2/\text{day}$

$$1.4 \mu\text{g}/\text{cm}^2/\text{day}/24 \text{ hrs}$$

$$= 0.058 \mu\text{g}/\text{cm}^2/\text{h}$$

$$= 6 \times 10^{-5} \text{ mg}/\text{cm}^2/\text{h}$$

Calculated K_p values based on Hostynek et al. (1993)

$$\text{Applied concentration } 5 \text{ mg}/500 \mu\text{l} = 0.01 \text{ mg}/\mu\text{l} = 10 \text{ mg}/\text{ml} = 10 \text{ mg}/\text{cm}^3$$

$$= 3 \times 10^{-5} \text{ mg}/\text{cm}^2/\text{h} / 10 \text{ mg}/\text{cm}^3 = 3 \times 10^{-6} \text{ cm}^2/\text{h}$$

$$= 6 \times 10^{-5} \text{ mg}/\text{cm}^2/\text{h} / 10 \text{ mg}/\text{cm}^3 = 6 \times 10^{-6} \text{ cm}^2/\text{h}$$

14 day

Time weighted average diffusion rate calculations:

2.75% percutaneous absorption at 14 days (Grecian formula)

$$5 \text{ mg} * 0.0275/14 = 0.01 \text{ mg/day}$$

$$0.01 \text{ mg}/10 \text{ cm}^2 * \text{day} = 0.001 \text{ mg}/\text{cm}^2/\text{day}$$

$$= 0.001/24 \text{ hr} = 4 \times 10^{-5} \text{ mg}/\text{cm}^2/\text{h}$$

3.58% percutaneous absorption at 14 days (ethanol)

$$5 \text{ mg} * 0.0358/14 = 0.013 \text{ mg/day}$$

$$0.013 \text{ mg}/10 \text{ cm}^2 * \text{day} = 0.0013 \text{ mg}/\text{cm}^2/\text{day}$$

$$= 0.0013/24 \text{ hr} = 5 \times 10^{-5} \text{ mg}/\text{cm}^2/\text{h}$$

5.6% percutaneous absorption at 14 days

$$5 \text{ mg} * 0.056/14 = 0.02 \text{ mg/day}$$

$$0.02 \text{ mg}/10 \text{ cm}^2 * \text{day} = 0.002 \text{ mg}/\text{cm}^2/\text{day}$$

$$= 0.002/24 \text{ hr} = 8 \times 10^{-5} \text{ mg}/\text{cm}^2/\text{h}$$

K_p calculations

$$= 4 \times 10^{-5} \text{ mg/cm}^2/\text{h} / 10 \text{ mg/cm}^3 = 4 \times 10^{-6} \text{ cm/h}$$

$$= 5 \times 10^{-5} \text{ mg/cm}^2/\text{h} / 10 \text{ mg/cm}^3 = 5 \times 10^{-6} \text{ cm/h}$$

$$= 8 \times 10^{-5} \text{ mg/cm}^2/\text{h} / 10 \text{ mg/cm}^3 = 8 \times 10^{-6} \text{ cm/h}$$

28 days (4 weeks)

$$\text{Dose} = 5 \text{ mg} \times 3 \text{ days/week} \times 4 \text{ weeks} = 60 \text{ mg}$$

Time weighted average diffusion rate calculations:

3.28% percutaneous absorption at 4 weeks

$$60 \text{ mg} \times 0.0328 / 28 = 0.0703$$

$$0.07 / 10 \text{ cm}^2/\text{day} = 0.007 \text{ mg/cm}^2/\text{day}$$

$$= 0.007 / 24 \text{ hr} = 3 \times 10^{-4} \text{ mg/cm}^2/\text{h}$$

3.91% percutaneous absorption at 4 weeks

$$60 \text{ mg} \times 0.039 / 28 = 0.08$$

$$0.084 / 10 \text{ cm}^2/\text{day} = 0.0084 \text{ mg/cm}^2/\text{day}$$

$$= 0.0084 / 24 \text{ hr} = 3 \times 10^{-4} \text{ mg/cm}^2/\text{h}$$

3.58% percutaneous absorption at 4 weeks

$$60 \text{ mg} \times 0.0358 / 28 = 0.08$$

$$0.08 / 10 \text{ cm}^2/\text{day} = 0.008 \text{ mg/cm}^2/\text{day}$$

$$= 0.008 / 24 \text{ hr} = 3 \times 10^{-4} \text{ mg/cm}^2/\text{h}$$

K_p calculations

$$\text{Applied concentration } 5 \text{ mg} / 500 \mu\text{l} = 0.01 \text{ mg}/\mu\text{l} = 10 \text{ mg/ml} = 10 \text{ mg/cm}^3$$

$$3 \times 10^{-4} \text{ mg/cm}^2/\text{h} / 10 \text{ mg/cm}^3 = 3 \times 10^{-5} \text{ cm/h}$$

$$3 \times 10^{-4} \text{ mg/cm}^2/\text{h} / 10 \text{ mg/cm}^3 = 3 \times 10^{-5} \text{ cm/h}$$

$$3 \times 10^{-4} \text{ mg/cm}^2/\text{h} / 10 \text{ mg/cm}^3 = 3 \times 10^{-5} \text{ cm/h}$$

Reported Flux (Hostynek et al. 1993): $\sim 5 \mu\text{g/cm}^2/\text{day}$

$$5 \mu\text{g/cm}^2/\text{day} / 24 \text{ hrs}$$

$$= 0.21 \mu\text{g/cm}^2/\text{h}$$

$$= 2 \times 10^{-4} \text{ mg/cm}^2/\text{h}$$

Calculated K_p values based on Hostynek et al. (1993)

$$\text{Applied concentration } 5 \text{ mg} / 500 \mu\text{l} = 0.01 \text{ mg}/\mu\text{l} = 10 \text{ mg/ml} = 10 \text{ mg/cm}^3$$

$$= 2.1 \times 10^{-4} \text{ mg/cm}^2/\text{h} / 10 \text{ mg/cm}^3 = 2.1 \times 10^{-5} \text{ cm/h}$$

56 day (8 weeks)

$$\text{Dose} = 5 \text{ mg} \times 3 \text{ days/week} \times 4 \text{ weeks} = 60 \text{ mg}$$

(note: dosing stopped at 4 weeks)

Time weighted average diffusion rate calculations:

4.44% percutaneous absorption at 8 weeks

$$60\text{mg} \cdot 0.044 / 56 = 0.05$$

$$0.05 / 10\text{cm}^2 / \text{day} = 0.005 \text{ mg/cm}^2 / \text{day}$$

$$= 0.005 / 24 \text{ hr} = 2 \times 10^{-4} \text{ mg/cm}^2 / \text{h}$$

4.14% percutaneous absorption at 8 weeks

$$60\text{mg} \cdot 0.0414 / 56 = 0.044$$

$$0.044 / 10\text{cm}^2 \cdot \text{day} = 0.004 \text{ mg/cm}^2 / \text{day}$$

$$= 0.004 / 24 \text{ hr} = 2 \times 10^{-4} \text{ mg/cm}^2 / \text{h}$$

4.27% percutaneous absorption at 8 weeks

$$60\text{mg} \cdot 0.0427 / 56 = 0.046$$

$$0.05 / 10\text{cm}^2 \cdot \text{day} = 0.005 \text{ mg/cm}^2 / \text{day}$$

$$= 0.005 / 24 \text{ hr} = 2 \times 10^{-4} \text{ mg/cm}^2 / \text{h}$$

K_p calculations

$$\text{Applied concentration } 5\text{mg}/500\mu\text{l} = 0.01 \text{ mg}/\mu\text{l} = 10 \text{ mg/ml} = 10 \text{ mg/cm}^3$$

$$2.0 \times 10^{-4} \text{ mg/cm}^2 / \text{h} / 10 \text{ mg/cm}^3 = 2.0 \times 10^{-5} \text{ cm/h}$$

$$1.7 \times 10^{-4} \text{ mg/cm}^2 / \text{h} / 10 \text{ mg/cm}^3 = 1.7 \times 10^{-5} \text{ cm/h}$$

$$1.9 \times 10^{-4} \text{ mg/cm}^2 / \text{h} / 10 \text{ mg/cm}^3 = 1.9 \times 10^{-5} \text{ cm/h}$$

Calculations from Bress and Bidanset (1991)

Species: human (skin)

Surface area of skin treated: 1.3 cm²

Dose of Pb applied: 10 mg

Applied dose: (load): 7.7 mg/cm²

Pb in receptor fluid: 5 μg @37°C

Diffusion rate

Total Pb applied:

$$7.7 \text{ mg/cm}^2 \cdot 1.3 \text{ cm}^2 = 10 \text{ mg} = 10000 \mu\text{g}$$

Receptor fluid fraction calculation:

$$5.0 \mu\text{g} / 10000 \mu\text{g} = 0.0005$$

Avg diffusion rate calculation

$$(0.0005 \cdot 7.7 \text{ mg/cm}^2) / 24 \text{ hr} = 2 \times 10^{-4} \text{ mg/cm}^2 / \text{h}$$

Note: Franken et al (2015) and Hostynek et al. (1993) calculated the same diffusion rate value

Species: guinea pig (skin)

Surface area of skin treated: 1.3cm²

Dose of Pb applied: 10 mg

Applied dose: (load): 7.7 mg/cm²

Pb in receptor fluid: 5 μg @37°C and 3 μg @23°C

Diffusion rate

Total Pb applied:

$$7.7 \text{ mg/cm}^2 * 1.3 \text{ cm}^2 = 10 \text{ mg} = 10000 \text{ ug}$$

Receptor fluid fraction calculation:

$$3.0 \text{ ug}/10000 \text{ ug} = 0.0003 \text{ (@}23^\circ\text{C)}$$

$$5.0 \text{ ug}/10000 \text{ ug} = 0.0005 \text{ (@}23^\circ\text{C)}$$

Avg diffusion rate calculation

$$\text{Skin at } 37^\circ\text{C}: (0.0003 * 7.7 \text{ mg/cm}^2)/24 \text{ hr} =$$

$$9.6 \times 10^{-5} \text{ mg/cm}^2/\text{h}$$

$$\text{Skin at } 23^\circ\text{C}: (0.0005 * 7.7 \text{ mg/cm}^2)/24 \text{ hr} =$$

$$1.6 \times 10^{-4} \text{ mg/cm}^2/\text{h}$$

Receptor fluid fraction calculation:

$$\text{Skin at } 37^\circ\text{C} - 3.0/10000 = 0.0003$$

$$\text{Skin at } 23^\circ\text{C} - 5.0/10000 = 0.0005$$

Calculations from Pan et al. (2010)

Concentration of Pb applied: 120 mM Pb in 0.5 ml in double distilled water or synthetic sweat (39.03 mg/ml) (0.6 ml applied)

Surface area of skin treated: 0.785 cm² diameter

Applied dose: (load): 24.86 mg/cm²

$$120 \text{ mM Pb acetate} = 39.03 \text{ mg/ml} = 39.03 \text{ mg/cm}^3$$

Cumulative dose (receptor)

intact skin (Water)-0.23 ug/cm²

SC stripped skin (water)- 0.40 ug/cm²

Intact skin (synthetic sweat)- 0.13 ug/cm²

$$39.03 \text{ mg/ml} * 0.5 \text{ ml} = 19.52 \text{ mg.}$$

$$19.52 \text{ mg}/0.785 \text{ cm}^2 = 24.86 \text{ mg/cm}^2 = 24860 \text{ ug/cm}^2$$

Receptor fluid fraction calculation:

$$\text{Intact skin (water): } (0.23 \text{ ug/cm}^2)/(24860 \text{ ug/cm}^2) = 9.25 \times 10^{-6}$$

$$\text{SC stripped skin (water): } (0.4 \text{ ug/cm}^2)/(24860 \text{ ug/cm}^2) = 1.6 \times 10^{-5}$$

$$\text{Intact skin (synthetic sweat): } (0.13 \text{ ug/cm}^2)/(24860 \text{ ug/cm}^2) = 5.2 \times 10^{-6}$$

Avg diffusion rate calculation

$$\text{Intact skin (water): } (9.25 \times 10^{-6} * 24.86 \text{ mg/cm}^2)/10 \text{ hr} = 2.3 \times 10^{-5} \text{ mg/cm}^2/\text{h}$$

$$\text{SC stripped skin (water): } (1.6 \times 10^{-5} * 24.86 \text{ mg/cm}^2)/10 \text{ hr} = 4.0 \times 10^{-5} \text{ mg/cm}^2/\text{h}$$

$$\text{Intact skin (synthetic sweat): } (5.2 \times 10^{-6} * 24.86 \text{ mg/cm}^2)/10 \text{ hr} = 1.3 \times 10^{-5} \text{ mg/cm}^2/\text{h}$$

K_p calculations

Intact skin (water): $2.3 \times 10^{-5} \text{ mg/cm}^2/\text{h} / 39.03 \text{ mg/ml} = 5.9 \times 10^{-7} \text{ cm/h}$

SC stripped skin (water): $4.0 \times 10^{-5} \text{ mg/cm}^2/\text{h} / 39.03 \text{ mg/ml} = 1.0 \times 10^{-6} \text{ cm/h}$

Intact skin (synthetic sweat): $1.3 \times 10^{-5} \text{ mg/cm}^2/\text{h} / 39.03 \text{ mg/ml} = 3.3 \times 10^{-7} \text{ cm/h}$

Cumulative dose (skin)

Intact skin (Water)- 11.1 ug/mg

SC Stripped skin- 28 ug/mg (approx.)

Synthetic sweat – 2ug/mg (approx.)

Pb oxide and Pb metal studies

Calculations from Filon et al. (2006)

Concentration of Pb applied: The dosing was reported as 10mg of total Pb. No information was provided on how the Pb was dosed on the skin.

Applied dose: (load): 5 mg/cm^2

Surface area of skin treated: 3.14 cm^2

Receptor fluid fraction calculation:

$(0.0000029 \text{ mg/cm}^2) / (5 \text{ mg/cm}^2) = 5.8 \times 10^{-7}$

Avg diffusion rate calculation

$(5.8 \times 10^{-7} * 5 \text{ mg/cm}^2) / 24 = 1.2 \times 10^{-7} \text{ mg/cm}^2/\text{h}$

The median background corrected median concentration in the receiving solution was $0.0029 \text{ } \mu\text{g/cm}^2$

Note: Same value was calculated by Julander et al. (2020)

Calculations from Bress and Bidanset (1991)

Concentration of Pb applied: The dosing was reported as 10mg of total Pb oxide. No information was provided on how the Pb was dosed on the skin.

Model (in vitro/in vivo): *in vitro*

Study design: experimental, J diffusion tube

Species: guinea pig (skin)

Surface area of skin treated: 1.3 m^2

Applied dose: (load): 7.7 mg/cm^2

Pb content in the receptor fluid was below the LOD ($1 \text{ } \mu\text{g}$).

Total Pb applied:

$7.7 \text{ mg/cm}^2 * 1.3 \text{ cm}^2 = 10 \text{ mg} = 10000 \text{ ug}$

Avg diffusion rate calculation

$(0.0001 * 7.7 \text{ mg/cm}^2) / 24 \text{ hr} < 3 \times 10^{-5} \text{ mg/cm}^2/\text{h}$

Note: Same value was calculated by Hostynek et al. (1993)

Other results:

Receptor fluid fraction calculation:

$<1.0\mu\text{g}/10000\mu\text{g} = 0.0001$

Pb content in tissue ($\mu\text{g}/\text{wet gram tissue}$)

Blood- $0.33\pm 0.02 \mu\text{g}/\text{g}$ (control- 0.35 ± 0.05)

Brain- $0.36\pm 0.04 \mu\text{g}/\text{g}$ (control- 0.40 ± 0.03)

Liver- $0.37\pm 0.05 \mu\text{g}/\text{g}$ (control- 0.33 ± 0.04)

Kidney- $0.36\pm 0.03 \mu\text{g}/\text{g}$ (control- 0.40 ± 0.03)

Model: *In vivo*

Study design: Experimental

Species: Guinea Pig

Other results:

Pb content in tissue ($\mu\text{g}/\text{wet gram tissue}$)

Blood- $0.33\pm 0.02 \mu\text{g}/\text{g}$ (control- 0.35 ± 0.05)

Brain- $0.36\pm 0.04 \mu\text{g}/\text{g}$ (control- 0.40 ± 0.03)

Liver- $0.37\pm 0.05 \mu\text{g}/\text{g}$ (control- 0.33 ± 0.04)

Kidney- $0.36\pm 0.03 \mu\text{g}/\text{g}$ (control- 0.40 ± 0.03)

Other Results from Sun et al. (2002)

Metal: Pb oxide

The cumulative Pb in urine collected after 12 days of exposure compared to pre-dosing levels was 115.9 ng in the Pb nitrate exposed group vs. 10.8 ng in the control group.

Metal: Pb metal

The cumulative Pb in urine collected after 12 days of exposure compared to pre-dosing levels was 736.6 ng in the Pb nitrate exposed group vs. 10.8 ng in the control group.

Pb nitrate

Calculations from Pan et al. 2010

Concentration of Pb applied: 120 mM Pb in 0.5 ml in double distilled water or synthetic sweat (39.74 mg/ml)

Surface area of skin treated: 0.785 cm^2

Applied dose: (load): $25.31 \text{ mg}/\text{cm}^2$

Contact time (duration of application): 10 hours

$120\text{mM Pb nitrate} = 39.74 \text{ mg}/\text{ml} = 39.74 \text{ mg}/\text{cm}^3$

Cumulative dose (receptor)

intact skin (Water)- $0.20 \pm 0.13 \mu\text{g}/\text{cm}^2$

SC stripped skin (water)- $0.43 \pm 0.12 \mu\text{g}/\text{cm}^2$

Intact skin (synthetic sweat)- $0.19 \pm 0.12 \mu\text{g}/\text{cm}^2$

39.74 mg/ml * 0.5ml= 19.52 mg.
19.52mg/0.785 cm²= 25.31 mg/cm²= 25310 ug/cm²

Receptor fluid fraction calculation:

Intact skin (water): $(0.20 \mu\text{g} / \text{cm}^2) / (25310 \text{ug} / \text{cm}^2) = 8 \times 10^{-6}$
SC stripped skin (water): $(0.43 \mu\text{g} / \text{cm}^2) / (25310 \text{ug} / \text{cm}^2) = 1.7 \times 10^{-5}$
Intact skin (synthetic sweat): $(0.19 \mu\text{g} / \text{cm}^2) / (25310 \text{ug} / \text{cm}^2) = 7.5 \times 10^{-6}$

Avg diffusion rate calculation

Intact skin (water): $(8.0 \times 10^{-6} * 25.31 \text{ mg} / \text{cm}^2) / 10 \text{ hr} = 2.0 \times 10^{-5} \text{ mg} / \text{cm}^2 / \text{h}$
SC stripped skin (water): $(1.7 \times 10^{-5} * 25.31 \text{ mg} / \text{cm}^2) / 10 \text{ hr} = 4.3 \times 10^{-5} \text{ mg} / \text{cm}^2 / \text{h}$
Intact skin (synthetic sweat): $(7.5 \times 10^{-6} * 25.31 \text{ mg} / \text{cm}^2) / 10 \text{ hr} = 1.9 \times 10^{-5} \text{ mg} / \text{cm}^2 / \text{h}$

Intact skin (water): $2.0 \times 10^{-5} \text{ mg} / \text{cm}^2 / \text{h} / 39.74 \text{ mg} / \text{ml} = 5.0 \times 10^{-7} \text{ cm} / \text{h}$
SC stripped skin (water): $4.2 \times 10^{-5} \text{ mg} / \text{cm}^2 / \text{h} / 39.74 \text{ mg} / \text{ml} = 1.1 \times 10^{-6} \text{ cm} / \text{h}$
Intact skin (synthetic sweat): $1.9 \times 10^{-5} \text{ mg} / \text{cm}^2 / \text{h} / 39.74 \text{ mg} / \text{ml} = 4.8 \times 10^{-7} \text{ cm} / \text{h}$

Cumulative dose (skin)

Intact skin (Water)- 14.38 $\mu\text{g} / \text{mg}$
SC Stripped skin- 0.43 $\mu\text{g} / \text{mg}$ (approx.)
Synthetic sweat – 3 $\mu\text{g} / \text{mg}$ (approx.)

Other results

Pb concentrations:

Skin: 1.8 $\mu\text{g} / \text{mg}$ (approx.)
Liver- 0.00038 $\mu\text{g} / \text{mg}$ (approx)
Kidney- 0.016 $\mu\text{g} / \text{mg}$ (approx.)

Histological results:

Mild to moderate chronic inflammation of subcutis and dermis layers. Significant chronic inflammation in subcutis layer was observed in another area. Mild fat necrosis in dermis layer was also observed.

Proteomic analysis:

19 proteins were upregulated and 3 proteins were downregulated. 4 proteins showed a consistent >2.5 fold increase in upregulation compared to controls. These 4 proteins were identified as glucose- related protein precursor (GRP)78, K14, alpha-actin, and Rho GDP-dissociation inhibitor 2 (RhoGDI2)

Other Results from Sun et al. (2002)

The cumulative Pb in urine collected after 12 days of exposure compared to pre-dosing levels was 736.6 ng in the Pb nitrate exposed group vs. 10.8 ng in the control group.

Pb subacetate

Other results from King et al. 1978

Pb was detected in 3 of 4 layers in the 20 minute collection and 4 of 4 layers in the 90 minute collection, with decreasing concentrations observed in deeper layers. The 90 minute samples showed an increased amount of Pb in deeper layers of skin compared to the 20 minute samples, suggesting an increasing penetration over time, though this this was not confirmed with statistical analyses.

Pb orthoarsenate

Other results from Kunze and Laug, 1948

Tissue fraction calculation

Intact skin dosing: $0.85 \mu\text{g}/101500\text{ug} * 100 = 0.0008\%/g$ wet tissue

Pb content (μg) in wet grams of kidney

0.85 $\mu\text{g}/g$ (Intact skin dosing)

0.55 $\mu\text{g}/g$ (control)

Total Pb applied: $3.5\text{mg}/\text{cm}^2 * 29 \text{cm}^2 = 101.5 \text{mg} = 101500 \text{ug}$

Other results from Sun et al., 2002

The cumulative Pb in urine collected after 12 days of exposure compared to pre-dosing levels was 123.1 ng in the Pb sulfate exposed group vs. 10.8 ng in the control group.

Appendix 3. K_p and Diffusion Rate Calculation Based on Skin Penetration Studies in Chapter 3

Study 1

Franz cell surface area: 0.79cm^2

Dosing solution: $12.68\ \mu\text{g}/\text{ml} = 12.68\ \mu\text{g}/\text{cm}^3$

Volume applied (infinite dose study): $4.5\ \text{ml}$

Pb in skin layer: $0.51\ \mu\text{g}$ (total skin)

Diffusion rate

$$0.51\ \mu\text{g}/0.79\ \text{cm}^2 = 0.65\ \mu\text{g}/\text{cm}^2$$

$$0.65\ \mu\text{g}/\text{cm}^2/24\ \text{h} = \mathbf{0.027\ \mu\text{g}/\text{cm}^2/\text{h}}$$

$$0.027\ \mu\text{g}/\text{cm}^2/\text{h}/12.68\ \mu\text{g}/\text{cm}^3 = \mathbf{2.13 \times 10^{-3}\ \text{cm}/\text{h}}$$

Study 2

Wetting agent: DI water

Franz cell surface area: $0.79\ \text{cm}^2$

Dosing solution concentration: $14,508\ \mu\text{g}/\text{ml} = 14,508\ \mu\text{g}/\text{cm}^3$

Mass of Pb applied on skin (finite dose study): $290.16\ \mu\text{g}$

Applied dose: $367.29\ \mu\text{g}/\text{cm}^2$

Time of study: $24\ \text{h}$

Pb in skin layer: 91.68 (total skin)

Diffusion rate

$$91.68\ \mu\text{g}/0.79\text{cm}^2 = 116.05\ \mu\text{g}/\text{cm}^2$$

$$116.05\ \mu\text{g}/\text{cm}^2/24\text{h} = \mathbf{4.84\ \mu\text{g}/\text{cm}^2/\text{hr}}$$

K_p

$$4.84\ \mu\text{g}/\text{cm}^2/\text{hr}/14,508\ \mu\text{g}/\text{cm}^3 = \mathbf{3.33 \times 10^{-4}\ \text{cm}/\text{hr}}$$

Wetting agent: SSFL

Franz cell surface area: 0.79cm^2

Dosing solution concentration: $17,948\ \mu\text{g}/\text{ml} = 17,948\ \mu\text{g}/\text{cm}^3$

Mass of Pb applied on skin: $290.16\ \mu\text{g}$

Applied dose: $367.29\ \mu\text{g}/\text{cm}^2$

Time of study: $24\ \text{h}$

Pb in skin layer: 47.81 (total skin)

Diffusion rate

$$47.81\ \mu\text{g}/0.79\text{cm}^2 = 60.52\ \mu\text{g}/\text{cm}^2$$

$$60.52\ \mu\text{g}/\text{cm}^2/24\text{h} = \mathbf{2.52\ \mu\text{g}/\text{cm}^2/\text{hr}}$$

K_p

$$2.52 \mu\text{g}/\text{cm}^2/\text{hr}/14,508 \mu\text{g}/\text{cm}^3 = \mathbf{1.73 \times 10^{-4} \text{cm}/\text{hr}}$$

Study 3

Wetting agent: DI water

Franz cell surface area: 0.79cm^2

Dosing solution concentration: $17,948 \mu\text{g}/\text{ml} = 17,948 \mu\text{g}/\text{cm}^3$

Mass of Pb applied on skin: $1076.88 \mu\text{g}$

Applied dose: $1363.13 \mu\text{g}/\text{cm}^2$

Time of study: 72 h

Pb in skin layer: $251.48 \mu\text{g}$ (total skin)

Diffusion rate

$$251.48 \mu\text{g}/0.79 \text{cm}^2 = 318.33 \mu\text{g}/\text{cm}^2$$

$$318.33 \mu\text{g}/\text{cm}^2/72 \text{h} = \mathbf{4.42 \mu\text{g}/\text{cm}^2/\text{hr}}$$

K_p

$$4.42 \mu\text{g}/\text{cm}^2/\text{hr}/17,948 \mu\text{g}/\text{cm}^3 = \mathbf{2.46 \times 10^{-4} \text{cm}/\text{hr}}$$

Wetting agent: SSFL

Franz cell surface area: 0.79cm^2

Dosing solution concentration: $17,948 \mu\text{g}/\text{ml} = 17,948 \mu\text{g}/\text{cm}^3$

Mass of Pb applied on skin: $1076.88 \mu\text{g}$

Applied dose: $1363.13 \mu\text{g}/\text{cm}^2$

Time of study: 72 h

Pb in skin layer: $194.37 \mu\text{g}$

Diffusion rate

$$194.37 \mu\text{g}/0.79 \text{cm}^2 = 246.03 \mu\text{g}/\text{cm}^2$$

$$246.03 \mu\text{g}/\text{cm}^2/72 \text{h} = \mathbf{3.42 \mu\text{g}/\text{cm}^2/\text{hr}}$$

K_p

$$3.42 \mu\text{g}/\text{cm}^2/\text{hr}/17,948 \mu\text{g}/\text{cm}^3 = \mathbf{1.90 \times 10^{-4} \text{cm}/\text{hr}}$$

Study 4

Franz cell surface area: 0.79cm^2

Mass of Pb applied on skin: $769.02 \mu\text{g}$

Dosing solution concentration: $38,451 \mu\text{g}/\text{ml} = 38,451 \mu\text{g}/\text{cm}^3$

Applied dose: $973.44 \mu\text{g}/\text{cm}^2$

Time of study: 24 h

Wetting agent: DI water

Pb in skin layer: 43.28

Diffusion rate

$$43.28 \mu\text{g}/0.79\text{cm}^2 = 54.78 \mu\text{g}/\text{cm}^2$$

$$54.78 \mu\text{g}/\text{cm}^2/24\text{h} = \mathbf{2.28 \mu\text{g}/\text{cm}^2/\text{hr}}$$

K_p

$$2.28 \mu\text{g}/\text{cm}^2/\text{hr}/38,451 \mu\text{g}/\text{cm}^3 = \mathbf{5.94 \times 10^{-5} \text{cm}/\text{hr}}$$

Franz cell surface area: 0.78cm²

Mass of Pb applied on skin: 769.02 μg

Dosing solution concentration: 38,451 $\mu\text{g}/\text{ml}$ = 38451 $\mu\text{g}/\text{cm}^3$

Applied dose: 973.44 $\mu\text{g}/\text{cm}^2$

Time of study: 24 h

Wetting agent: SSFL

Pb in skin layer: 91.22

Diffusion rate

$$91.22 \mu\text{g}/0.79\text{cm}^2 = 115.47 \mu\text{g}/\text{cm}^2$$

$$115.47 \mu\text{g}/\text{cm}^2/24\text{h} = \mathbf{4.81 \mu\text{g}/\text{cm}^2/\text{hr}}$$

K_p

$$4.81 \mu\text{g}/\text{cm}^2/\text{hr}/38,451 \mu\text{g}/\text{cm}^3 = \mathbf{1.25 \times 10^{-4} \text{cm}/\text{hr}}$$